INTERACTION OF GASES IN THE SURFACE OF NICKEL OXIDE

K. KLIER and M. JIRATOVA

Institute of Physical Chemistry, Czechoslovak Academy of Sciences, Prague, Czechoslovakia

Abstract: An investigation has been made of the processes occurring on the surface of nickel oxide in the presence of carbon monoxide carbon dioxide and oxygen under various conditions. Apart from adsorption-desorption and electric conductivity measurements, exchange reactions of radio-carbon have been employed for the analysis of the adsorbate. Radio-carbon is exchanged between the adsorbate and gases according to the character of the adsorbate: $CO_{(ads)}$ exchanges group CO and $CO_{2(ads)}$ or carbonate exchanges group CO_2. The results show that carbon monoxide forms oxidized surface species with lattice oxygen of the nickel oxide at 20°C, this reaction being enhanced by increasing temperature and pressure. When oxygen is preadsorbed, oxidized species are preferably created by reaction with adsorbed oxygen with simultaneous disappearance of $CO_{(ads)}$. Also carbon dioxide reacts with adsorbed oxygen with charge transfer, presumably due to the reaction

$$CO_2 + O^-_{(ads)} + Ni^{2+} \rightarrow CO_3^{2-} + Ni^{3+} .$$

1. INTRODUCTION

Interactions of gases CO, CO_2 and O_2 on the surface of nickel oxide have hitherto been investigated by several methods, including chemical analyses of gases [1], adsorption [2-5,9,13], calorimetric [6,7], infrared spectra [8], electric conductivity [2,9,10], thermoelectric power [11] and optical spectra [12] measurements. As a result of these investigations, it has been well established that oxygen is adsorbed in anionic form ($O^{\delta-}$), the negative charge of the adsorbate being compensated by mobile positive charge inside nickel oxide (Ni^{3+}). Thus oxidized nickel oxide can be fully reduced to its original electronic state (Ni^{2+}) by carbon monoxide adsorption at room temperature [9]. Increased adsorption heats of carbon monoxide on surface precovered by oxygen and of oxygen on surfaces precovered by CO and CO_2, as compared with bare surfaces, have indicated reactions of adsorbing gases with the adsorbate [6,7]. Effect of self-poisoning by CO_2 of NiO for carbon monoxide oxidation, first observed by Roginski and Tselinskaya [1], has later been confirmed by other authors [6,14] and explained to be due to the occupation by CO_2 of sites available for CO and O_2 adsorption.

However, there has been considerable disagreement among different workers concerning the adsorbed amounts of CO and O_2, formulas of adsorbed complexes, and the possibility of reactions with lattice oxygen at room temperature [7,15]. Also the behaviour of CO_2 in this system has not been fully elucidated. Some authors observed localization of electrons in

the adsorbate and release of mobile holes into nickel oxide during CO_2 adsorption [2,11], others observed no such effect [9,13]. These results suggested that a study of the influence due to the various factors (temperature, pressure, purity of the surface) on the behaviour of this system as well as the application of new methods to analysis of adsorbed complexes would be of value.

In this work, interactions of gases with and in the surface of nickel oxide have been investigated by means of adsorption-desorption measurements, analyses of gaseous phase, electric conductivity measurements, and exchange reactions of radio-carbon between adsorbate and different gases, and have been exploited for the analysis of the adsorbate. The present results provide information about the composition of and the reactions in the adsorbed layer under various conditions.

2. EXPERIMENTAL PART

2.1. *Apparatus*

Apparatus of the type described earlier [16] was used, allowing measurements to be made of amounts adsorbed and desorbed simultaneously with electric conductivity, measured in situ by a high frequency method [16,17] at 1 Mc/s. Volume of apparatus was 1576 ml for experiments at pressures lower than 10^{-1} mm Hg and 1142 ml for experiments at pressures of about 2 mm Hg. Pressure was measured by Pirani gauges [16,17] up to 10^{-1} mm Hg and by a MacLeod gauge up to 2.5 mm Hg. Two freezing traps in the measuring part of apparatus were maintained at -78°C except when analyses were made for CO and CO_2 by freezing out carbon dioxide at -190°C. In the latter case, due corrections were made for changes of volume. Installed in the wall of the reaction vessel space was also a thin mica window (1 mg/cm^2) of diameter 30 mm sealed by Araldite to a glass opening in the wall. The joint was vacuum tight and the apparatus was evacuable to 10^{-7} mm Hg. The radioactivity was measured by an alpha G-M counter, set close to the mica window outside the reaction space. The solid sample was located inside the reactor in such a position that the radiation of ^{14}C from adsorbate was completely absorbed by the glass and could not reach the counter window. Only radioactivity of the gas was thus measured. Due corrections were made for background radiation and dead time of the counter. Radioactivity of the labelled gases was proportional to their pressure. Conveniently, specific activity of a gas is defined as the number of counts per minute (cpm) per one molecule of this gas in the apparatus. Two specific activities were used in the present work: 8.2×10^{-15} cpm molecule^{-1} (^{14}CO, experiments 1-7, and $^{14}CO_2$, experiment 10 in table 1 below) for low pressure experiments, and 2.29×10^{-15} cpm molecule^{-1} for high pressure experiments (^{14}CO, experiments 8 and 9 in table 1).

2.2. *Materials*

Commercial ^{14}CO (0.61 mC/ml) was used and purified in situ by vacuum distillation from active charcoal. $^{14}CO_2$ was prepared in situ by oxidation of

^{14}CO by oxygen on a heated platinum filament and subsequent freezing with evacuation. Preparation of inactive gases CO, CO_2 and O_2 is described elsewhere [4]. The carbon oxide contained less than 5×10^{-3} % of O_2.

Nickel oxide of high purity and surface area 99 m^2/g was prepared according to ref. 3 and 17 by vacuum decomposition of nickel hydroxide at 200°C for 15 hours (final pressure 10^{-6} mm Hg). The nickel oxide contained some amount of non-decomposed hydroxide [3, 18]. The following experiment allowed us to assess the maximum possible contamination of the surface. Adsorption of 9.2×10^{17} molecules of oxygen on 0.26 g sample caused electric conductivity to increase from 0.33×10^{-6} ohm^{-1} to 0.46×10^{-6} ohm^{-1}, which effect was completely reversed by subsequent adsorption of CO. On the other hand, when carbon monoxide was adsorbed on a clean nickel oxide, no change of conductivity occured, similarly as in [9]. From estimated error of our conductivity measurements, 0.02×10^{-6} ohm^{-1}, one is able to see that no more than 1.7×10^{17} molecules of oxygen could have been adsorbed on the initial clean nickel oxide, which is less than 0.1% of surface coverage [6].

2.3. *Procedure*

First, carbon monoxide labelled by ^{14}C was allowed to be adsorbed for 200 minutes (adsorbed amount a), then the gaseous phase with desorbable part of the adsorbate was removed by pumping for 30 min, the amount desorbed being measured and analyzed for CO (amount d) and CO_2 in a separate volume behind the gas collection pump. The adsorbate remaining on the surface was then subjected to exchange reactions at the same temperature as adsorption. First, inactive CO was admitted, its adsorbed amount (b), amount of CO in gas (g) and CO_2 in gas (q) measured and ^{14}C activity (y) in gaseous carbon monoxide followed with time. After the concentration of radioisotope in the gaseous carbon monoxide (y/g) had reached an equilibrium value, the gaseous mixture was pumped out and analyzed. Subsequently, non-radioactive CO_2 was admitted to the sample, amounts of CO_2 adsorbed (c), CO_2 in gas (h) and CO in gas (p) were measured and ^{14}C activity determined both in gaseous carbon dioxide (activity z) and in gaseous carbon monoxide until the concentration of isotope (z/h) reached an equilibrium value. For some experiments, the sequence of admissions of CO and CO_2 was reversed.

Each experiment (1-10 in table 1) was carried out with a newly prepared sample (0.26 g) of reproducible properties.

3. RESULTS

3.1. *Carbon monoxide on nickel oxide*

3.1.1. Kinetics and extent of adsorption

Fig. 1 shows the courses of adsorption at various temperatures, pressures and degrees of preadsorption by oxygen. In this graph is not included CO adsorption on nickel oxide precovered by 118×10^{17} molecules of oxygen, because both the extent and the rate of adsorption were very high.

Table 1

Experimental data for adsorption and exchange reactions

	1	2	3	4	5	6	7	8	9	10	11	12	13	14
Experiment	Temperature	Sequence	Note	a	d	g_∞	$\frac{g_0}{g_\infty}$	h	$\frac{z_\infty}{h_\infty}$	b	c		m	n
1**	20°C	CO-CO_2		17.6	3.3 (0.5)	14.2	2.05	3.7	0.085	4.7	448.3		6.3	4.7
2**	20°C	CO_2-CO		17.3	2.9 (0.2)	17.8	1.55	4.4	0.091	2.5	445.6	2.2 [p]	4.3	4.7
3**	55°C	CO-CO_2		15.7	1.1 (0.3)	17.0	1.92	5.3	0.11	3.7	381.7		6.5	5.4
4**	100°C	CO_2-CO		19.8	0.7 (0.2)	17.9	1.00	5.0	0.26	1.5	272.0	1.6 [p]	2.5	8.9
5**	150°C	CO-CO_2		30.5	2.15 (0.3)	20.4	1.30	2.6	0.87	2.9	142.0		4.1	17.5
6**	20°C	CO-CO_2	preadsorbed 9.35×10^{17} molecules O_2	21.5	1.7 (0.3)	13.4	1.48	2.9	0.20	4.9	401.1		4.0	9.9
7**	20°C	CO-CO_2	preadsorbed 118×10^{17} molecules O_2	81.9	0.6 (0.1)	4.1	0.83	3.3	1.31	2.9	374.7		0.7	70.0
8**	20°C	CO-CO_2	initial pressure 2.25 mm Hg	152.8	25.0 (1.1)	560	0.186	116.7	0.074	5.4	514.5	3.0 [q]	50.2	21.0
9**	20°C	CO_2-CO	initial pressure 2.26 mm Hg	154.0	32.1 (1.2	*	*	155.7	0.074	*	582.0		*	24.7
10**	20°C	CO_2	adsorbed $^{14}CO_2$	127.4				2.4	2.18		290.0		0	106.0

STAT

LEGEND TO TABLE 1

a, amount adsorbed in 200 min; expts. 1-9: adsorption of ^{14}CO
expt. 10 : adsorption of $^{14}CO_2$

d, amount desorbed in 30 min by pumping after the 200 min adsorption; upper values: ^{14}CO desorbed; lower values in brackets: $^{14}CO_2$ in desorbate

g_∞, amount of CO in gas at the end of exchange with carbon monoxide

h_∞, amount of CO_2 in gas at the end of exchange with carbon dioxide

$\frac{y_\infty}{g_\infty}$, specific activity of CO in equilibrium with the adsorbate, cpm molecule^{-1} x 10^{15}

$\frac{z_\infty}{h_\infty}$, specific activity of CO_2 in equilibrium with the adsorbate, cpm molecule^{-1} x 10^{15}

b, amount of CO adsorbed during exchange with carbon monoxide

c, amount of CO_2 adsorbed during exchange with carbon dioxide

p, amount of CO_2 displaced from the adsorbate during exchange with CO

m, amount of adsorbate exchangeable with CO, computed from (2)

n, amount of adsorbate exchangeable with CO_2, computed from (3)

The quantities $a, d, g, h, b, c, p, q, m$ and n are in molecules x 10^{-17}

The amounts p and q were pumped out of the system

* Exchange with CO was not carried out in this experiment

** Initial pressure 5.6 x 10^{-2} mm Hg

Experiments 1-5 and 8-10 carried out on bare NiO.

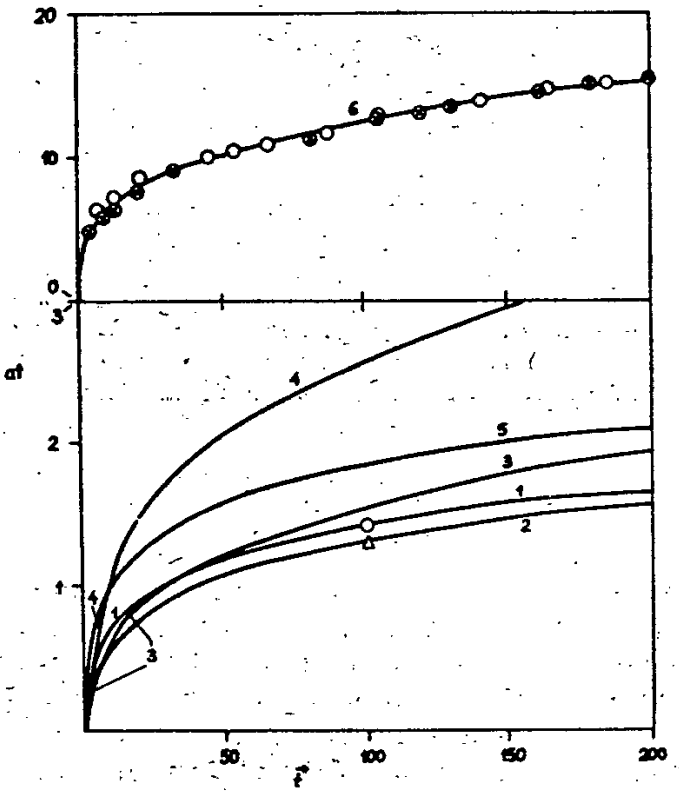

Fig. 1. Adsorption of carbon monoxide
a, adsorbed amount in molecules x 10^{-17} per 0.26 g sample
t, time in min.
Initial pressure 5.6 x 10^{-2} mm Hg (1-4 clean nickel oxide):
curve 1: 20°, curve 2: 55°, curve 3: 100°, curve 4: 150°,
curve 5: 20°, 9.35 x 10^{17} molecules O_2 preadsorbed.
curve 6: 20°C, initial pressure 2.25 mm Hg, clean nickel oxide ○ ⊛ two independently prepared samples.

Data for this experiment are presented in table 1 together with other data concerning exchange reactions.

Kinetics of adsorption obeyed the well known equation (fig. 2)

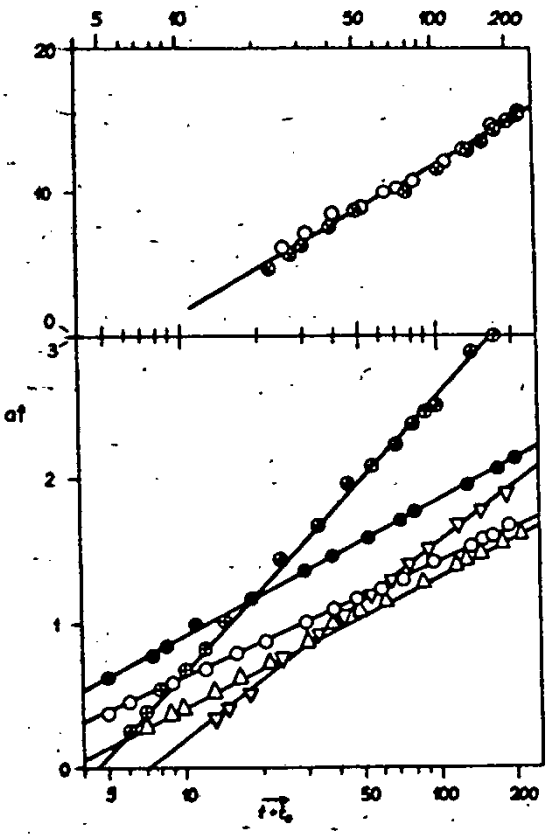

Fig. 2. Plots of data from fig. 1 according to equation (1) $t + t_0$ in min, logarithmic scale. Lower figure: ○ correspond to curve 1 in fig. 1; △, to 2, ▽, to 3; ⊕, to 4; ●, to 5.

$$a = \frac{2.3}{b} [\log(t + t_0) - \log t_0] \qquad (1)$$

(a, adsorbed amount in molecules, t, time, b and t_0 constants), the values of $2.3/b$ and t_0 being summarized in table 2 in the discussion. Reproducibility of results was very good as demonstrated in fig. 1 by a comparison of adsorptions on different samples, including those taken from our earlier work [4], open circles for 20°C adsorption and triangles for 55°C adsorption. Since all the adsorptions studied with ^{14}CO and those in earlier work with non-radioactive CO gave the same results, one can exclude isotopic effect on the extent of adsorption. At 150°C, measuring devices indicated the presence of hydrogen during CO adsorption. This is most likely a product of the reaction of CO with non-decomposed nickel hydroxide contained in the sample under the catalytic action of nickel which is being produced by the reaction of carbon monoxide with the lattice oxygen of NiO. The partial pressure of CO in the gaseous mixture during adsorption was determined at

Table 2
Constant of equation (1) and amount of oxidized CO ($l + n$)

Temperature °C	Conditions of experiment	$\frac{2.3}{b}$	t_o	$l + n$
20	*	8.25	4	8.0
55	*	8.89	5	8.1
100	*	13.4	10	15.0
150	*	18.6	5	24.2
20	9.35 10^{17} molecules O_2 preadsorbed	9.21	3.5	15.8
20	low pressure adsorption clean NiO, initial pressure of CO adsorption 2.25 mm Hg	100	20	77.6

$l + n$ and $\frac{2.3}{b}$ in molecules $\times 10^{-17}$ per 0.26 g of adsorbent,

t_o in minutes

* Unless otherwise stated, adsorptions were carried out from the initial pressure 5.6×10^{-2} mm Hg on a clean nickel oxide.

this temperature from the radioactivity due to a non-condensable gas, which is associated only with carbon monoxide. No hydrogen was evolved during exchange experiments.

3.1.2. Exchange reactions

Exchange reactions were carried out after the adsorption of ^{14}CO lasting 200 min. The results are presented in fig. 3 (exchange of ^{14}C between adsorbate and gaseous carbon monoxide) and in fig. 4 (exchange between adsorbate and-carbon dioxide). The final values of the concentration of ^{14}C in $CO_{(g)}$ and in $CO_{2(g)}$ were equilibrium ones and did not change for another ten hours; they are presented in table 1 (col. 7 and 9) with other data for adsorption and results of analyses of the gaseous phase. All experiments, except those showing the effect of pressure (table 1, experiments 8 and 9), were carried out at low pressures (initial pressure of ^{14}CO adsorption 5.6×10^{-2} mm Hg, pressure during exchange reactions 10^{-2} - 10^{-3} mm Hg). Effect of temperature was studied in experiments 1-5 for the range 20-150°C. Effect of oxygen preadsorption on CO adsorption and exchange reactions at 20°C was investigated in experiments 6 and 7. Oxygen was always preadsorbed at 150°C because at this temperature all oxygen adsorbs irreversibly in ionic form [17]. In some experiments, the exchanging gas displaced a certain amount of the other gas from the adsorbate into the gaseous phase; this amount was measured and is given in column 12 of table 1.

Experiments with reversed sequence of the two exchanging gases provide information about mechanism of both exchange reactions (see Discussion). The sequences are indicated in column 2 of table 1 as $CO\text{-}CO_2$ and $CO_2\text{-}CO$ according to order of admissions of exchanging gases.

A note has to be added on the maximum on high pressure exchange (⊗) in fig. 3. Theory [19] predicts very low maxima on all curves for exchange

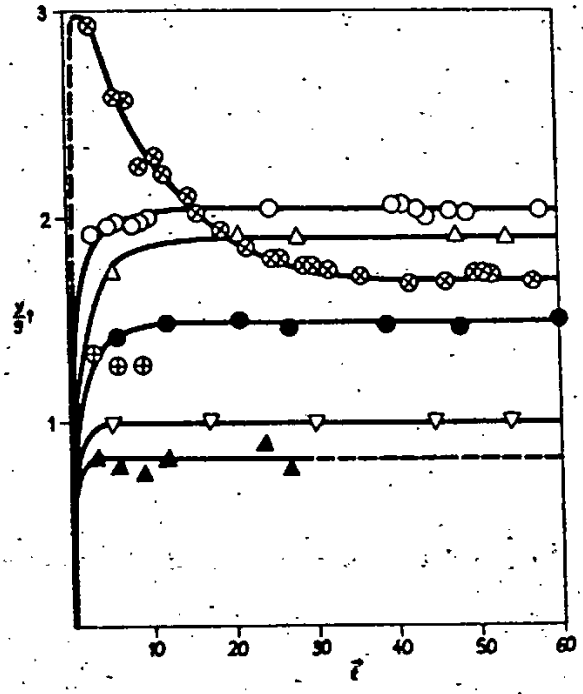

Fig. 3. Exchange reactions of ^{14}C between adsorbate and carbon monoxide
$\frac{y}{g}$, concentration of ^{14}C in $CO_{(g)}$, cpm molecule^{-1} x 10^{15},
t, time (min). For ⊗ scale reduced 10 ×.
Pressure below 10^{-1} mm Hg, clean nickel oxide; ○ 20°C (experiment 1) △ 55°C (experiment 3), ▽ 100°C (experiment 4), ⊕ 150°C (experiment 5).
Pressure below 10^{-1} mm Hg, oxygen precovered nickel oxide:
● 20°C, 9.35 x 10^{17} molecules O_2 preadsorbed (experiment 6).
▲ 20°C, 118 x 10^{17} molecules O_2 preadsorbed (experiment 7)
⊗ 20°C, pressure about 2 mm, clean nickel oxide (experiment 8).

with carbon monoxide, which would not be detectable by the experimental techniques employed at present. The high maximum on the curve mentioned is a diffusion effect: at 2 mm Hg, diffusion coefficient of gas becomes much lower than that at 5×10^{-2} mm; the radioactive gas is rapidly exchanged from the surface into the gaseous phase where its high concentration reaches first the counter window and then slowly diffuses into the other parts of apparatus.

3.2. *Carbon dioxide on nickel oxide*

Carbon dioxide adsorbs to a much higher extent than carbon monoxide. Kinetics of adsorption were not measured because most of the adsorption is a very rapid process. At low pressures the adsorption amounted to 4.17×10^{19} molecules (amounts a plus c in experiment 10 in table 1) with final pressure 4.3×10^{-3} mm Hg. The quantity c (col. 11, table 1) shows the influence of various factors on CO_2 adsorption. There is a little effect when carbon monoxide is preadsorbed at 20°C (row 1), a slight decrease with preadsorption of oxygen (rows 6 and 7), decrease with increasing temperature (rows 1-5) and a slight enhancement of adsorption with increased pressure (rows 8, 9).

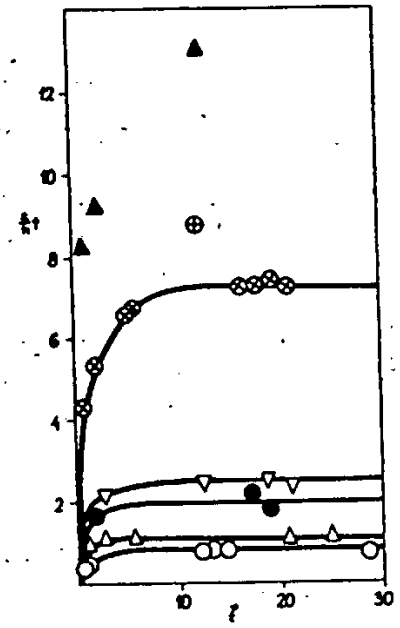

Fig. 4. Exchange reactions of ^{14}C between adsorbate and carbon dioxide
$\frac{x}{h}$, concentration of ^{14}C in $CO_{2(g)}$, cpm molecule^{-1} x 10^{17}
t, time (hours). For ⊗ scale reduced 10 times.
The same symbols as in fig. 3 used for varions experiments.

An experiment on exchange of adsorbed $^{14}CO_2$ with inactive carbon dioxide was also carried out and the results are given in table 1, row 10. The half time of this exchange reaction was about one hour.

Measurements of electric conductivity revealed that on clean nickel oxide, CO_2 adsorbs without changing electric conductivity of NiO, whereas adsorption of CO_2 on NiO with preadsorbed oxygen leads to an increase of conductivity linearly dependent on the amount of adsorbed CO_2 (fig. 5).

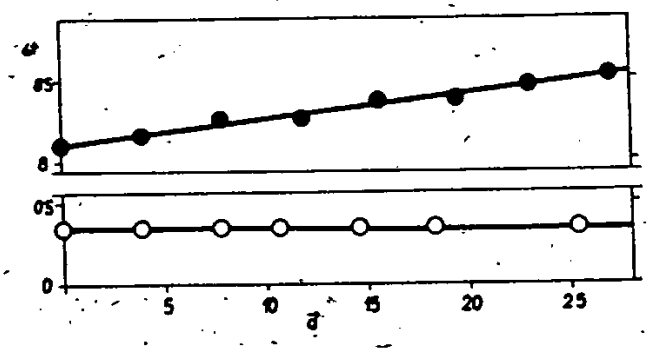

Fig. 5. Changes of electric conductivity with adsorption of CO_2
σ, conductivity, ohm^{-1} x 10^8; a, molecules x 10^{-18} of CO_2 adsorbed
○, clean nickel oxide
●, nickel oxide with 103.6 x 10^{17} preadsorbed oxygen molecules.

4. DISCUSSION

4.1. *Interpretation of exchanged amounts*

It is evident from figs. 3 and 4 and from table 1 that under comparative conditions the equilibrium amounts of ^{14}C exchanged with CO decrease with increasing temperature of ^{14}CO adsorption and with increased amount of preadsorbed oxygen, while reversed effect is observed in exchange with CO_2. This is a clear indication that a part of adsorbing ^{14}CO becomes oxidized to carbon dioxide or carbonate which is then able to exchange group CO_2 with gaseous carbon dioxide; this part is the greater the higher is the temperature of ^{14}CO adsorption and the more oxygen is preadsorbed.

Further evidence is obtained from experiments with reversed sequences of exchanging gases which reveal mechanism of the two exchange reactions. If one part (M) of adsorbate exchanges only with CO and not with CO_2 and another part (N), only with CO_2 and not with CO (mechanism I), the amounts exchanged under comparative conditions with the two gases will not depend on the sequence of the exchanging gases. If, on the other hand, the same molecules of adsorbate were able to exchange ^{14}C with both CO and CO_2 (mechanism II), one would always expect high radioactivity appearing in the gas admitted first and low activity in the gas admitted next and, therefore, great differences in the amounts exchanged with CO in the two experiments in which CO is admitted before and after exchange with CO_2; the same would apply for exchange with CO_2.

Results of experiments 1 and 2, and 8 and 9 in table 1 indicate that mechanism I takes place, since the final isotope concentrations are dependent to a very small extent on the sequence of exchanging gases. Quantitative analysis of the data fully confirms these conclusions and allows us to determine the number of carbon atoms in both parts M and N. At equilibrium, a uniform distribution of radio-carbon among the mutually exchangeable species must be attained. Part of exchanging gas, which was originally not radioactive, adsorbs and this adsorbate (amount b in exchange with CO and c in exchange with CO_2, table 1) also participates in exchange *.

Let m and n be numbers of carbon atoms in parts M and N, and X the concentration of radio-carbon in adsorbing ^{14}CO. Then, according to mechanism I, amount mX of ^{14}C labelled molecules of adsorbate M become uniformly distributed, at the end of exchange with CO, among the gaseous $CO((y_\infty/g_\infty)\, g_\infty)$, the original adsorbate $M((y_\infty/g_\infty)m)$ and the newly adsorbed $CO((y_\infty/g_\infty)b)$:

$$\frac{y_\infty}{g_\infty}(g_\infty + b + m) = mX \qquad \text{(2) exchange of M with CO}$$

Similarly, amount nX of ^{14}C labelled molecules of adsorbate N becomes uniformly distributed at the end of exchange with CO_2 among the gaseous

* In exchange with CO_2, a small fraction of c molecules of CO_2 adsorbate does not exchange as is seen from experiment 10 in table 1. We shall assume for the purpose of discussion that all molecules c are exchangeable, being aware of a slight inaccuracy introduced by the assumption.

CO_2 ($(z_\infty/h_\infty)\ h_\infty$), the original adsorbate N ($(z_\infty/h_\infty)\ n$) and newly adsorbed CO_2 ($(z_\infty/h_\infty)\ c$):

$$\frac{z_\infty}{h_\infty}(h_\infty + c + n) = nX \qquad \text{(3) exchange of N with } CO_2$$

Formulae (2) and (3) are identical with those obtained from kinetic treatment of mechanism I [19].

For mechanism II, the conditions for uniform distribution of radiocarbon are different and depend on the sequence of exchanging CO and CO_2. When the sequence CO-CO_2 is employed, one obtains

$$\frac{y_\infty}{g_\infty}(g_\infty + b + m + n) = (m + n)\ X \qquad \text{(4) exchange with CO}$$

$$\frac{z_\infty}{h_\infty}(h_\infty + c + m + n) = (m + n)\frac{y_\infty}{g_\infty} \qquad \text{(5) exchange with } CO_2$$

while with the reversed sequence CO_2-CO holds

$$\frac{z_\infty}{h_\infty}(h_\infty + c + m + n) = (m + n)\ X \qquad \text{(6) exchange with } CO_2$$

$$\frac{y_\infty}{g_\infty}(g_\infty + b + m + n) = (m + n)\frac{z_\infty}{h_\infty} \qquad \text{(7) exchange with CO}$$

Values of m and n can be computed for mechanism I when inserting measured quantities in (2) and (3), and values $m+n$ for mechanism II from (4) - (7). These values must be self-consisent for the two reversed experiments, if the respective mechanism operates.

The following excellent agreement is obtained between amounts m and n in the two reversed experiments, calculated by means of (2) and (3), which confirms that mechanism I is operating:

m(expt. 1) = 6.3×10^{17} molec.; m'(expt. 2) = 6.5×10^{17} molec.
n (expt. 1) = 4.7×10^{17} molec.; n (expt. 2) = 4.5×10^{17} molec.
n'(expt. 8) = 24 $\times 10^{17}$ molec.; n (expt. 9) = 24.7×10^{17} molec.

The value m' (n') is a sum of amount m (n), determined from exchange reactions (col. 14 table 1), and number of molecules of labelled adsorbate which were displaced from the surface in preceding exchange (col. 12 table 1) and removed from the system, so that they could not participate in subsequent exchange.

Calculations according to (4)-(7) lead to many orders, discrepancies and even negative values of $m + n$ for different sequences of exchanging gases. Slight interference of mechanism II with mechanism I would lead to gross discrepancies and therefore our results show that mechanism I alone is operating.

Apart from the two adsorbates M and N, there is a part (L) which is not capable of exchange with either CO or CO_2. The number of carbon atoms in part L is $l = a - d - m - n$. The following diagramme shows the magnitudes of l, m, n and d for various conditions employed in the present research.

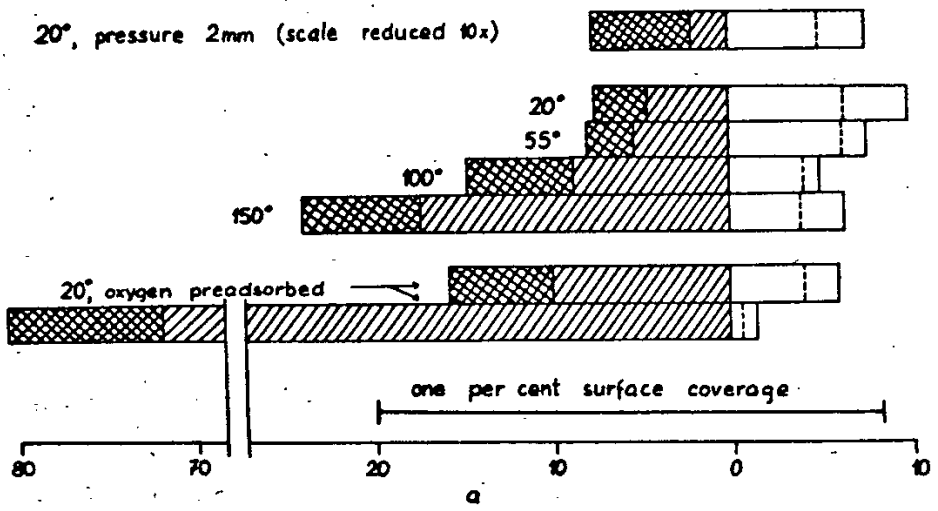

Diagramme 1: part M
part D
part N
part L

a, molecules $\times 10^{-17}$

Number of experiment from up down: 8, 1, 3, 4, 5, 6, 7.

The nature of parts D (desorbable CO, amount *d*) and M is weakly chemisorbed CO which is in dynamic equilibrium with the gaseous carbon monoxide as the rapid courses of exchange reactions indeed show. Part N is adsorbed CO_2 or carbonate which exchanges whole group CO_2 with gaseous carbon dioxide and does not dissociate under the formation of CO (no exchange with CO). Its character is the same as that of the product of CO_2 adsorption, since the half time of its exchange with CO_2 is close to the half time of $^{14}CO_{2(ads)}$ - $CO_{2(g)}$ exchange, 1 hour. The presence of carbonate formed with lattice oxygen at some stage of CO_2 adsorption has been proved by exchange of ^{18}O between $Ni^{18}O$ and CO_2 at 20°C on the present preparation of NiO [20]. Therefore, once adsorbed carbon dioxide is formed, it will form carbonates with lattice oxygen and vice versa. The non-exchangeable part L is a very strongly bonded or sterically hindered adsorbate. Since its extent increases simultaneously with that of part N, it also is very likely a carbonate or adsorbed CO_2. Further evidence for this is obtained from the exchange of $^{14}CO_{2(ads)}$ with CO_2, which shows that a certain part of the adsorbed carbon dioxide does not exchange with CO_2. Mode L is also a product of interaction of adsorbed oxygen with CO and it may well be true that this very strongly bonded adsorption mode actually poisons nickel oxide catalysts for the low temperature oxidation of carbon monoxide.

Since the starting nickel oxide in experiments 1-5 and 8-9 was free from adsorbed oxygen, the $CO_{2(ads)}$ or carbonate must be formed in these experiments by the reaction of adsorbing CO with lattice oxygen of the nickel oxide. This is a reduction process which produce lower valency states of nickel cations, either Ni^0 or Ni^+, e.g.,

$$CO + O^{2-}_{lattice} + Ni^{2+} \rightarrow CO_{2(ads)} + Ni^{0} + \square \quad (8)$$

$$CO_{2(ads)} + O^{2-}_{lattice} \rightleftharpoons CO_3^{2-} + \square \quad (9)$$

Electrons in these states are localized in d-shells of nickel and therefore no change of electric conductivity occurs, as observed in [9] and also in the experiment quoted in the experimental part of this work. However, change of electronic structure of cation at temperatures as low as 20°C is indicated by the change of visible spectrum of the clean nickel oxide during the adsorption of carbon monoxide [10]. The presence of lower valency states of nickel will certainly contribute to the adsorptive properties of nickel oxide. Particularly, considerable amount of adsorbate exchangeable with CO may be bonded to these lower valency states, e.g., Ni-CO, carbonyl on atomic scale. Increased amount of weakly bonded carbon monoxide at 150°C as compared with that at lower temperatures may well be due to this kind of adsorption.

4.2. *Reactions with adsorbed oxygen ions*

Oxygen is adsorbed at 150°C in the surface of NiO as atomic anions [17]. Total increase of CO adsorption on nickel oxide with preadsorbed (150°C) oxygen as compared with clean nickel oxide (fig. 1) is due to a large increase in the amounts of modes N and L, accompanied by a marked decrease in the amounts of modes M and D. When a sufficient amount of CO is allowed to react with adsorbed oxygen, electric conductivity of nickel oxide drops to the value observed on oxygen-free samples [9] and the colour of clean nickel oxide is restored. The reaction

$$CO + O^{-}_{(ads)} + Ni^{3+} \rightarrow CO_{2(ads)} + Ni^{2+} \quad (10)$$

explains both electric conductivity and ^{14}C exchange observations.

It is interesting that reaction of CO_2 with adsorbed oxygen ions takes place with charge transfer also. Namely, the increase of conductivity during CO_2 adsorption on oxygenated samples can be interpreted as

$$CO_2 + O^{-}_{(ads)} + Ni^{2+} \rightarrow CO_3^{2-} + Ni^{3+} \quad (12)$$

where Ni^{3+} ions are produced to increase conductivity, while the reaction of CO_2 with lattice oxygen (9) does not lead to any change of conductivity of the clean nickel oxide.

Only a small part of the oxygen adsorbate participates in reaction (12), as the effect on conductivity is very small compared with the effect induced by a comparable amount of adsorbed oxygen.

4.3. *Relation between adsorption kinetics and mode of adsorption*

For experiments on clean nickel oxide, correlation exists between the values of the constant b (eq. (1)) and the amounts of CO oxidized by lattice oxygen, $l + n$, as shown in table 2. This means that adsorption decelerates more slowly when reaction with lattice oxygen is enhanced, which happens either on increasing the temperature or the pressure. This also explains the crossing of kinetic curves for various temperatures in fig. 1. If the

constant b contributes to activation energy of adsorption according to

$$\frac{dq}{dt} = A \exp\left[-\frac{E_0 + bRTq}{RT}\right] \qquad (13)$$

(q, adsorbed amount in time t, E_0 and A, constants), then the above mentioned correlation means that increased extent of reaction with lattice oxygen makes the whole process less dependent on adsorbed amount of CO, in other words, the reaction with lattice oxygen is more uniform with respect to activation energy than the production of $CO_{(ads)}$. A similar but smaller effect is observed with CO adsorption on oxygen precovered NiO.

4.4. *Comparison with other work*

The present results show that carbon monoxide adsorption at 20°C and 5.6×10^{-2} mm Hg on a clean NiO is very low (~0.6% surface coverage in 200 min adsorption) and yet, part of this process is the result of reaction which has already taken place with lattice oxygen. The effect of increasing pressure is to increase both the extent of reaction with lattice oxygen and the amount of weakly adsorbed CO. The latter finding confirms considerations [15] which explain the differences in the amounts of CO adsorbed found in various works, in terms of low adsorption heat of CO and reactions with lattice oxygen. There is, however, another factor strongly influencing the CO adsorption at low pressures, namely, adsorbed oxygen present on the surface of NiO. This explains why other authors [2, 5] found, at comparable pressures, amounts adsorbed higher than that in the present work. At higher pressures (about 40 mm), the effect of oxygen preadsorption on CO adsorption is small [3] because reaction with lattice oxygen at these pressures becomes very extensive and numbers of adsorption sites on the surfaces with and without adsorbed oxygen are not substantially different.

ACKNOWLEDGEMENT

The authors wish to thank Professor R. Brdička, Director of the Institute of Physical Chemistry in Prague, for his constant interest in their work. They are also indebted to Dr. F. S. Stone from Bristol University and Dr. J. Haber from Kraków Mining Academy for helpful discussion of their work.

REFERENCES

1) S. Z. Roginski and T. S. Tselinskaya, J. Phys. Chem. USSR 21 (1947) 919, 22 (1948) 1360.
2) N. P. Keier, L. N. Kutseva, Izv. Akad. Nauk USSR, Otd. chim. nauk 1959, 797.
3) S. J. Teichner, R. P. Marcellini and P. Rué, Advances in Catalysis 9 (1957) 458.
4) K. Klier, Coll. Czech. Chem. Commun. 28 (1963) 2996.
5) Y. Kubokawa and O. Toyama, Bull. Chem. Soc. Japan 35 (1962) 1407.
6) R. M. Dell and F. S. Stone, Trans. Farad. Soc. 50 (1954) 501.

7) P. Ch. Gravelle, Dissertation, University of Lyon, May 1963.
8) M. Courtois and S. J. Teichner, J. Chim. Phys. 1962, 272.
9) R. P. Marcellini, R. E. Ranc and S. J. Teichner, Actes du deuxième Congrès international de catalyse, Technip, Paris 1960, 289.
10) A. Bielanski, J. Dereń, J. Haber and J. Sloczynski, Zeit. Physik. Chem. N. F. 24 (1960) 345.
J. Dereń, J. Haber and J. Sloczynski, Bull. Acad. Sci. Pologne 8 (1960) 391, 8 (1960) 399.
11) G. Parravano and C. A. Domenicali, J. Chem. Phys. 26 (1957) 359.
12) K. Klier, Kinetika i Kataliz 3 (1962) 65.
13) P. Rué, Dissertation, University of Lyon, June 1963.
14) R. Ranc, Dissertation, University of Lyon, March 1963.
15) F. S. Stone and K. Klier, Actes du deuxième Congrès international de catalyse, Technip, Paris 1960, 323.
16) T. I. Barry and K. Klier, Discussions Faraday Soc. 31 (1961) 219.
17) K. Kuchynka and K. Klier, coll. Czech. Chem. Commun. 28 (1963) 148.
18) K. Kuchynka, Dissertation, Czechoslovak Academy of Sciences, Prague, October 1963.
19) K. Klier, Coll. Czech. Chem. Commun. (1964) to be published.
20) K. Klier and Z. Herman, Coll. Czech. Chem. Commun. (1964) to be published.

ON THE MAGNETIC PROPERTIES AND CATALYTIC ACTIVITY OF NICKEL OXIDE

D. MEHANDJIEV and G. BLIZNAKOV

Institute of General and Inorganic Chemistry, Bulgarian Academy of Sciences, Sofia, Bulgaria

Abstract: An attempt is made to present additional information on the reaction $CO + \frac{1}{2}O_2 \rightarrow CO_2$ with NiO as catalyst and to explain the contradictory results obtained by a number of authors, concerning the activation energy and the influence of various additives. Tc this end, the catalytic activity of pure nickel oxide was studied simultaneously with its magnetic properties and the content of oxygen in excess of the stoichiometric amount. It was shown that when the excess of oxygen is increased, the specimens of nickel oxide pass from antiferromagnetic into paramagnetic state with traces of ferromagnetism. This leads to a sharp change of the activation energy of reaction. While for the antiferromagnetic specimens the activation energy is of the order 4-9 kcal/mole, for the paramagnetic ones it is about 13-17 kcal/mole. The rate constant changes in an analogous manner. The magnetic moment calculated for the paramagnetic specimens shows that Ni^{+3} is formed at the expence of oxygen in excess of the stoichiometric amount, the crystal lattice being preserved, as is evident from the X-ray analysis.

1. INTRODUCTION

The catalytic and adsorption properties of NiO have been studied thoroughly. The oxidation of CO to CO_2 on a NiO catalyst (pure and with additives) is investigated in the works [1-5]. The values of the activation energy of reaction presented in these publications are rather contradictory. While for pure nickel oxide Keier et al. [3], Kutseva [5] and Parravano [1] give low values of the activation energy (3-5 kcal/mole), Schwab and Block [2] present about 16 kcal/mole. Further, Keier [3] and Parravano [1] state that introduction of monovalent ions (Li^+, Ag^+) increases the activation energy, while trivalent ions decrease it. Schwab and Block [2] maintain the opposite: trivalent ions increase and monovalent ions decrease the activation energy.

The general conclusion from the studies on the magnetic properties of nickel oxide [6-13] has been that stoichiometric NiO is antiferromagnetic with an antiferromagnetic temperature of 377°C [7]. With increasing content of oxygen in excess of the stoichiometric amount, nickel oxide becomes ferromagnetic [8] or displays non-compensated antiferromagnetism [13]. The addition of Li ions, according to Perakis [8], leads to ferromagnetic properties. As to the character of the curve: susceptibility-composition of nickel oxide, there is contradiction only in the region of slight deviations from the stoichiometric compound. While according to Klemm and Haas [6], specific susceptibility in the above mentioned region increases sharply, the data of Shirokov [13] show a value which is almost constant.

Studies on other physical-chemical properties of nickel oxide have also been published. The conductivity of nickel oxide with respect to additives is studied in the works [14, 15]. The electronic properties of nickel oxide are investigated in [16-19].

With the purpose of explaining the mechanism of the reaction $CO + \frac{1}{2} O_2 \rightarrow CO_2$, some authors studied the adsorption of the initial products on NiO and that of the products of reaction [20-27]. Irrespective of the great number of studies, the mechanism of this reaction has not been established. Still more uncertain is the reason for the different values of activation energy obtained. While the authors of most of the magnetic studies take into consideration the excess of oxygen, others, especially authors investigating the catalytic properties of NiO (the work of Kutseva [5] excepted), only give the conditions of preparation, considering the nickel oxide obtained to be stoichiometric NiO. Assuming that the catalytic properties of NiO depend on its content of oxygen in excess of the stoichiometric amount, this explains in all cases the differencies between the results of the investigations, if the nickel oxide obtained contained various amounts of oxygen. Considering the data, published for the activation energy, it is evident that they are grouped about two values: some authors give a high value, about 14-18 kcal/mole, while others present a lower value of about 3-8 kcal/mole. According to the data obtained by Kutseva [5], with changing the content of excessive oxygen, the activation energy changes but little. However, small amounts of lithium or chromium added sharply change the activation energy, but with the increase of additives, the change of activation energy is insignificant.

For this reason, the present investigation had the purpose of studying the catalytic activity of nickel oxide together with its magnetic properties, taking into consideration the deviations from stoichiometry as well.

2. EXPERIMENTAL

Specimens of nickel oxide, containing various amounts of an excess of oxygen, were obtained by decomposing basic nickel carbonate in air, at a temperature, varied from 300° up to 1000°C, in the course of 3 to 24 hours. The ratio between nickel and oxygen in the specimens was determined complexometrically, as well as gravimetrically, through the content of nickel in each specimen. Magnetic susceptibility was measured in an apparatus for magnetic investigations by Gouy's method, in the temperature interval from 0°C to 100°C, with an accuracy of 1%. Catalytic activity was studied in a static apparatus, in the temperature interval from 60° to 100°C and pressures from 8×10^{-1} to 4×10^{-1} mmHg. A stoichiometric mixture of CO and O_2 was used for the experiments and CO_2 produced was gathered in a trap of liquid nitrogen. Before each experiment, the specimen was heated out for an hour at 100°C, under a pressure of 10^{-4} mm Hg. A higher temperature of heating out led to a decrease of the excess of oxygen. The activation energy and the pre-exponential coefficient were calculated after finding the dependence $\lg \tau_{\frac{1}{2}} - 1/T$ (Here $\tau_{\frac{1}{2}}$ is the half period and T, the absolute temperature).

The specific surfaces of the specimens were determined by means of low-temperature-adsorption of nitrogen by the BET method.

3. RESULTS

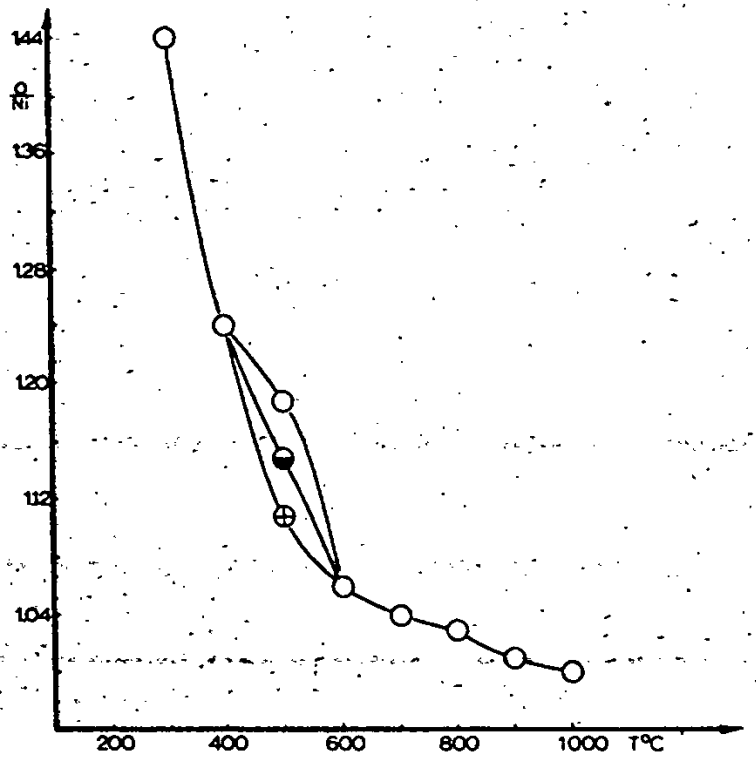

Fig. 1. Atomic ratio (O/Ni) between oxygen and nickel in dependence with the temperature of preparation of the specimens. Period of heating for the specimen, obtained at 500°; -O- 3 hours; -⊖- 24 hours; -⊕- 80 hours.

Fig. 1 gives the dependence between the content of oxygen in excess of the stoichiometric amount and the temperature of decomposition of the specimens. It is evident, that the excess of oxygen decreases with the increase of temperature; at 1000°C stoichiometric nickel oxide was obtained. The specimen decomposed at 500°C displays a different character. While with the rest of the specimens, the period of heating has practically no effect upon the ratio between nickel and oxygen, in the above mentioned specimen the content of oxygen decreases with longer heating. Furthermore, the sample decomposed at 500°C containing oxygen in excess amounting to O/Ni = 1.19 is paramagnetic, while the remaining two samples decomposed at the above temperature are antiferromagnetic.

Fig. 2 shows the specific susceptibilities of the specimens as functions of the content of oxygen in excess of the stoichiometric amount. The specific susceptibility decreases with the decreasing content of excessive oxygen. In the interval O/Ni = 1.15 to 1.12, the functions change their sign. While above 1.15 susceptibility decreases with temperature, i.e. the specimens

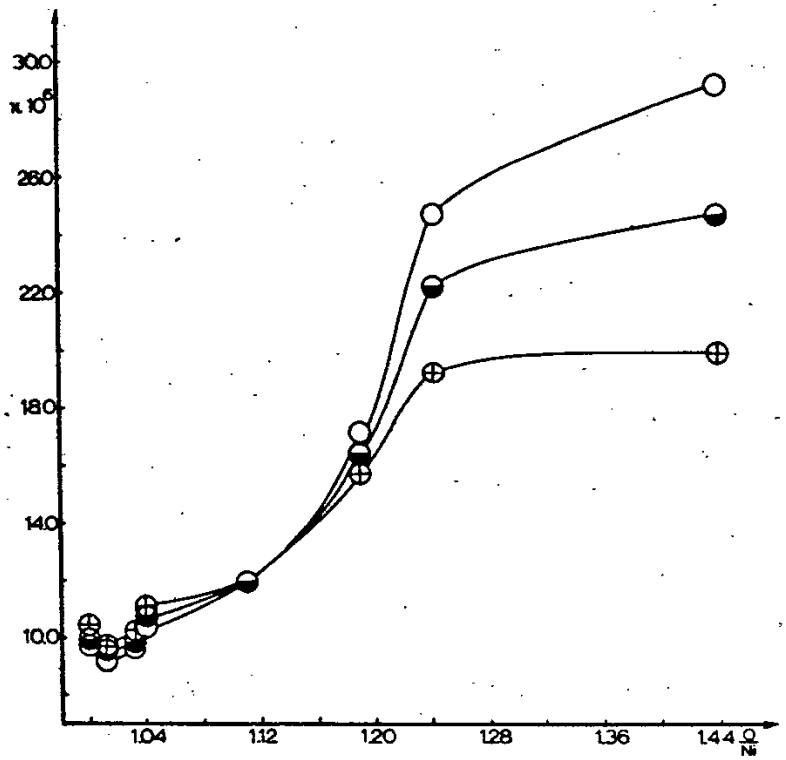

Fig. 2. Specific susceptibility (κ) of the specimens in dependence with the atomic ratio (O/Ni) and the temperature of measuring the susceptibility. -O- 25°C; -⊖- 50°C; -⊕- 80°C .

are paramagnetic with traces of ferromagnetism (their susceptibility is only slightly influenced by the magnetic field), below 1.12 susceptibility increases with the increasing temperature, i. e. the specimens are antiferromagnetic. In the interval between 1.12 and 1.15 susceptibility increases slightly with temperature.

For the paramagnetic specimens were calculated the effective magnetic moments and Weiss' constants, from the dependence $1/\kappa - T$, shown in fig. 3. It is evident that the effective magnetic moment is lower for the specimens with higher content of oxygen. The latter being in agreement with the assumption of Ray [28] that Ni with valency higher than 2 has a low magnetic moment. For the specimen $NiO_{1.19}$, the magnetic moment corresponds to the theoretically calculated, under the condition that the orbital component is frozen.

The change of sign of Weiss' constant is also very characteristic. The results from the determination of the activation energy of reaction in dependence with the composition of nickel oxide are shown in fig. 4. While for the paramagnetic specimens, with O/Ni above 1.15, the activation energy is of the order 13-17 kcal/mole, transition into the antiferromagnetic state leads to a sharp decrease of activation energy, down to 4-9 kcal/mole. The dependence between the activation energy and the temperature of decomposition of the specimens is analogous to the dependence between the activation energy and the composition of the nickel oxide. In the specimens

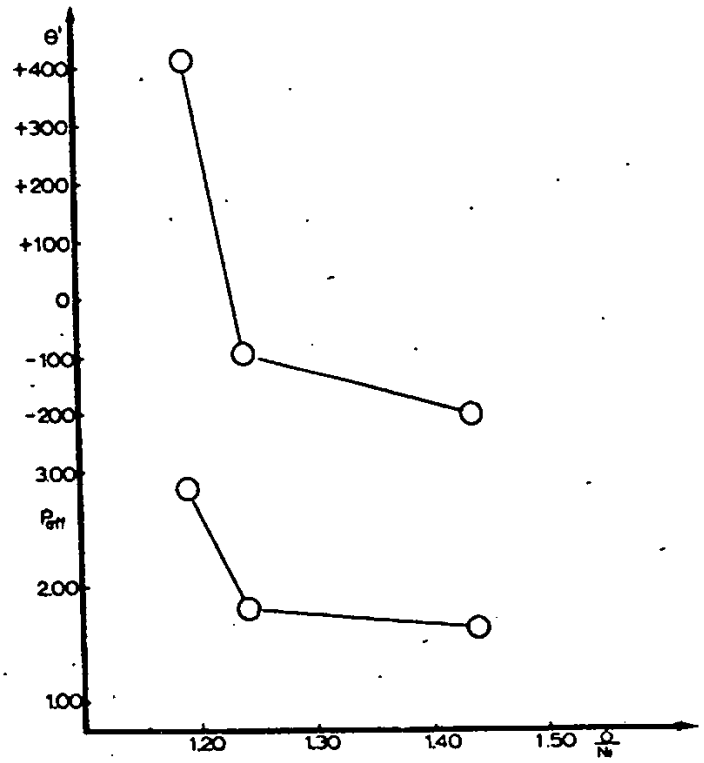

Fig. 3. Dependence between the effective magnetic moment (P_{eff}) in Bohr magnetons, Weiss' constant and the atomic ratio (O/Ni) of oxygen to nickel.

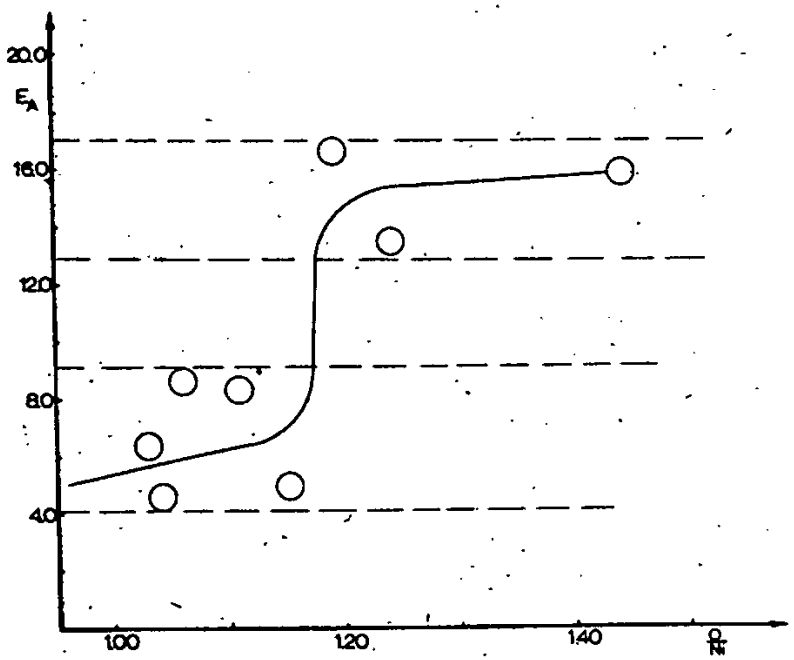

Fig. 4. Dependence between the activation energy of the reaction $CO + \frac{1}{2}O_2 \rightarrow CO_2$, ($E_A$) in kcal/mole and the atomic ratio (O/Ni) of oxygen to nickel.

decomposed at 500°C, a change in the ratio O/Ni by only 0.04, with almost equal specific surfaces, leads to a change of activation energy amounting to about 10 kcal/mole. The results obtained for the pre-exponential coefficient are analogous. Transition from one magnetic state into another calls forth an analogous sharp change here of the pre-exponential coefficient.

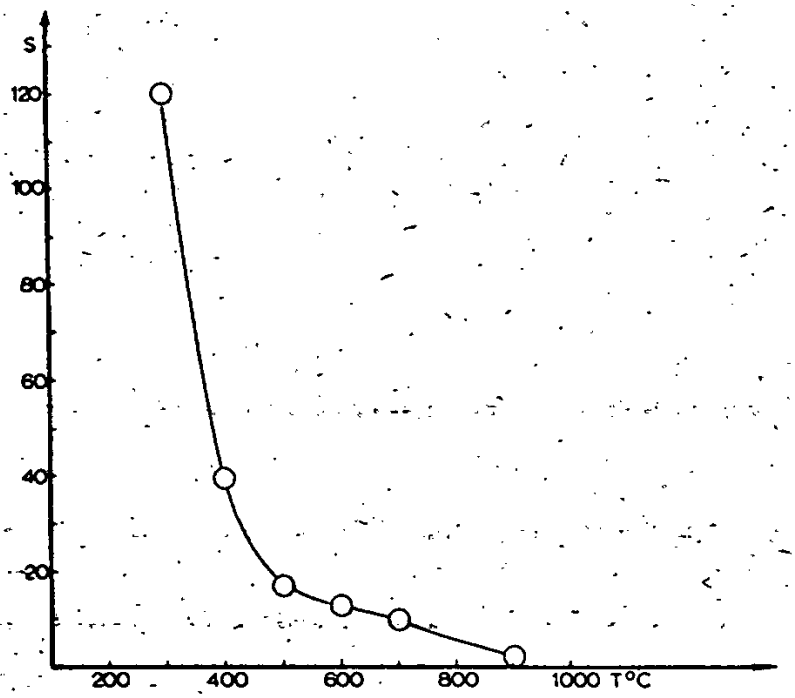

Fig. 5. Dependence of the specific surface (S) of the specimens in m^2/g and the temperature of preparation.

Fig. 5 shows the specific surfaces as a function of the temperature of decomposition. The change of specific surface at lower temperature is rather great (almost twice the initial value) for the specimens decomposed at 300° and at 400°C. X-ray analysis was carried out, in order to study the crystal lattice of the specimens. The following results were obtained for the parameter of the lattice in dependence of the temperature of decomposition of the specimens. For the specimen decomposed at 300°C the parameter obtained was 4.211 Å, for the specimen at 400°C - 4.180 Å, 500°C - 4.186 Å, 600°C - 4.171 Å, 700°C - 4.169 Å and 1000°C - 4.184 Å. There is a tendency toward a slight deformation of the lattice. The lines of nickel oxide are preserved in all the specimens. The lines in the specimen decomposed at 300°C are not very distinct, but they are still there, i.e. the acceptance of oxygen and likely the formation of Ni_2O_3 takes place without the lattice of NiO being distorted. These results coincide with the data of Shimomura [8].

4. DISCUSSION

It is evident from the above results that in the oxidation of CO to CO_2 and probably in other reactions also, the magnetic state of the catalyst is an important factor, determining its catalytic activity. When nickel oxide is antiferromagnetic, the activation energy is low (4-9 kcal/mole); the reaction takes place with a high rate. When nickel oxide is paramagnetic, the activation energy is of the order 13-17 kcal/mole. The fact that with the monotonous change of the content of oxygen in excess of the stoichiometric amount, the catalytic parameters (activation energy, rate constant, etc.) are sharply changed and this sharp change coincides with the transition from paramagnetism to antiferromagnetism, shows that the excess of oxygen affects mainly through changing the magnetic state of the catalyst and less by changing the number of active centres or the crystal structure. It is evident, this is a case of magneto-catalytical effect, which could also be observed at a constant temperature, if a possibility exists for a definite way of changing the magnetic state of the substance. The increase of the excess of oxygen disturbs the strong interaction in the antiferromagnetic specimens and they become paramagnetic with traces of ferromagnetism, due to the incomplete suppression of the strong interaction. Transition from the antiferromagnetic to the paramagnetic state can also take place with raise of temperature. Therefore, in discussing the results, the history of nickel oxide must also be taken into consideration, i.e. its composition and the temperature of determining its catalytic activity. These conclusions are confirmed by data of other authors and explain the contradictions in their results. For example, Kutseva [5] has worked with specimens, showing O/Ni up to 1.12 and temperatures up to 200°C (the data are calculated from the graphs in the publication). Hence, the specimens are antiferromagnetic and it should follow that the activation energy would be lower. The experimental data show values from 3 to 5 kcal/mole.

For the specimen of pure nickel oxide Parravano [1] gives two values for two different temperature intervals. This can be explained, taking into consideration that, according to the method of preparation, the specimens should be antiferromagnetic and the activation energy lower. For the temperature interval 100-180°C, it actually is about 3 kcal/mole. The increase of activation energy in the second temperature interval is due to reaching the antiferromagnetic temperature and the transition into the paramagnetic state. A lowered antiferromagnetic point could be expected here, because it depends upon the dimensions of the particles as well [10]. Schwab's specimens are also antiferromagnetic, but because the catalytic measurements were made at a higher temperature, the activation energy ought also to be higher, as is actually observed.

As to the specimens with various additives, the foretelling on the activity of the catalyst could be made, if the ratio between Ni, O and the element added, as well as the magnetic state of the catalyst, are known. We are of the opinion that when the specimen is antiferromagnetic and the catalytic reaction takes place below the antiferromagnetic temperature, every kind of additive should lead to an increase of the activation energy, if it disturbs

the strong interaction. With the paramagnetic state the problem is more complicated and depends on whether this state has been reached through an additive or is due to a content of oxygen in excess of the stoichiometric amount, or after increasing the temperature. The data for the magnetic moments calculated show that Ni^{+3} is obtained at the expence of the excess of oxygen. The crystal structure however is preserved almost to the full transformation of NiO into Ni_2O_3 (the specimen with O/Ni = 1.44). Here, a deformation of the lattice is observed and the lines of the specimen decomposed at 300°C are already slightly diffused. Hence, in this case the existence of two phases can no more be assumed.

The authors wish to express their thanks to Mrs. K. Hristova for the complexometric and gravimetric analyses and to Mr. I. Tsolovski for the X-ray studies.

REFERENCES

1) G. Parravano, J. Am. Chem. Soc. 72 (1953) 1452.
2) G. M. Schwab and J. Block, Z. Elektrochem. 58 (1954) 756.
3) N. P. Keier, S. Z. Roginsky and N. Sazonova, Doklady Akad. Nauk SSSR 106 (1956) 859.
4) A. Bielanski, Z. Phys. Chem. (DDR) 24 (1960) 345.
5) L. N. Kutseva, Doklady Akad. Nauk SSSR 138 (1961) 409.
6) W. Klemm and K. Haas, Z. anorg. allgem. Chem. 219 (1934) 81.
7) M. Föex and C. H. La Blanchetais, Compt. rend. 228 (1949) 1579.
8) Y. Shimomura, I. Tsubokawa and M. Kojima, J. Phys. Soc. Japan 9 (1954) 521.
9) N. Perakis, A. Serres and G. Parravano, Compt. rend. 242 (1956) 1275.
10) J. T. Richardson and W. O. Milligan, J. Phys. Chem. 60 (1956) 1223.
11) W. L. Roth, Phys. Rev. 110 (1958) 1333.
12) T. I. Barry, Atomic Energy Research Establ. (Great Britain) R-3493 (1960) 1.
13) Yu. G. Shirokov and I. P. Kirilov, Izvest. Ucheb. Vysshikh Zavedenii, Khim. i Khim. Tekhnol. 4 (1961) 599.
14) A. Bielanscki, Y. Deren and D. Haber, Trans. Faraday Soc. No. 1 (1962).
15) G. M. Schwab, J. Appl. Phys. 33 (1962) 426.
16) G. H. Wanmer, Element of solid state (Cambridge, 1959) p. 169.
17) S. Van Houten, Phys. Chem. Soc. 17 (1960) 7.
18) K. Hauffe, Z. Elektrochem. 56 (1952) 366; 57 (1953) 762.
19) K. Hauffe, Semiconductor surface physics.
20) N. P. Keier, Problemy Kinetiki i Kataliza, Akad. Nauk SSSR No. 10 (1960) 73.
21) K. Hauffe, Z. Elektrochem. 65 (1961) 321.
22) Y. Kubokawa, Bull. Univ. Osaka Perfect. A9 (1961) 45.
23) M. Courtois, Chim. mod. 6 (1961) 195.
24) K. Klier, Kinetika i Kataliz 3 (1962) 65.
25) S. J. Teichner, K. P. Marcellini and P. Rué, Adv. Catalysis 9 (1962) 458.
26) I. Matsuure, Technol. Repts. Kansai Univ. No. 3 (1961) 63.
27) K. Kuchynka and K. Klier, Collection Czech. Chem. Commun. 28 (1963) 148.
28) P. Ray, A. Bhaduri and B. Sarme, J. Indian Chem. Soc. 25 (1948) 51.

INTERACTION BETWEEN ADSORBED MOLECULES AND THE MECHANISM OF THE ELEMENTARY ACTS IN THE DEHYDRATION OF ALCOHOLS ON OXIDE CATALYSTS

V. E. VASSERBERG

The N.D. Zelinsky Institute of Organic Chemistry, Academy of Sciences, Moscow, USSR

Abstract: The presence of foreign substances greatly affects the kinetics of alcohol dehydration in the adsorption layer over Al_2O_3, leading either to retardation or acceleration (conjugated dehydration) of the reaction. The mutual effect on the adsorbed molecules can also be observed at ordinary pressures, but at low temperature, in the "pre-catalytic" region. In particular it is manifested in the newly discovered reaction of what may be called isotope-radical exchange, wherein a radioactive label is transferred under conditions of catalytic dehydration. The degree of transfer depends upon the nature of the catalyst. The character of the catalytic heterogeneity of the surface and the number of active centres have been determined for a number of Al_2O_3 catalysts. Active intermediate complexes have been shown to be formed in the adsorption layer during the dehydration reaction. These possess many properties characteristic of free radicals, catalyzing for instance the para-ortho hydrogen reaction, polymerization of olefins, etc. The existence of two dehydration mechanisms has been suggested: (a) a high temperature mechanism whereby olefins are formed directly from primary complexes and (b) a low temperature "collective" or polymolecular mechanism associated with the formation and decomposition of secondary complexes resulting from interaction of the adsorbed molecules.

1. INTRODUCTION

It is generally accepted that all heterogeneous catalytic reactions take place in the adsorption layer formed by the reactant molecules on the catalyst surface. Hence in order to judge the true mechanism of the reaction and the nature of its elementary acts one can not merely confine oneself to a study of the reaction kinetics by determining the changes taking place in the compositon of the liquid or gaseous phases, but the behavior of the adsorbed molecules themselves must be accounted for. For this one can utilize IR spectroscopy (as is now being done, following the pioneer work of Terenin[1] and Eishens[2]) or direct kinetic determinations of reactions in the adsorption layer. Despite its unquestionable merits the latter method has not been used to a great extent. Among the few works in this direction mention should be made of the classical studies by Dohse et al.[3] carried out as far back as in 1929-1933 and also some later ones[4-9]. In recent years this method has been systematically employed in A. A. Balandin's laboratory for studying the dehydration of lower aliphatic alcohols and ethers on a number of Al_2O_3 catalysts of different origins.

2. EXPERIMENTAL

2.1. *Mutual effect of the adsorbed molecules and the inhomogeneity of alumina*

Our method, a modification of Dohse's technique, is as follows: A sample of the catalyst (from 0.1 to 7.0 g) is put on the pan of a springlever balance [10] placed in the circulating system of a vacuum set-up and degassed at 450° until a pressure of 10^{-5} mm Hg has been reached. Then at the temperature of the run (from 40° for tert. C_4H_9OH until 220° for C_2H_5OH) a certain amount of reactant vapor (measured both manometrically and directly from the gain in weight of the catalyst due to adsorption) is introduced into the system. After that the rate of reaction in the adsorption layer is followed by the increase in the pressure of the olefin formed, water remaining firmly bound to the catalyst.

In this way many pecularities of the reaction playing an essential part in its mechanism could be revealed, and those which are frequently hidden when carrying out the reaction under ordinary conditions, i.e. in a flow system at atmospheric pressure. For instance, it was found that alcohols are dehydrated in the adsorption layer at measurable rates (the half decompositon period $\tau_{0.5}$ = 2 - 30 min) already at quite moderate temperatures (100-140° for iso-C_3H_7OH) i.e. when this reaction is not noticeable under ordinary conditions. Furthermore catalysts most active in the monolayer reaction may not prove to be optimal under atmospheric pressure [11]. Also there is no regular relation between the corresponding activation energies.

Interesting data have been obtained in the adsorption layer study of the concurrent dehydration of isopropanol and ethanol. The reaction turned out to be always hindered for iso-C_3H_7OH, but accelerated in a number of cases for ethanol. This phenomenon of conjugated catalytic dehydration has been explained by the interaction between the active intermediate complexes formed by the respective alcohols in the catalyst surface under the reaction conditons [12]. Later, together with Balandin and Silskova we decided to see whether such a conjugated process occurs under ordinary conditions, carrying out the reaction at low temperatures, i.e. in the "pre-catalytic" region. Dehydration of C_2H_5OH, iso-C_3H_7OH and their binary mixtures was studied in a recycling system [13] at 150-250° and 1 atm pressure, the gas being analyzed by partition chromatography in a stream of CO_2. It was found that at 150° the reaction does not take place at all; at 200-225° the over-all amount of ethylene formed from an equimolar mixture of the alcohols was by 2.3-4.9 times larger than that obtained from pure C_2H_5OH. At 250° the amount of C_2H_4 was less than from pure ethanol. The amount of C_2H_4 was just what should have been expected from the trivial assumption that dehydration of both alcohols takes place independently, the relative yield of the reaction products being determined only by their competition for the active centers. The amount of ethylene formed is still less for equimolar mixtures of C_2H_5OH with CH_3OH or H_2O.

In previous studies [14, 15] examples were presented of the mutual effect of adsorbed molecules on the rate and direction of reaction for a large number of binary systems. It was found that even small amounts of, say,

acetone, dioxane, acetonitrile and ethyl acetate can almost completely inhibit the dehydration of 5-7 times the amount of iso-C_3H_7OH in the adsorption layer. Further in a number of cases, when the degree of coverage was very low, polymerisation of the olefins was observed, indicating that surface diffusion of the adsorbed molecules takes place.

In the co-operation with Balandin and Georgievskaya the character of the inhomogeneity of the surface of a number of alumina catalysts and the shape of the active center distribution curve were determined. In this study, instead of the usual integral method of Dohse (determination of the over-all rate of decomposition of the adsorbed alcohols as a function of the degree of surface coverage σ a new, differential method was employed. This was aimed at determining the dehydration kinetics of a small amount of a given alcohol adsorbed on various regions of the surface. This is achieved by preliminarily blocking a part of the surface by various amounts of a preadsorbed inert substance (water) (fig.1.).

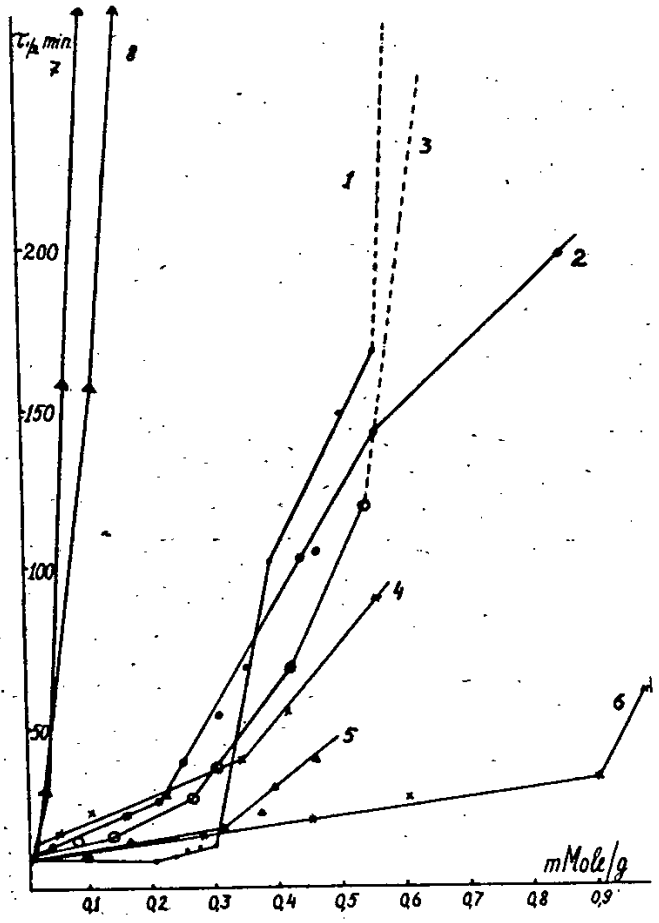

Fig. 1. The half decomposition period of the adsorption layer dehydration iso-C_3H_7OH on various alumina catalysts as function of amount of preadsorbed blocking substance (curves 1-6: water, curves 7-8: dioxane).
1 and 7 - Catalyst no. 1, 140°; 2 - Catalyst no. 2, 110°; 3 - Catalyst no. 3, 120°; 4 - Catalyst no. 4, 120°; 5 - Catalyst no. 5, 120°; 6 and 8 - Catalyst no. 6, 130°.

On the basis of the "effective specific adsorption area" ω of the given catalyst [16] and the value of ω ordinarilly accepted in the literature for water $\omega = 10.2$ Å^2); the number of active sites ω and the fraction of the active surface S_{act} in the various catalysts could be determined from the position of the point of inflexion of the curves on fig.1. The following alumina catalysts were employed: (1) commercial grade A-1; (2) precipitated from sodium aluminate solution by CO_2 at 0°; (3) prepared by the hydrolysis of aluminium isopropilate; (4) precipitated from aluminium nitrate solution by aqueous ammonia at 100°; (5) ditto, but with $Zn(NO_3)_2$ added to the solution to obtain 0.5% (molar) ZnO referred catalyst; (6) ditto, with 10% ZnO.

It can be seen that Z lies between 8×10^{19}/g and 1.7×10^{20}/g (which corresponds to $3.6 - 5.8 \times 10^{17}$/m^2 of the catalyst surface) and S_{act} from 12% to 30% of the overall surface. Further experimental investigations of this question led to quite unexpected results. Thus it was found that dehydration of iso-C_3H_7OH practically stops altogether if dioxane molecules are present in $\frac{1}{5}$th to $\frac{1}{10}$th the amounts necessary to cover all the active centers (we had determined for the given specimen). Furthermore for the same temperature $\tau_{0.5}$ can drop to $\frac{1}{5}$th - $\frac{1}{10}$th the former value if the reaction is carried out at very greatly diminished surface coverage (0.004 - 0.02 mmole/g instead of usually employed values of 0.06 - 0.1 mmole/g). In this case the break in $\sigma - \tau_{0.5}$ curve (similar to that determined by Dohse), sets in already at 0.06 mmole/g. This is about $\frac{1}{3}$rd the value we had obtained for the same catalyst by the differential method, but on the other hand it is in very good agreement with that obtained by Dohse for bauxite ($2 - 3 \times 10^{19}$/g). It thus follows that the lifetime of the intermediate complex and hence the reaction rate depends not only upon the activity of the center and the nature of the adsorbate, but also upon the presence or absence of other molecules in its immediate vicinity. In other words the rate of dehydration of "isolated" molecules is higher than that of the molecules with neighbors.

Similar acceleration of the reaction was observed for iso-C_3H_7OH in the "pre-catalytic" region when working in a recycling system under dilution with argon, nitrogen or CO_2.

The low temperature decomposition of ethanol (at 120-140°) may serve as an example of the inverse mutual interaction of adsorbed molecules we observed on some alumina catalysts. The reaction in this case assumes a noticeable rate only after a certain threshold value of the surface concentration of alcohol (fig.2.).

2.2. *Radical-like intermediate complexes in dehydration catalysis*

The formal similarity of many of the above-mentioned phenomena with free radical reactions led to the assumption that under the conditions prevailing in our experiments the reactants form radical-like intermediates on the surface of the catalyst. Such types of intermediates in heterogeneous catalysis have been postulated by numerous workers (Zelinsky and Shchuikin [17], Eidus [18], Temkin [19], Semenov, Voevodsky and Vol'kenstein [20], Myasnikov [21], Kemball [22] et al. [23]. Direct experimental evidence of their existence has been provided in the works of the author together with Balandin

and Davydova [24] and Davydova and Georgievskaya [25], when it was shown that the active intermediates formed in the $MgSO_4$ and Al_2O_3 catalysed dehydration of alcohols and ethers possess such characteristic properties of free radicals as the ability to induce the para-ortho hydrogen conversion.

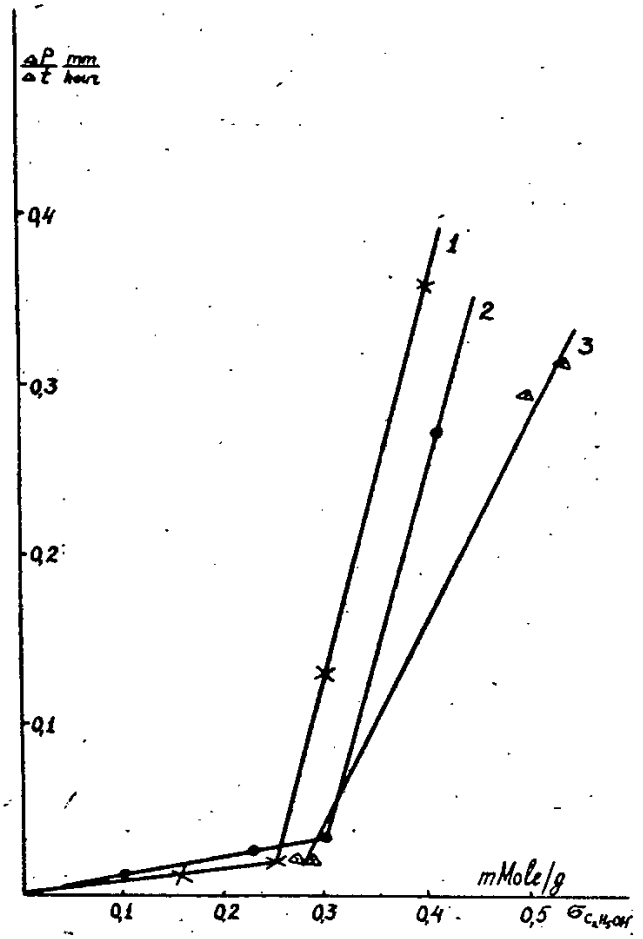

Fig. 2. The threshold value of the surface concentration of alcohol in the low-temperature adsorption layer dehydration of C_2H_5OH. 1 - Catalyst no. 1, 140°; 2 - Catalyst no. 2, 140°; 3 - Catalyst no. 3, 120°.

Later together with Georgievskaya it was shown that the adsorbed layer dehydration of iso-C_4H_9OH on some alumina catalysts was accompanied by initiated polymerization, also a characteristic property of free radicals. If propylene or isobutylene is preliminarily added to the system (at pressures of 0.05 - 0.1 mm Hg) dehydration is accompanied not by a monotonous increase in pressure resulting from more of the isobutylene being formed from the alcohol, but the pressure falls instead below the initial value and begins to rise after. The polymerization process associated with the pressure drop is not observed before dehydration sets in and rapidly ceases on its completion (fig.3.).

2.3. *Catalytic radical-isotope exchange and interaction between adsorbed molecules*

Interaction between adsorbed molecules in the pre-catalytic region was demonstrated by Balandin, Levy and the author [26, 27] with the aid of a radiochemical method.

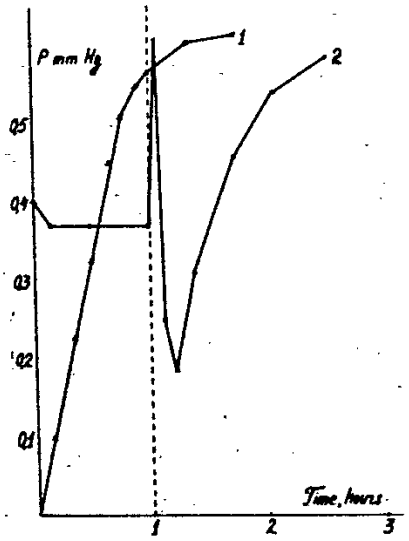

Fig. 3. Initiated polymerization of isobutylene by concurrent adsorption layer dehydration of iso-C_4H_9OH on Al_2O_3 + 10% ZnO catalyst at 120°. 1 - Pure iso-C_4H_9OH; 2 - Isobutylene + iso-C_4H_9OH. Vertical line - addition of the isobutanol.

We concluded that such interaction if it takes place could lead to an exchange of particles or groups between the reacting molecules and hence, with tracer atoms to a change in the isotopic composition. For this purpose $C^{14}H_3OCH_3$ ($C^{14}H_3OH$ in some runs) was chosen as the label donor because of its stability under the experimental conditions, since, while forming the same intermediate surface complexes as the other alcohols, it cannot undergo dehydration. As second components of the mixture, with the dimethyl ether to be passed over the alumina catalyst , were other alcohols, ethers, ketones, olefins, etc. In many cases this gave rise to a new type of reaction, radical-catalytic exchange of the label between the methyl ether and other compounds. Later we showed that the degree of exchange depends upon the nature of the catalyst. Thus on passing a mixture of oct-1-ene and $C^{14}H_3OH$ in a ratio 5:1 at 225° under various catalysts, namely Al_2O_3 treated with potassium hydroxide, $Al_2O_3 + Fe_2O_3$, untreated Al_2O_3, alumosilicate cracking catalyst and $Ca_3(PO_4)_2$, the specific radioactivity of octene in the catalysate was 0, 50, 60, 190, 170 and 25 imp/min-mg $BacO_3$, respectively.

3. DISCUSSION OF RESULTS

The data on the surface heterogeneity of the alumina catalyst led to the following conclusions.

1) It is not at all a generale rule that all active centers should be identical as found by Dohse. One can see from fig.2 that the initial part of the

curve is parallel to abscissa axis only for one catalyst.

2) The large differences in activity of the catalysts (the $\tau_{0.5}$ value at 120° for isopropanol on various specimens varied between 6 and 27 min) under our experimental conditions when the entire alcohol was adsorbed and there was no competition for the active centers, could be explained only by differences in the activity of the unitary centers, rather than their number. Under ordinary condtions, the catalytic activity is probably the total result of the average activity of the working active centers, their number and also their mobility, i. e. the ease with which they are regenerated after completion of a unit reaction act.

3) The Al_2O_3 surface contains sites that are devoid of catalytic activity. Thus it can be seen on the curve that after the surface concentration of H_2O reached about 3-4 μmole/m^2 the reaction stops almost completely, although the coverage is far from that corresponding to a complete monolayer and the surface still contains some adsorbed alcohol. The conclusion regarding the presence of inactive sites could be made only on the basis of the differential and not the integral approach.

We shall now attempt to treat the available material from a single viewpoint, assuming that the adsorbed reactants form labile, radical-like intermediate complexes on the active sites of the catalyst surface. At the limit such complexes may be regarded as free radicals, stabilized by the surface*. Our studies have demonstrated their existence at the relatively low temperatures of 150-250°, but it is only natural to assume that they can occur at all temperatures of the dehydration reaction. However, the direction of their further transformation depends upon the reaction conditions. They must have a short lifetime at relatively high temperatures of the order of 350-450°, the main direction of reaction possibly being immediate breakdown to the ultimate olefin. These strongly adsorbed radical-like forms have a longer lifetime at 100 - 200°, under conditions of reaction in the adsorption layer or in the "pre-catalytic" region and by their residual valencies can bind other molecules either of the same or other species migrating on the surface. New intermediate forms then arise possessing a different (frequently higher) stability, and manifest themselves by changing the rate and even the direction of the reaction. As for the rate of decomposition of the foreign molecules bound to the initially formed complex, this may even increase (example of conjugated dehydration).

The proposed mechanism in the case of conjugated dehydration and transfer of the radioactive label can be represented schematically as follows:

* The existence of such surface stabilized radicals has been repeatedly discussed in the literature in recent years.

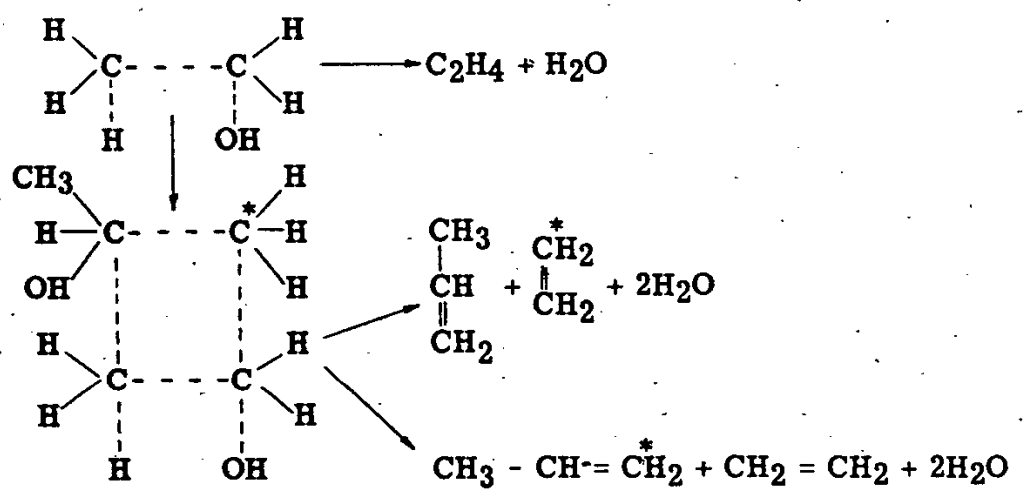

If the conditions induce considerable interaction between the reacting molecules, an appreciable proportion of the end products can originate not from the primary "singlet" active complexes, but from the secondary complexes resulting from the additon reaction. The " collective", polymolecular decomposition mechanism will then begin to play a considerable or even predominant part in the reaction. The differences in the adsorption layer and ordinary dehydration kinetics can be explained by the possibility of such dual reaction. The high temperature under the ordinary conditions is detrimental to the formation of interaction products so that they cannot be detected in the catalysate.

The collective reaction mechanism is in harmony with the basic principle of the multiplet theory of catalysis according to which the active intermediate complex is a molecule with partially ruptured bonds. The bonding electrons of the atoms comprising the "multiplet reaction index" are partially delocalized due to interaction with the atoms of the catalyst. There is therefore no difference between such a formation and a free surface-stabilized radical, since in this case delocalization of the unpaired electron of the radical also takes place. Hence such a complex should possess enhanced reactivity and form bonds with its neighbors.

Because of this reactivity, the failure of attempts to detect such radicals by EPR when the reactions were carried out under usual conditions becomes understandable. In that case the secondary polymolecular complexes are formed causing considerable loss of the radical-like properties. Thus when carrying out the dehydration of alcolhols under the usual conditions we also could not observe the para-ortho hydrogen convertion, in contrast to the monolayer reaction.

If it is assumed that the concept of the radical-like character of the primary intermediate complexes here developed is of a general nature, then in the light of this theory a number of other observed phenomena will become understandable. This for instance is the case for the effect of the space velocity and inert gases on the rate and selectivity of a number of catalytic reactions, in particular etherification. It also sheds new light on numerous

data concerning the effect of the solvent species and of various poisons which as a rule had been explained by selective adsorption of foreign molecules on the active sites. Attempting to account for the specificity and highly varied nature of the action of these foreign substances one had then to postulate a large assortment of active sites responsible for the respective reactions and selectively sorbing the poisons. We however, believe ti more likely that these substances form with the adsorbed reacting molecules various secondary complexes, differing in stability and in the direction of further reaction.

The available experimental data does not allow one to judge as yet the structure of the polymolecular intermediate complexes or the number of constituent molecules. Neither are we able to tell their mutual arrangement whether on a single plane or in different layers (sandwich structure), etc. However the concept of their existence is in conformity with all the data obtained in the present work and can therefore be considered to be sufficiently based on fact to merit further attention.

Table 1
Inhomogeneity of the active surface of alumina catalysts of different origins

No. of the catalyst	Sp. surface by N_2 m^2/g)	Capacity of monolayer mmole/g		Surface coverage at the point of breaks in the curves fig. 1, in mmole/g		Amount of dioxane*** at complete inhibition, mmole/g	Number of active centers, Z		S_{act} (%)	Catalytic activity in the adsorbed layer	
		for H_2O	for iso-propanol	for* H_2O	total**		$10^{18}/m^2$	$10^{19}/g$		E (kcal/mole)	Half period of decompos $\tau_{0.5}$ (min) at 120°
1	130	2.1	0.66	0.30	0.14	0.06	0.70	9.0	23	17	27
2	222	3.6	1.14	0.20	0.13	0.06	0.36	8.0	13	25	6
3	210	3.4	1.12	0.26	0.16	0.07	0.53	11.0	12	24.5	8
4	236	3.8	1.10	0.32	0.18	0.06	0.51	12.0	14	20.5	13
5	247	4.0	0.91	0.30	0.13	0.04	0.33	8.0	14	19.0	10
6	290	4.6	0.93	0.90	0.28	0.07	0.59	17.0	30	21.0	24

* Experimentally determined.

** The total effective coverage is expressed in mmole of isopropanol for 1 g of the catalyst, taking into account the differences in values of the elementary adsorption areas, i.e. that one molecule of iso-C_3H_7OH is equivalent approximately to 3 molecules of H_2O.

*** For dioxane the value of ω on Al_2O_3 is equal roughly to ω for iso-C_3H_7OH, as it was demonstrated in the paper [28].

REFERENCES

1) A.N.Terenin, in: Poverhnostnye khimicheskije soiedinenia i ih rol v iavlenash adsorbzii (Surface chemical compounds and their part in the adsorption phenomena), (Moscow, 1957) p.206.
2) R.P.Eishens, W.A.Pliskin, Adv. Catalysis 9 (19) p. 662.
3) H.Dohse and coll. Z.phys. Chem. B5, (1929) 131; B6 (1929) 343; B14 (1931) 349; B23 (1933) 33; Z. Elektrochem. 36 (1938) 677.

4) A.A. Balandin, V.E. Vasserberg, Acta Physicochimica URSS 81 (1946) 678.
5) E. Wicke, Z. Elektrochem. 83 (1949) 279.
6) V.I. Levin, in: Problemy kinetiki i kataliza (Problems in kinetics and catalysis) (Moscow, 1949) Vol. 7, p. 205.
7) N.P. Keyer, in: Problemy kinetiki i kataliza (Problems in kinetics and catalysis) (Moscow, 1965) Vol. 8, p. 224.
8) E.A. Andreev, in: Problemy kinetiki i kataliza (Problems in kinetics and catalysis) (Moscow, 1949) Vol. 6, p. 293.
9) D.P. Dobychin, in: Poverhnostnye khimicheskije soiedinenia..., (Moscow, 1957) p. 341.
10) V.E. Vasserberg, Kinetika i Kataliz 3 (1962) 556.
11) V.E. Vasserberg and A.A. Balandin, Problemy kinetiki i kataliza 10 (1960) 356.
12) V.E. Vasserberg, A.A. Balandin and T.V. Georgievskaya, Dokl. Akad. Nauk SSSR 134 (1960) 371.
13) G.I. Levy and V.E. Vasserberg, Kinetika i Kataliz 3 (1962) 527.
14) V.E. Vasserberg, A.A. Balandin and T.V. Georgievskaya, Dokl. Akad. Nauk SSSR 140 (1961) 859.
15) V.E. Vasserberg, A.A. Balandin and T.V. Georgievskaya, Dokl. Akad. Nauk SSSR 140 (1961) 1110.
16) V.E. Vasserberg, A.A. Balandin and M.P. Maksimova, Izvest. Akad. Nauk SSSR, Otdel. Khim. Nauk (1959) 363; Zhur. Fiz. Khim. 36 (1961) 858.
17) N.D. Zelinsky and N.I. Shuikin, Dokl. Akad. Nauk SSSR 3 (1934) 225.
18) Ya.T. Eidus and N.D. Zelinsky, Izvest. Akad. Nauk SSSR, Otdel. Khim. Nauk (1940) 289;
Ya.T. Eidus and N.V. Ershov, Izvest. Akad. Nauk SSSR, Otdel. Khim. Nauk (1959) 1655.
19) M.I. Temkinand L.O. Apelbaum, in: Problemy fizicheskoi Khimii (Problems in Physical Chemistry) (Moscow, 1958) p. 1, 94.
20) V.V. Voevodsky, N.N. Semenov and F.F. Vol'kenstein, in: Voprosy khimitcheskoi kinetiki, kataliza i reakzionnoi sposobnosti (Problems in chemical kinetics, catalysis and reactivity (Moscow, 1955) p. 423.
21) M.Y. Myasnikov, Zhur. Fiz. Khim. 34 (1960) 385.
22) C. Kemball, Bull. Soc. Chim. Belg. 63 (1958) 373.
23) E.G., papers in the books Problemy kinetiki i kataliza 10 (Moscow, 1960) Vol. 10, p. 369–428 and Voprosy khimitcheskoi kinetiki..., (Moscow, 1955) pp. 423–632.
24) V.E. Vasserberg and I.R. Davydova, Kinetika i Kataliz 2 (1961) 773.
25) V.E. Vasserberg, A.A. Balandin and I.R. Davydova, Dokl. Akad. Nauk SSSR 136 (1961) 376.
26) V.E. Vasserberg, A.A. Balandin and G.I. Levy, Kinetika i Kataliz 2 (1961) 61.
27) G.I. Levy and V.E. Vasserberg, Kinetika i Kataliz 2 (1961) 758.
28) V.E. Vasserberg, A.A. Balandin and M.P. Maksimova, Izvest. Akad. Nauk SSSR, Otdel. Khim. Nauk (1962) 1865.

MOLECULAR MECHANISM OF SOME CATALYTICAL REACTIONS AS REVEALED BY MEANS OF ISOTOPIC KINETICAL EFFECTS AND EXPERIMENTS WITH TRACER MOLECULES

S.Z.ROGINSKY

Institute for Chemical Physics, Moscow, USSR

Abstract: The measurement of hydrogen and oxygen isotopic kinetical effects in the oxidation of hydrogen on platinum points to the participation of oxygen and the non-participation of hydrogen in the limiting step of the oxidation of hydrogen. The step-wise scheme of this process is considered; the promoting effect of oxygen and the heterogeneity of the surface are taken in account. Results of the investigation of the T mechanism of Fisher-Tropsh process on cobalt catalysts by means of the distribution of the radiocarbon mark in the products and the isotopical kinetical effect are exposed. The possibility of a considerable simplification and selectivity of the hydrogenation processes by conducting them in a chromatographic separating method was shown, as well as the perspectivity of a simultaneous application of radiochromatography and a chromatographic column in the study of reactions and catalysts.

1. INTRODUCTION

The participation of solid surfaces in heterogenous catalysis involves intermediate forms and reaction mechanisms which are very difficult to elucidate. For a considerable number of the homogeneous chemical reactions of gases and liquids the molecular mechanism is unambiguously stated. The mechanism of heterogenous reactions remains open to discussion, even for the most investigated and simple gaseous contact reactions, proceeding with the formation of one stable product and the breaking or formation of only 2 or 3 chemical bonds. Still less clear is the mechanism of the complicated contact reactions, where the main function of the catalyst is a kibernetic regulator of reaction routes and a control of chemical and spacial structure of the complex end products.

This situation shows, that the orthodox methods of research in catalysis are not sufficient for an elucidation of the deep reaction mechanism. In this report I shall expose some results, obtained by investigating the mechanism by means of other (mainly isotopic) methods.

2. OXIDATION OF HYDROGEN ON PLATINUM

For this system the main features are: a low activity of the degased metal, the possibility of strong activation of Pt by means of oxygen uptake

from O_2 or from the reacting mixture [1, 2] and a strong catalytic corrosion [3]. The reaction kinetics are different on Pt-specimens with different histories.

For stoichimetric mixtures the reaction order is usually $\frac{1}{2}$: ($w = kp^{\frac{1}{2}}$). In some cases this order results from a true first order for oxygen and a $-\frac{1}{2}$ order for hydrogen $w \sim [O_2]/[H_2]^{\frac{1}{2}}$, in other cases there exists a true $\frac{1}{2}$ order for oxygen and a zero order for hydrogen. These peculiarities of the reaction kinetics led us to a probable stepwise reaction scheme. The process starts with chemisorption of oxygen, which is charged negatively by the metal's electrons. The limiting step involves oxygen, but not hydrogen [2].

To check this conclusion the magnitudes of isotopical kinetic effects (α) of hydrogen and oxygen were measured.

For reactions, consisting of $\geqslant 2$ steps it is important to distinguish between the values α_i - (obtained by the comparison of velocity constants of the two separately conducted isotopic reactions) and α_s (obtained from the magnitude of isotopic separation, accompanying reactions of a mixture of isotopic molecules). For a stationary process in the simplest case α_i equals the ratio of velocity constants of the limiting step. In the presence of auxiliary equilibria, α_i can contain (as factors) thermodynamic isotopical effects.

Accumulation of α of different kinetic steps is impossible. Owing to competition between the isotopic molecules α_3 can be observed on each bifurcation for the element, whose isotopes do not participate in the limiting step. For the same reason in multi-step reactions, α_s-values may differ from those of the single steps [4]. If there is no redistribution provoked by isotopic exchange, or if this is strictly taken in account, the α_s-values can be measured with greater reliability and precision, than the α_i-values. Therefore for oxygen measurements of only α_s were real. For hydrogen both values of α were determined with deuterium (mass-spectrometrically and by water density measurements). In a large temperature range for low total pressures (0.1 mm Hg) and for atmospheric pressure, $\alpha_i \approx 1$. The data, obtained at low temperatures and low pressures (see fig. 1) are the most convincing.

Evidently the assumption [5] about the value $\alpha_i \approx 1$ for hydrogen is true. The coincidence of the curves of fig.2 to a great extent shows that the reaction velocity is independent of $[H_2]$. This fact, together with $\alpha_i = 1$, almost unambiguously excludes a participation of free or bonded hydrogen in the limiting step of the hydrogen oxidation.

For platinum, poisoned with respect to the isotopic exchange: $DH + H_2O \rightarrow DHO + HD$, there was found earlier an α_s-value, changing from 1.3 to 1.1 in the temperature range 95°-300°C [6]. When the temperature is lowered to 20°C this α-value increases up to 1.8 (fig.3), which is greater than (m_{HD}/m_H). This fact indicates the presence of an isotopic bifurcation with a chemical mechanism. Under different conditions the α_s-values for oxygen are found to vary from 1.01 to 1.05. Experiments were performed with a gas, containing 13 atom % O^{18}; so only the molecules O^{16} O^{18} and O_2^{16} have to be taken in account. The values $\alpha_s > 1$ for oxygen and the explicit dependance of the stationary velocity of the process upon oxygen concentration indicate that oxygen participates in the limiting step. This result,

in conjuction with other data for the same system leads to the following step scheme: Scheme I

$$\text{I. } Pt + O_2 \xrightarrow{1} \overset{*}{Pt}\,; \quad \overset{*}{Pt} + O_2 \xrightarrow{2} \overset{*}{PtO}{}^{(-)}_{2chs}\,; \quad \overset{*}{PtO}{}^{(-)}_{2chs} \xrightarrow{3} 2\overset{*}{PtO}{}^{(-)}_{chs}\,;$$

$$\text{II. } Pt + \tfrac{1}{2}H_2 \xrightarrow{1} PtH^{(-)}_{chs}\,; \quad \overset{*}{Pt} + H_2 \xrightarrow{2} \overset{*}{PtH}{}^{(+)}_{2ads}\,;$$

$$\overset{*}{Pt} + \tfrac{1}{2}H_2 \xrightarrow{3} \overset{*}{PtH}{}^{(-)}_{chs}\,; \quad PtH^{(-)}_{chs} \xrightarrow{4} Pt + H_2O\,;$$

$$\text{III. } O^{(-)}_{chs} + H^{(+)}_{2ads} \xrightarrow{1} H_2O\,; \quad O^{(-)}_{2ads} + H^{(+)}_{2ads} \xrightarrow{2} H_2O_2 \xrightarrow{3} O^{(-)}_{chs} + H_2O\,;$$

$$O^{(-)}_{2chs} + H \xrightarrow{4} O^{(-)}_{chs} + OH\,.$$

We should like to emphasize the introduction of a preparatory step - the formation of the active surface of platinum ($\overset{*}{Pt}$).

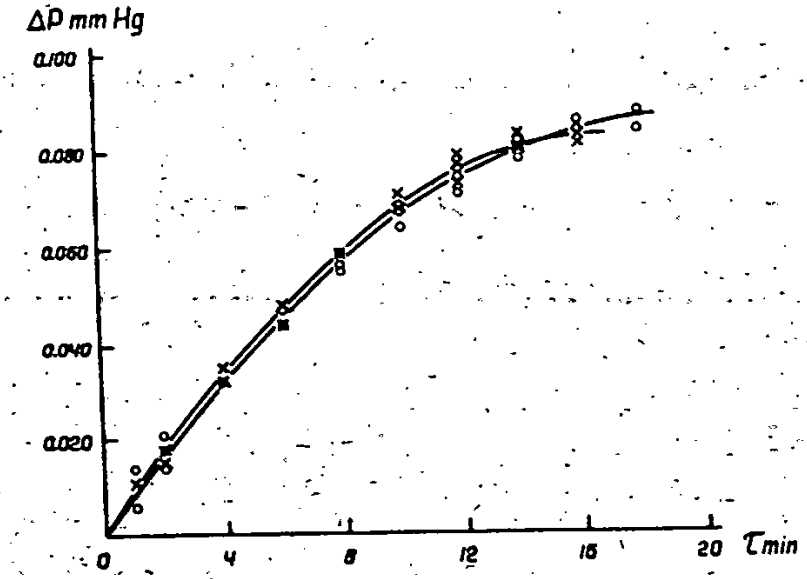

Fig. 1. Reaction kinetics of stoichiometric mixtures of oxygen with protium and deuterium at - 78°. $(P_O)_{mixt} \cong 0.107$ mm Hg
x - protium
o - deuterium .

This step is a result of the oxygen uptake by the metal. This activation can be prevented by a firm uptake of other gases and in particular, of hydrogen. $\overset{*}{Pt}$ probably consists of sites, of a two-dimensional oxide PtO. After long work a 3-dimensional oxide layer is formed. This layer can be detected by electron diffraction (fig.4); it was identified as Pt_3O_4 [7]. According to Shishakof this stable peroxide may be Pt_2O_8, with O-O-bonds in the crystal lattice [8]. Platinum, covered with this oxide, is especially active.

Depending on external conditions and the state of the surface, the catalysis can be controlled either by the chemisorption of oxygen in the form of $\bar{O}_{2ads}I_2$, or by its transiton in dissociated state I_3. According to electrochemical data both forms can coexist [9, 10] and O_2^- and can react with water forming peroxide. Under special conditions the formation of peroxide can

occur also at the oxidation of H_2.

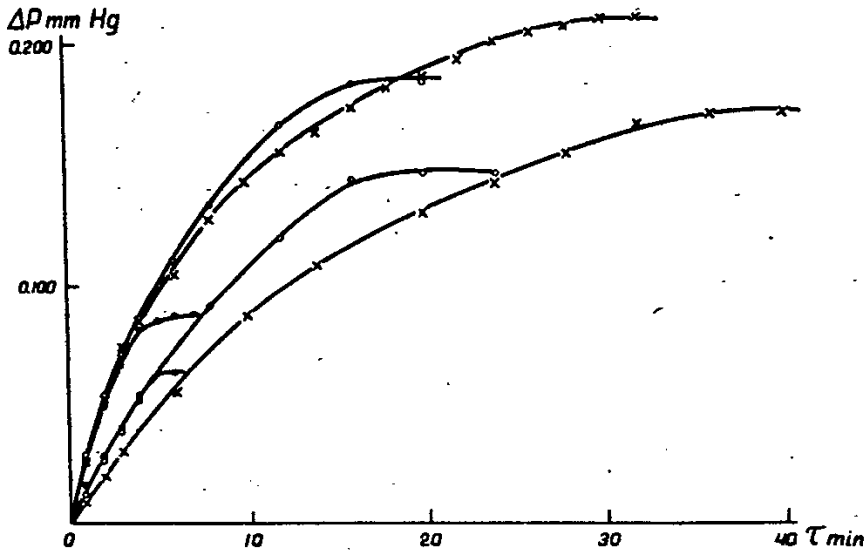

Fig. 2. Reaction kinetics in mixtures with constant oxygen volume and different amounts of hydrogen at - 78°C.
● - $O_2 : H_2 = 1 : 1$ $(P_o)_1 = 0.140$ mm Hg $(P_o)_2 = 0.104$ mm Hg
o - $O_2 : H_2 = 1 : 2$ $(P_o)_1 = 0.198$ mm Hg $(P_o)_2 = 0.157$ mm Hg
x - $O_2 : H_2 = 1 : 3$ $(P_o)_1 = 0.258$ mm Hg $(P_o)_2 = 0.214$ mm Hg
The upper bundle of curves corresponds to mixtures at high initial pressure.

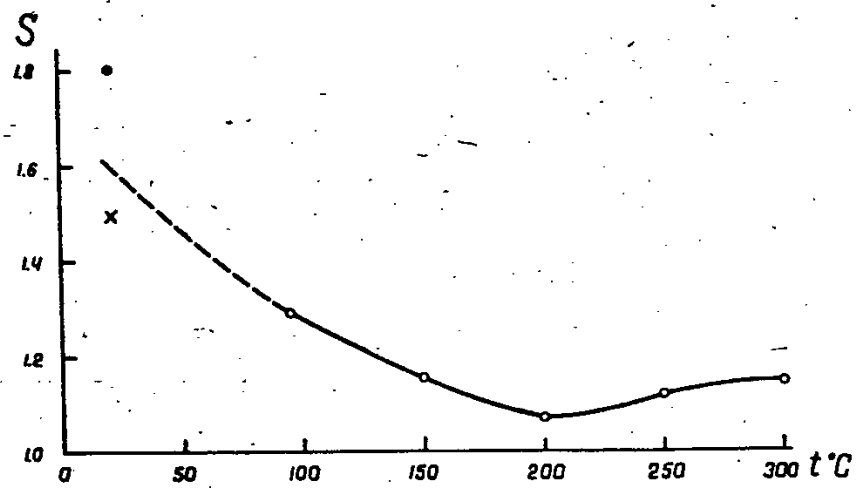

Fig. 3. Temperature dependence of the separation degree S_1, corresponding to 10% conversion in a mixture of H_2 and HD (atmospheric pressure, dynamical conditions),
● - $\alpha_{H_2;HD}$, x - $S_{10\%}$ (P_o = 0.2 mm Hg statics).

Under usual conditions the peroxide is unstable in contact with platinum, therefore as a rule only water is formed in a gaseous medium.

$w \sim [O_2]$ when the velocity and kinetics are controlled by step I_2; and $w \sim O_2^{\frac{1}{2}}$ when by step $-I_3$. It is very difficult to give a more concrete defi-

nition of the adsorbed forms of hydrogen and oxygen, participating in the catalytic process, because the adsorption of both gases is complex as revealed by a study of the adsorption on surfaces which have been degased in an ultra-vacuum, and they affect one another. Let us suppose, as a working hypothesis, that O_2^- or O^- react with H_2^+, which, according to Mignolet [11] and others can be formed at adsorption on the first negatively charged hydride (or oxide) layer. Similarly O_2^- or O^- reacting on Pt, lie in the second layer.

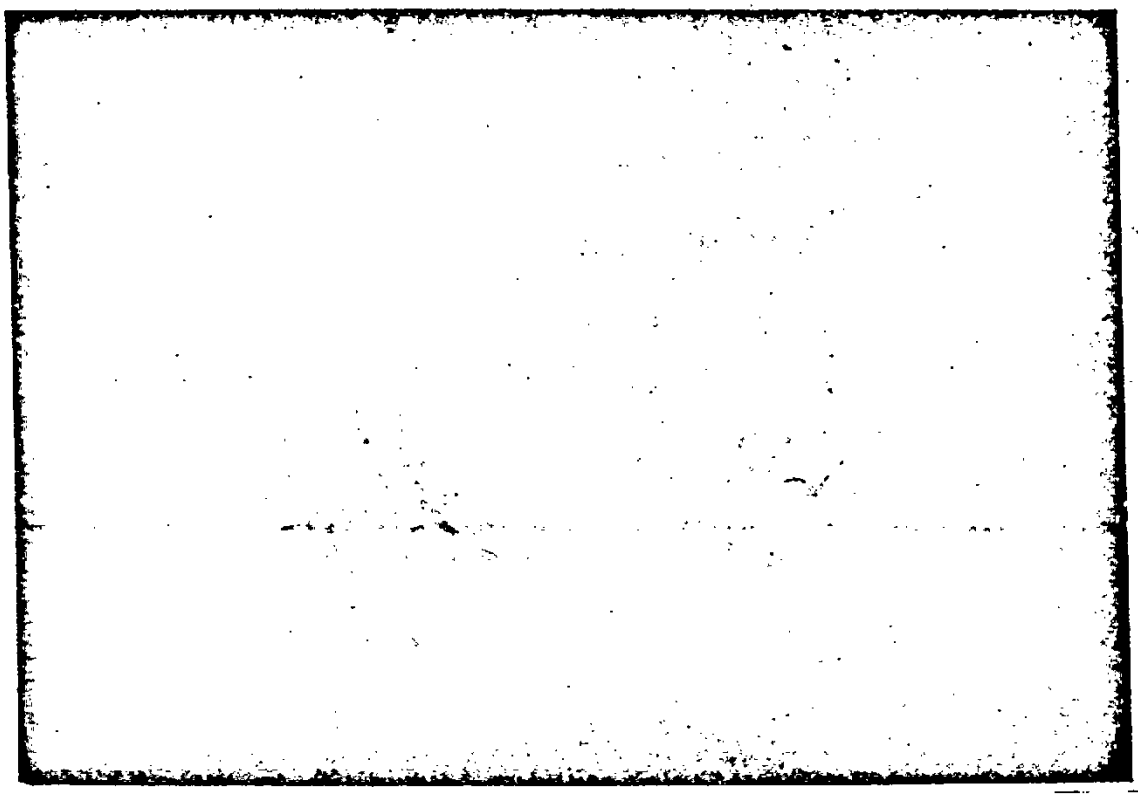

Fig. 4. a. Electron diffraction picture of a fresh platinum plate.
b. Electron diffraction picture of platinum after catalytic oxidation of hydrogen.

Supplementary complications are introduced into the mechanism and kinetics of hydrogen oxidation and of the majority of other contact reaction by the catalytical and chemosorbtional heterogeneity of the surface and by the modifying interaction of adsorbed molecules. In catalysis and adsorption it is impossible to distinguish between the influence of heterogeneity or interaction on the grounds of external manifestations. It is possible to do so by means of contemporary physical methods. Some isotopic methods, elaborated in our laboratory [12], are effective for the investigation and detection of heterogeneity.

To the study of the mechanism of catalytic isotopic hydrogen exchange on active platinum these methods were recently applied by Boreskov and Wasilewitch [13]. The kinetics of the low-temperature isotopic exchange of adsorbed tritium with D_2 and H_2 indicates a large inhomogeneity of the Pt-

surface relative to the velocities of isotopic exchange. The distribution of sites relative to activation energies of exchange is found to be nearly uniform. The part of highly active centres is small, as for homomolecular $H_2 + D_2$ - exchange.

The nature of these sites probably differs from those of the other surface regions. It is interesting to note the absence of an isotopic effect ($\alpha_i = 1$) in the exchange of H_2 and D_2 with the adsorbate. This indicates that H_2 and D_2 do not participate in the formation of transition complexes of the limiting step of exchange. It follows from the same data that chemosorbed H and T participate at this step.

3. SYNTHESES OF ALKANES FROM CO + H_2. HYDROPOLYMERISATION OF ETHYLENE.

The former processes is characterised by a simultaneous formation of several (many) members of the homological series. Depending on the choice of the catalyst and on the conditions of the synthesis there are formed chiefly C_nH_{2n+2} or $C_nH_{2n+1}OH$ from CO + H_2. Other homological series are represented in a much lesser degree. For the chemosorption of hydrogen on these catalysts there exist still more possible forms, than on Pt. For CO on metals the spectroscopical investigations of Eistens and others [14] indicate the possibility of several forms of chemosorption without and a dissociation. Besides that, the possibility of carbidising Me and of other reactions must be taken in account. Unfortunately the study of independent and combined chemisorption of CO and H_2 cannot alone give a clue to the specificity of these processes, because their direction and the composition of their products depend upon the following steps.

Of great principal importance was the pioneering work of Cummer and Emmett [15]. In their experiments, adding alcohols, marked with C^{14}, to the CO + H_2 - mixture, they found that carbon from the alcohol entered in products of synthesis. The molecular radioactivity (a_m), appearing in alkanes of different molecular weights, was constant. This result, obtained on Fe-catalysts, was considered by the authors as an indication, that the reactions are initiated by the alcohol or by a surface radical, formed from the alcohol. At the same time it was considered as a confirmation of the Storch and others [16] dehydration-condensation mechanism of the carbon chain growth. In our investigations the data [17] on the constance of the molar radioactivity of products were confirmed also for syntheses in the presence of alcohols on a cobalt-thorium-catalyst. But at the same time it was shown, that a similar effect is observed with the introduction of marked organic compounds of other functions, including olefins (fig.5). Under the same conditions the participation of olefins in the initiation is higher, than that of alcohols. Hence the assumption about the rôle of olefins or their direct convertion products (for instance methylenes) in the initiation of the methylene chain growth. Other authors later arrived at similar conclusions for cobalt and iron catalysts. The results of a comparison of the distribution of radioactivity in products of reactions, initiated by ketene

$H_2C = C = O$, marked with C^{14} in the methylene or the carbonyl groups only [18] are very convincing.

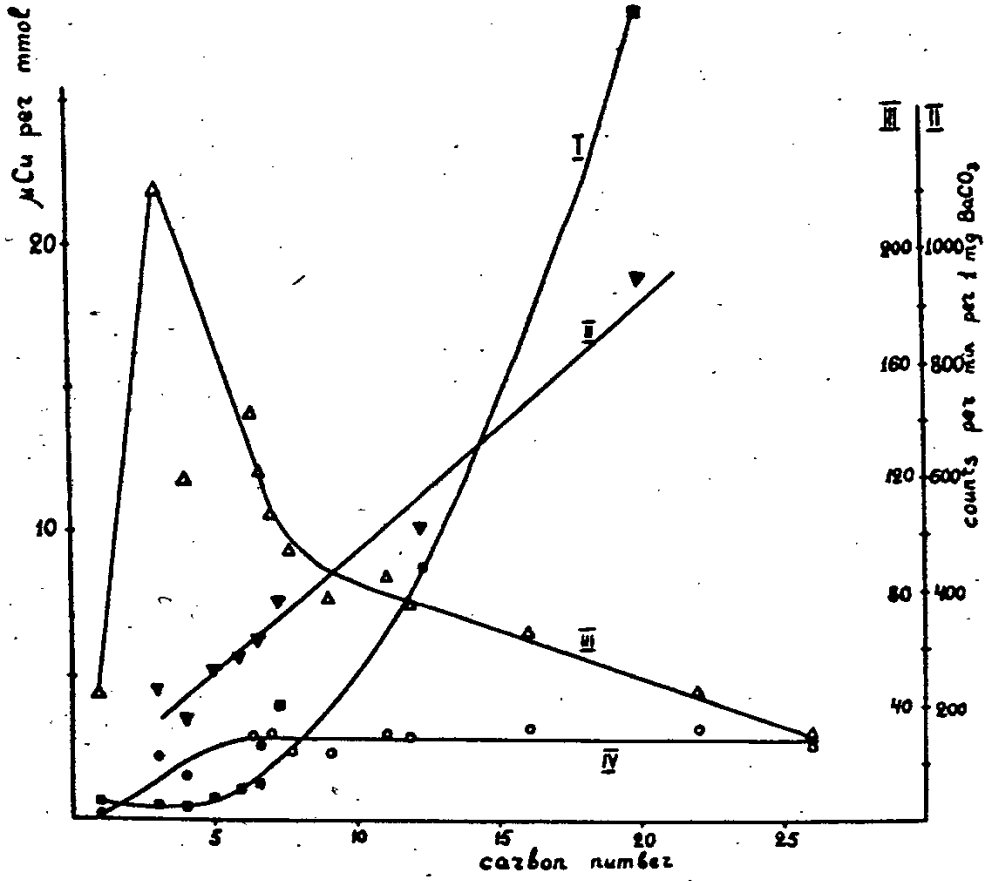

Fig. 5. a) Molar (I) and specific (II) radioactivity of hydrocarbons in the hydropolymerisation of ethylene in the presence of 2 at % of marked CO (8.6 μCu/mmol).
b) Specific (III) and molar (IV) radioactivity of hydrocarbons in the synthesis from a $CO + H_2$ - mixture, containing 1.45 at % of marked C_2H_2 (12.5 μCu/mmol).

Fig.6 shows that only for low atomic concentrations (~ 1%) of ethylene its rôle can be reducted to initiation. When its concentration is increased up to several percents an increase of a_m with the molecular weight of product is observed. In this case ethylene participates also in the chain growth. Hence a natural passage to hydrocondensation and Eidus hydropolymerisation in $H_2 + C_2H_4$ - mixtures containing additions of CO [19]. In this reaction the major part of methylene groups of the carbon chain is supplied by ethylene, so that, if the ethylene is marked, a_m must increase linearly with molecular weight.

Less clear is the rôle of CO in the hydropolymerisation. Besides the initiation, it can be a poisoning of harmful reactions - hydrogenation of ethylene, etc. At the hydropolymerisation of mixtures, containing 2% of marked CO, the specific radioactivity of hydrocarbons grows nearly linearly (quadratic increase of a_m) and the prepondering part of light hydrocar-

bons is formed without a participation of CO *.

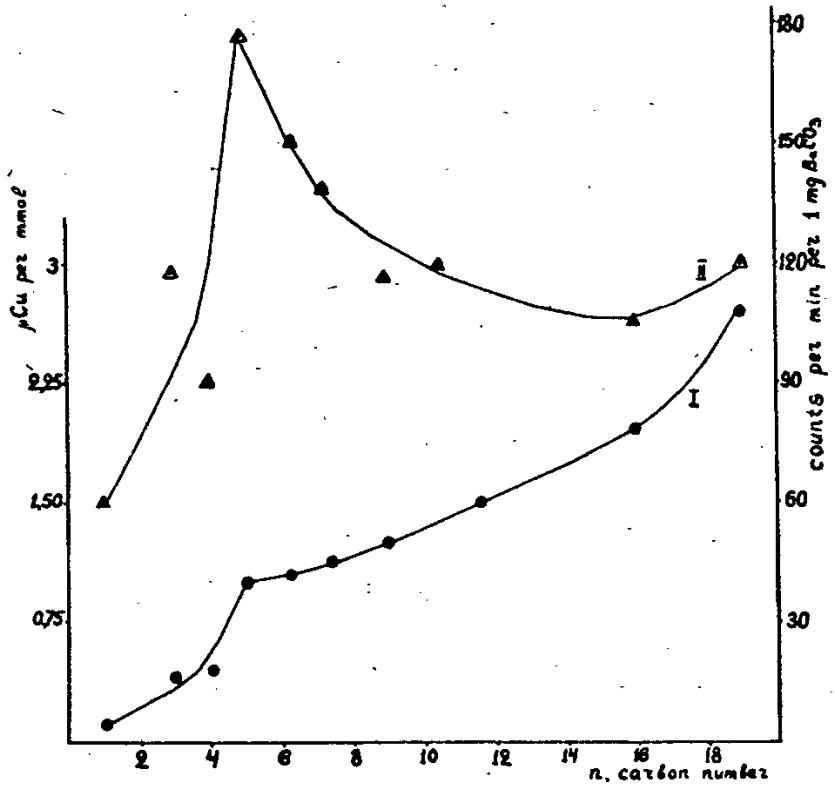

Fig. 6. Molar (I) and specific (II) radioactivity of hydrocarbons in the synthesis of hydrocarbons from a mixture of CO and H_2, containing 4.8 at % of marked C_2H_4 (1.53 m Cu/mmol).

The constant nature of a_m in conjunction with the non-participation of marked C_nH_{2n+2} in the synthesis confirms that in reactions of this group chemisorption is followed by steps of 3 main types:

a) Formation of the active form (priming), able to start a carbon chain of a hydrocarbons or alcohols:

b) Growth of the hydrocarbon chain, by means of a series of consecutive uniforms processes.

These processes proceed with the participation of CO and H_2.

c) Stopping of the single reaction, when the active form is converted in a molecule of the final product;

d) Removal of this molecule so that the active center gets free to repeat the same step sequence.

The whole process of formation of every separate molecule with any number of C proceeds without disengagement from the surface; according to the fixed chains mechanism without "relay-race" [17, 21]. Small and big molecules of the products of every homological series are formed independently. It is striking, that even additions, which participate strongly at the initiation, do not change considerably the velocity of the total process or the

* There is in this question a certain discrepancy in the data of Gibson et al. [20], who found a linear increase of a_m.

compositon of the products. This shows, that even in synthesis reactions without additions, the initiation phase, including the formation of the priming of a chain, able to grow and firmly bond on to the surface is short. The participation of additions at the initiation can be used as a relative measure of the probability of the priming formation. Assuming the mechanism of fixed chains, it seems natural to consider the priming (in the kinetic respect) as a whole with its active center. The surface is probably heterogenous relative to these centers in respect to the strength of the bond with the priming and the ability of chain growth. This can be an additional factor, defining the chemical and molecular composition of the products.

Every center must consist of several atoms, because during the prolonged exclusion of atoms, bonded with the priming; there must be available sites of an other type for the chemisorption of CO and H_2, (which take part in the growth), and perhaps also for the slipping down of the product and the "step over", postulated by some authors.

Considering detailed atomic models, we show here one of the possible schemes of the process prematurely.

Let us design active sites, on which the growing chain is fixed, with $\overset{*}{S}$, and the other sites, participating at the process, with S. $\overset{*}{S}$ can differ from S by its structure and by content of modifying additons. $\overset{*}{S}$ can be metallic atoms, adjoining to dislocations or to microcrystalls of ThO_2. The growing chain priming can get fixed at the surface, as a result of the direct bonding of the active part of the molecule with bare Me-atoms. Our experiments with olefins, the experiments of Emmett with ketene [18] lead to the assumption, that the priming consists of a radical, not containing oxygen. In scheme 2 it is supposed that it is $\overset{*}{S}\text{-}\overset{*}{C}H_2$, - some sort of simplest surface carbonium - ion. The chain grows by the following steps II_1-II_7. Some indications of the character of the limiting step are given in the work of Sakkaroff and Dokukina [22]. For the reaction of CO they got α_i (H_2, D_2) = 0.77. The value: $\alpha_i < 1$ excludes every diffusion control as well as the control through hydrogen adsorption and hydrocarbon desorption. This speaks also against any step, in which the transition state is formed under participation of free hydrogen molecules. The obtained α_i-values, in conjunction with the kinetic equation of the process [23] $w = (\kappa[H_2])/(1+b[H_2O]/[CO])$ shows that one of the steps of formation of additional methylene groups must be the limiting step. In this step, hydrogen and CO in the adsorbed state must both participate in this step. Data, obtained in our laboratory on C^{14} distribution in hydrocarbons from the marked surface carbide, may also be mentioned here. This distribution is identical to the C^{14} - distribution from marked CO or CO_2. Consequently, we must exclude a direct participation of carbidic carbon at the initiation and at the growth.

4. DEHYDROGENATION IN THE CHROMATOGRAPHIC METHOD. RADIOCHROMATOGRAPHY

The combination of the fast and fine chromatographic analysis of complex mixtures and performing the reactions in the separating chromatographic columns [24] is very appropriate for the investigation of complex pro-

Scheme II

1. *Formation of priming*

a) 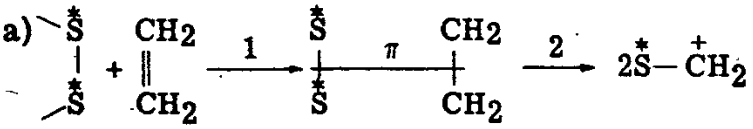

b) 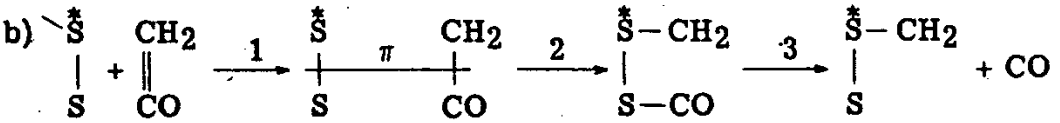

II. *Chain growth*

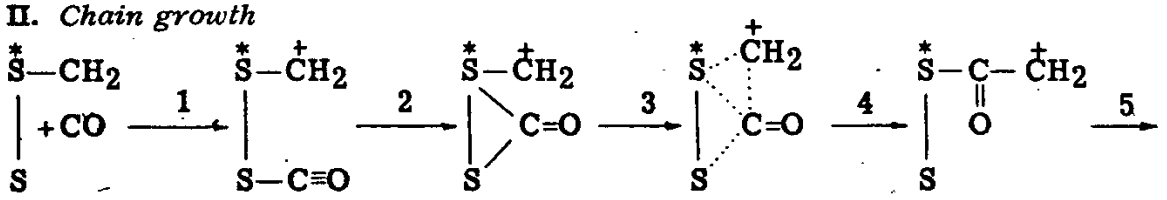

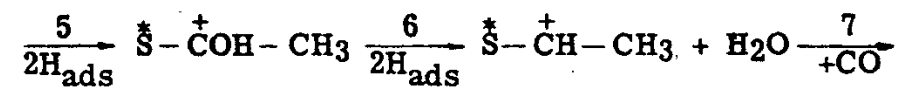

III. *Ruin of priming and break of the chain*

a) 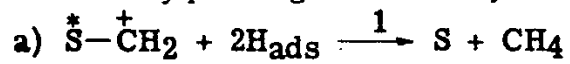

b) 

$\overset{\pi}{+\!\!+}$ bond in the surface π-complex.

cesses and catalysts. The efficiency of these methods is increased even more when the radiochromatographic technique is used to investigate simultaneously the isotopic mark distribution in the reaction products [25]. The scheme of the apparatus used in such studies is shown on fig.7.

When the pulse passes through the reactor - a more or less total separation of all components of the reaction mixture (initial substance, products, catalytic poisons etc.) occurs during the reaction. The kinetic conditions get therefore much simpler. There arises a possibility for a fast study of such peculiarities of the processes and catalysts, which remain unrevealed when the reaction is performed in another regime. The theory of the chromatographic regime was explained in several publications [26]. We mention here some illustrations of its reality. On fig. 8 is shown an example of the possibility of eliminating the inverse reaction (for dehydrogenisation of butilene). Therefore an active platinum contacts the temperature of the beginning of a noticeable process decreases considerably. The percentage and absolute content of butadiene is much higher, than the highest possible without a separation. Chromatographic analysis shows, that there are no side products in the out going gas. At the dehydrogenation on the same catalyst at its normal working temperature (>400°C) the butadiene is soiled with cracking and other side products.

In fig. 9 is shown a direct radiochromatographic verification of the ab-

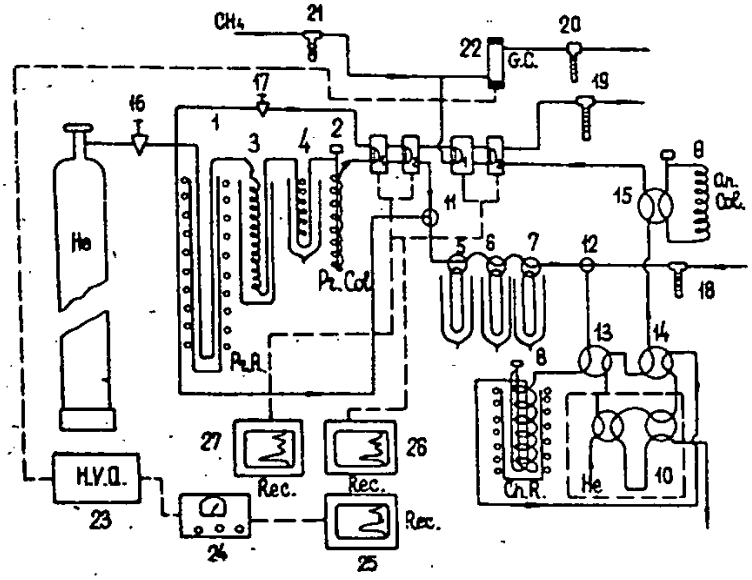

Fig. 7. Combined radiochromatographic apparatus for the investigation of catalytic reactions mechanism.
1 - preparative microreactor for the synthesis of individual components; 2 - preparative chromatographic column; 3, 4 - traps with liquid nitrogen; 5, 6, 7 - devise for the selection of chromatographically pure components; 8 - quartz reactor with catalyst; 9 - analytical chromatographic column; 10 - automatic dosator; 11, 12 - three-ways stopcock; 13, 14, 15 - four-ways-stopcocks; 16, 17 - fine regulation valve; 18, 19, 20, 21 - reometers; 22 - a stream Geiger counter; 23, 24, 25 - system for registration and writing down of radioactivity; 26, 27 - self-recording device; D_1 - ionisation detector; D_2 - heat conductivity detector (cataro-meter).

sence of an inverse process during the dehydrogenation of cyclohexane in the pulse regime - on the same catalyst. To the initial cyclohexane was added benzene, marked with C^{14}. In the outgoing cyclohexane radioactivity is practically absent. Some other conclusion of the theory were also verified [27]. In the ideal case the chromatographic column eliminates the possibility of side reactions between the separate products and the initial substance. It allows us to follow in detail the changes of selectivity in a series of catalysts during their reaction. By means of radiochromatography additonal peculiarities of the mechanism of the complex conjugated process of divinyl formation from alcohol (according to Lebedeff) was defined. Its main schemes were studied earlier by means of consecutive marking of all possible intermediate products [28, 29].

5. DISCUSSION

Thanks to the new experimental methods chemical adsorption receives a concrete physical meaning. Even in adsorption of simple diatomic molecules on simple catalysts there appear many surface forms with different

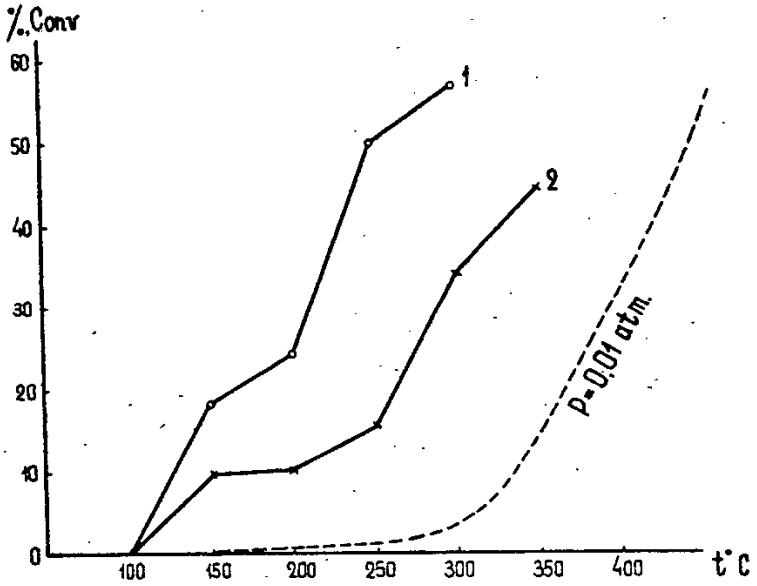

Fig. 8. Temperature dependence of divinyl yield at different stream velocities

1 - ω_1 = 17 cm^3/min

2 - ω_2 = 82 cm^3/min

The dotted line corresponds to equilibria yields of divinyl at hundred fold dilution.

topography, electrical charge, nature of bond with catalyst etc. The use of isotopic marks and kinetic isotopic effects α opens great possibilities for the elucidation of the rôle played by each of these forms in catalysis. Results of the isotopic studies often lead to a revision of seemingly firmly established schemes. Biographical heterogeneity is one of the causes of the appearance of the manifold forms and states of surface compounds, as well as the parallel and independent formation of different stable products (in alcohol decomposition, hydrocarbons oxidation etc.).

The second source of different stable product formation is the dual and more complex reactivity of intermediate products. A great rôle belongs in catalysis of complex reactions to the conjugation of surface processes: by means of commune active intermediary products, transfer of electrons through the solid and other collective mechanisms. Examples: mechanism of divinyl synthesis from ethanol, precised by means of isotopes [28] and the irreversible catalysis" of Zelinsky. The conjugation creates great possibilities for performing difficult processes, with a fine regulation of selectivity and of the product structure. Isotopes help to reveal latent conjugations and labile intermediates of catalysis. Examples: active associative complexes containing aldehyde and alcohol in the divinyl synthesis [28]; intermediate allyl radical with delocalised electrons in the catalytic propene oxidation to acrolein, studied with locally marked carbon and hydrogen [29]. Isotopic methods are especially effective in the investigation of complex catalytic processes, where other methods are difficult to apply. Results obtained in biochemical studies also confirm this conclusion.

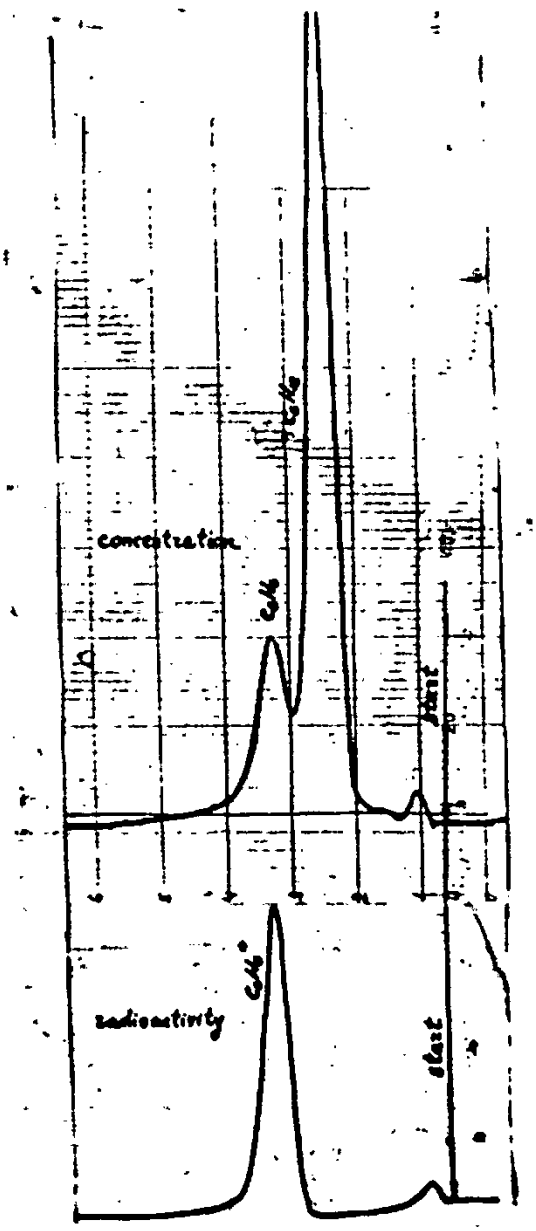

Fig. 9. Radiochromatographic prove of the absence of an inverse hydrogenation reaction. Pulse of cyclohexane and benzene mixture, marked with C^{14}. Reactor temperature 160°. Platinum catalyst.

REFERENCES

1) S. Z. Roginsky and V. S. Rozing, Uch. Zap. Leningr. Gos. Univ., Ser. Fiz. (1939) 67.
2) O. V. Krilov and S. Z. Rogincky, Izv. Akad. Nauk SSSR, Otd. Khim. Nauk (1956) 145.
3) S. Z. Roginsky, I. I. Tretiakov and A. B. Shekter, Dokl. Akad. Nauk SSSR 91 (1953) 881; Zhur. Fiz. Khim. 29 (1955) 1921.
4) S. Z. Roginsky, Kinetika i Kataliz 2 (1961) 694.
5) S. Z. Roginsky, Theoretical principles of isotopic methods for investigating chemical reactions (Consult. Bureau, Inc., New York, 1957).

6) V.I.Popov and S.Z.Roginsky, Dokl. Akad. Nauk SSSR 124 (1959) 1275; Kinetika i Kataliz 2 (1961) 77.
7) O.V.Krilov, S.Z.Roginsky and I.I.Tretiakov, Dokl. Akad. Nauk SSSR 91 (1953) 1353.
8) N.A.Shishakof, Osnovnie poniatia strukturnogo analiza, Izd. Akad. Nauk SSSR, M. (1961) ch. 5.
9) J.H.De Boer, Adv. Catalysis 9 (1957) 472.
10) J.P.Hoar, J. Electrochem. Soc. 109 (1962) 858;
L.Muller and L.Nekrassow, 14 meeting C.I.T.C.E., Moscow (1963).
11) J.Mignolet, J. Chem. Phys. 54 (1957) 19.
12) S.Z.Roginsky, Zhur. Fiz. Khim. 31 (1957) 2381; Kinetika i Kataliz 1 (1960) 15.
13) G.K.Boreskov and A.A.Vassilevitch, Actes du Deuxième Congrès Intern. de Catalyse (Editions Technip, Paris, 1960) Vol. 1, p. 1055.
14) R.P.Eishens and W.A.Pliskin, Adv. Catalysis 10 (1958) 1.
15) J.Kummer and P.H.Emmett, J. Am. Chem. Soc. 73 (1951) 564; 75 (1953) 5177.
16) H.Storch, N.Golumbic and R.Anderson, The Fischer-Tropsch and related syntheses (New York, 1951).
17) O.A.Golovina, S.Z.Roginsky, M.M.Sakkaroff and Ja.T.Eidus, Dokl. Akad.Nauk SSSR 108 (1956) 253;
O.A.Golovina, M.M.Sakkaroff, S.Z.Roginsky and E.S.Dokukina, Zhur. Fiz. Khim. 33 (1959) 2451.
18) G.Blyholder and P.H.Emmett, J. Phys. Chem. 63 (1959) 962; 64 (1960) 470.
19) N.J.Erchov and Ja.T.Eidus, Dokl. Akad. Nauk SSSR 115 (1957) 1126; 119 (1958) 1062.
20) A.W.Fletscher and E.J.Gibson, Proc. 2nd Radio-isotopes Conf. 2 (1954) 40;
E.J.Gibson and R.W.Clarke, J. Appl. Chem. (London) 11 (1961) 293.
21) S.Z.Roginsky, Probl. Kinetiki i Kataliza 10 (1960) 373.
22) M.M.Sakkaroff and E.S.Dokukina, Kinetika i Kataliz 2 (1961) 710.
23) W.K.Hall, R.J.Kokes and P.H.Emmett, J. Am. Chem. Soc. 82 (1960) 1027.
24) S.Z.Roginsky, M.I.Janovskii and G.A.Gaziev, Dokl. Akad. Nauk SSSR 140 (1961) 1125.
25) M.I.Janovskii and G.A.Gaziev. Vestn. Akad. Nauk SSSR (1960) no. 5, 27.
26) S.Z.Roginsky and A.L.Rozental, Dokl. Akad. Nauk SSSR 146 (1962) 155.
27) S.Z.Roginsky, M.I.Janovskii and G.A.Gaziev, Kinetika i Kataliz 3 (1962) 529.
28) O.M.Vinogradova, N.P.Keier and S.Z.Roginsky, Probl. Kinetiki i Kataliza 9 (1957) 200.
29) W.M.H.Sachtler, Rec. Trav. Chim. 82 (1963) 243;
H.H.Voge, C.D.Wagner and D.P.Stevenson, J. Catalysis 2 (1963) 58;
C.R.Adams and T.J.Jennings, J. Catalysis 2 (1963) 63.
30) V.M.Gryaznov and V.I.Shimulis, Dokl. Akad. Nauk SSSR 139 (1961) 870;
V.M.Gryaznov and V.D.Yagodovskii, Kinetika i Kataliz 4 (1963) 404.

THE INFLUENCE OF SURFACE STRUCTURE OF CrO_3-Al_2O_3 CATALYSTS ON THE MECHANISM OF REDOX CATALYTIC REACTION

J. DEREN, J. HABER and J. SIECHOWSKI

Department of Surface Phenomena, Research Institute of Physical Chemistry, Polish Academy of Sciences, Krakow, Poland

and

Department of Physical Chemistry, Normal School, Katowice, Poland

Abstract: The aim of the present research was to investigate the mechanism of processes taking place in the CrO_3-Al_2O_3 system in the course of thermal treatment, and their bearing upon the catalytic activity. Catalysts used were prepared by impregnation of $(\theta + \varkappa)$ - Al_2O_3 with chromic acid solutions and subsequent calcination in air and in vacuum. The investigations comprised the measurements of specific surface area, capillary structure, mean valence of chromium ions as determined in air and in vacuum, and thermovolumetric analysis. The decomposition of hydrogen peroxide has been chosen as the test reaction and its kinetics and activation energy were studied. The results indicate that from the catalytic point of view not only the concentration of Cr^{+6} acceptor centers but also their state of aggregation is of great importance. They hint also to the important role of Cr^{+6}/Cr^{+5} concentration ratio in the selectivity of chromia-alumina catalysts.

1. INTRODUCTION

The system consisting of chromium oxides supported on carriers has been a subject of many investigations [1-6]. Almost all of them however were carried out with catalysts, which previously were reduced with hydrogen or other reducing agents, whereas only a few dealt with the problem of thermal decomposition of CrO_3 supported on carriers. Although many interesting conclusions have been drawn concerning the valence state of chromium ions in chromium-oxide-on-carrier catalysts, the mechanism of the decomposition of CrO_3 supported on carriers and its relation to the catalytic activity of the resulting catalyst is not yet clear. The aim of the present research is to investigate the mechanism of the processes taking place in the CrO_3-Al_2O_3 system in the course of the thermal treatment, to determine the structure of the resulting catalyst and to find the correlation between the structure and the catalytic activity.

2. EXPERIMENTAL

2.1. *Preparation of catalysts*

The catalysts used in this study were obtained by impregnating an alumina support with chromic acid solutions at 20°.

The alumina was prepared according to Fricke and Jockers [7] by amalgamating an aluminium sheet (99.93% Al) with $HgCl_2$ and treating with redistilled water at 20°C. The preparation was slowly dried at room temperature. Its composition corresponded to the formula $Al_2O_3 \cdot 3.1H_2O$ and X-ray powder diagram showed the diffraction lines of bayerite only. The preparation was then calcined for 5 h at 1000°C. The resulting alumina was identified by X-ray analysis as $(\theta + \kappa)$-Al_2O_3. Its density was about 3.7 g/cm^3 and it contained 4.1% of water. $(\theta + \kappa)$-Al_2O_3 was used instead of γ-Al_2O_3 in order to eliminate the possibility of further changes of the carrier on subsequent thermal treatment of the catalysts.

The alumina was impregnated by contacting it with chromic acid solutions for 4 h. By changing the concentration of chromic acid catalysts were obtained with chromium concentration ranging from 0.065 to 8 wt %. Samples were dried for 20 h at 45°C and then calcined for 5 h at 100-500°C in air and in vacuum.

2.2. *Determination of the oxidation state of chromium*

The total amount of excess charges, corresponding to chromium ions in the valence states higher than +3, was determined by the Bunsen-Rupp method [8]. A sample of approximately 0.1 g was placed in a specially designed flask connected with a second flask containing the KI solution. 30 ml of conc. HCl was then added to the sample and the content boiled for 30 min. The iodine evolved was titrated with 0.01 N thiosulfate.

It had been found earlier by Matsunega [2] that chromia-alumina catalysts of low chromium concentration get re-oxidised after exposing them to air even at room temperature. Thus, the modified iodometric method as described elsewhere [9] was used in order to determine the amount of excess charges which remain in the sample after the heat treatment in vacuum. It enabled the analysis to be carried out directly after the heat treatment in vacuum without exposing the sample to air.

2.3. *Thermovolumetric analysis*

The question may be raised as to whether the excess charges found by chemical analysis in samples calcined at higher temperatures are really due to the incomplete decomposition of CrO_3 or to the re-oxidation of chromium ions, which might take place on cooling the sample after heat treatment. In order to answer this question a series of thermovolumetric analyses was carried out. The results are shown in fig. 1, whereon the amount of oxygen evolved on heating samples to 500°C is plotted as the function of chromium concentration. For comparison, the amount of active oxygen found by chemical analysis in samples calcined at 500°, is also given. The results are in good agreement within the experimental error and it may be concluded that re-oxidation or chemisorption of oxygen on cooling does not contribute to a greater extent to the results of chemical analysis.

2.4. *Surface area and capillary structure*

The evaluation of the surface area, the overall volume of pores and

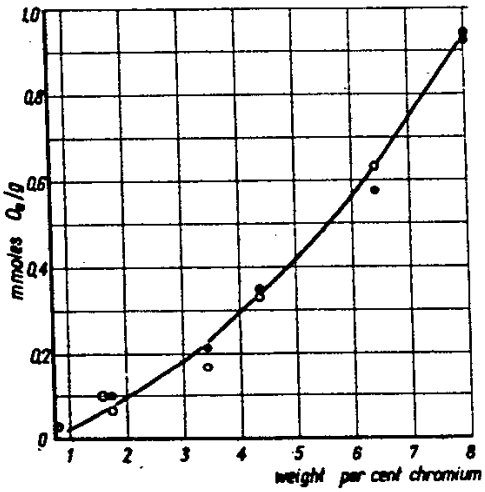

Fig. 1. The results of the thermovolumetric analysis.
O - mmoles of oxygen evolved on heating a sample to 500°C,
● - mmoles of active oxygen from chemical analysis of samples annealed at 500°C.

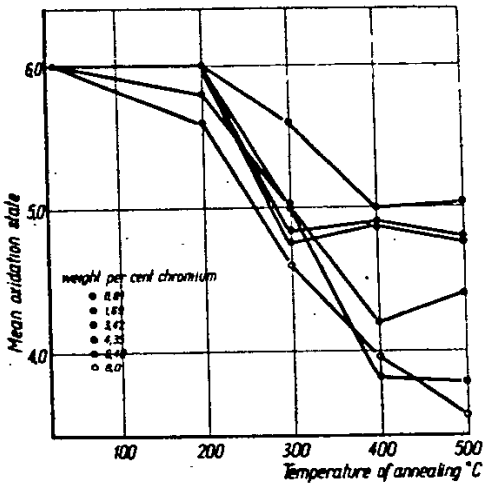

Fig. 2. The mean oxidation number of chromium ions as the function of the temperature of calcination.

pore size distribution was carried out by measuring the adsorption of argon at liquid nitrogen temperature. The specific surface area was calculated by means of the BET equation. The overall volume of pores was estimated from the amount of adsorption as p approaches p_0. The desorption branches of argon adsorption isotherms were used for the calculations of the pore size distribution, carried out on the basis of the Kelvin equation.

2.5. *Catalytic activity*

The decomposition of hydrogen peroxide has been chosen as the test reaction for comparison of the catalytic activity. The measurements of the kinetics of catalytic decomposition of hydrogen peroxide have been carried out in a way similar to that described previously [8]. 10 mg of catalyst were used for each run. The experiments were carried out for 30 min at five different temperatures between 20-40°C with each catalyst.

The analysis of the experimental data has been carried out on the assumption that the decomposition of H_2O_2 is a first order process. As the maximal conversion observed after 30 min never exceeded 0.05, it may be assumed in the first approximation that the reaction runs at the constant concentration of H_2O_2. In such conditions the integration of the first order equation gives:

$$V = V_0 + k.t$$

where V represents the volume of oxygen evolved and V_0 - volume of oxygen evolved to the moment, at which the time measurements started. In al experiments the linear dependence of the volume of oxygen evolved on time has been observed in accordance with the above equation. The rate constants have been computed from the slope of V versus t plots. The proportionality

of the rate constant to the amount of catalyst used has been taken as the evidence that the measurements were carried out in the kinetic region of the reaction. Additional experiments proved that the observed decomposition of hydrogen peroxide is a heterogeneous catalytic reaction and not a reaction catalyzed by small amounts of chromium ions which might have dissolved in the course of the measurement.

3. RESULTS AND DISCUSSION

According to the phase diagram of the system chromium-oxygen, constructed by Kubota [10], chromium anhydride is stable only at low temperatures. At 220° it decomposes into lower chromium oxides and at 400-450° Cr_2O_3 is eventually formed. Essentially similar results were obtained by Glemser et al. [11], although the nature and composition of the intermediate oxides remain still disputable. Entirely different situation is found in the case of chromic anhydride supported on alumina. Fig. 2 shows the mean oxidation number of chromium ions plotted as the function of the temperature of calcination for preparations of various chromium concentrations. Preparations containing less than about 4% of chromium show a practically constant +6 oxidation number up to about 200°C. Then the oxidation number decreases and at 300-400° attains the value of about +5, which remains constant on further annealing at higher temperatures. In the case of preparations with higher chromium concentrations the mean oxidation number decreases continuously with the increasing temperature of calcination, assuming a value between +3 and +4 for samples annealed at 500°.

Such changes of the oxidation number clearly demonstrate the pronounced stabilizing influence of the carrier on the +5 valence state of chromium ions. As suggested by Cossee and Van Reijen [4] the stabilization of the +5 valence state by alumina may be due to the crystal field effect. Such influence may be exerted only when chromic anhydride is well dispersed on the surface of alumina. In fact, it may be concluded from further experiments that in preparations containing low amount of chromium (< 4%) chromium oxide occurs in the state of molecular dispersion or small crystal nuclei. When chromium oxide is present in thicker layers as it is the case in preparations containing higher amount of chromium (> 4%) this stabilizing influence is relatively smaller and distinct phase of Cr_2O_3 is formed after calcination at higher temperatures. It is interesting to note that the amount of excess charges which remain after annealing these preparations at higher temperatures is practically independent of the concentration of chromium. They can be, however, completely removed by heating the samples at 200° in vacuum. It seems that the residual excess charges are due to the surface oxidation of the clumps of Cr_2O_3 formed on the surface of the carrier. On increasing the chromium concentration the clumps grow in thickness, their surface and the amount of excess charges remaining unchanged.

Fig. 3 represents the dependence of the specific surface area on the concentration of chromium for samples annealed at various temperatures. At very low chromium concentration (< 1%) the deposition of chromium oxide

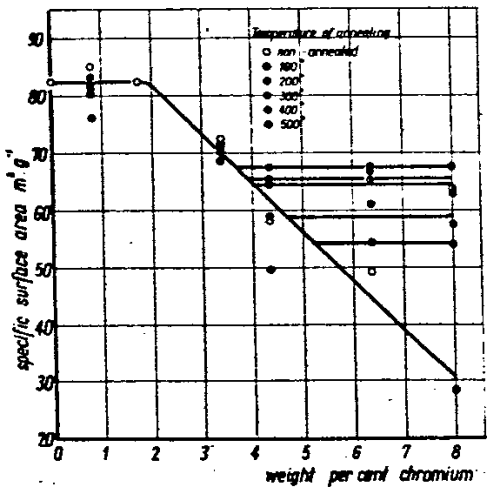

Fig. 3. Specific surface area as the function of chromium concentration.

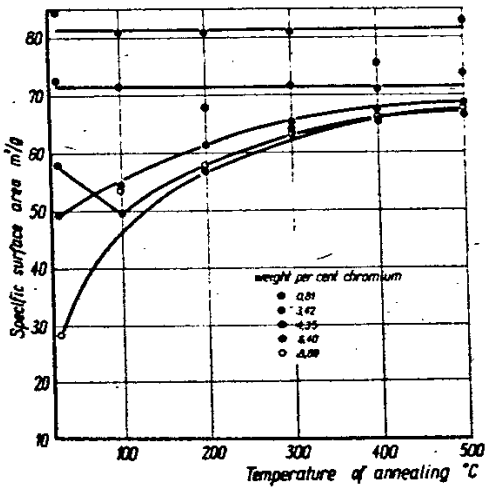

Fig. 4. Specific surface area as the function of the temperature of calcination.

on the surface of alumina has practically no influence on its surface area, independently of the temperature of calcination. On increasing the chromium concentration the surface area of non-calcined samples decreases to about 30 m^2/g for samples containing 8% of chromium. In the case of samples which were previously calcined the surface area decreases on increasing the concentration of chromium up to about 4% of chromium and then remains at a constant level, independent of the concentration. This level is the higher the higher is the temperature of calcination. This temperature dependence of the surface are is clearly visible from fig. 4, on which the surface area is plotted as the function of the temperature of calcination for several samples of various chromium concentrations. In the case of samples containing 0.8% and 3.4% of chromium the surface area is independent of the temperature of calcination, whereas it increases with rising of the calcination temperature for samples containing 6.4% and 8.0% of chromium and attains a constant value only at higher temperatures.

Thus, two characteristic concentrations of chromium on the surface of our carrier may be distinguished - one of about 1% and the second of about 4%. At concentrations below 1% the surface area remains independent of the concentration of chromium. In the range between 1% and 4% it decreases with increasing chromium concentration, but is independent of the temperature of annealing. At still higher concentration of chromium the surface area becomes independent of the concentration but depends on the temperature of annealing.

Eischens and Selwood [1] carried out a detailed study of the magnetic properties of chromia-alumina catalysts and concluded that at low concentration of chromium chromia occurs on the surface of alumina in the form of small crystal nuclei which are, on average, three layers thick. In the higher concentration range these crystal nuclei tend to grow and thicken, whereas they shrink as the concentration of chromium decreases and, at the

limit, chromium ions may be in two dimensional atomic dispersion. Kazansky et al. [3] also concluded from the results of EPR measurements that chromia is spred on the surface of alumina in form of thin plate-like crystallites. These ideas may be taken as the basis also for the interpretation of our results. It seems that at concentrations lower than 1% chromium ions occur in the state of atomic dispersion. In the region of about 1% the formation of crystal nuclei of CrO_3 begins, these being few layers thick as suggested by Eischens and Selwood. The region between 1-4% would correspond to the increase in the number of such crystal nuclei. They plug more and more small capillaries and the surface area decreases. At the concentration of about 4% all centers of nucleation are probably covered with crystal nuclei of CrO_3 and the latter begins to grow thick. The growth of crystal nuclei of CrO_3 may cause even larger capillaries to be plugged, what is reflected in further decrease of the surface area of non-calcined samples. On annealing, however, crystallites of CrO_3 decompose into Cr_2O_3 and these larger capillaries are re-opened. Thus, the surface area of calcined samples remains constant at concentrations higher than 4%. This model is consistent with the above mentioned results showing that at concentrations lower than about 4% of chromium chromium ions are stabilized by the carrier at the +5 oxidation state, whereas at its higher concentration Cr_2O_3 is formed on the surface in the course of calcination.

The analysis of the capillary structure of CrO_3-Al_2O_3 catalysts lends further support to the above presented model. Fig. 5 represents the volume

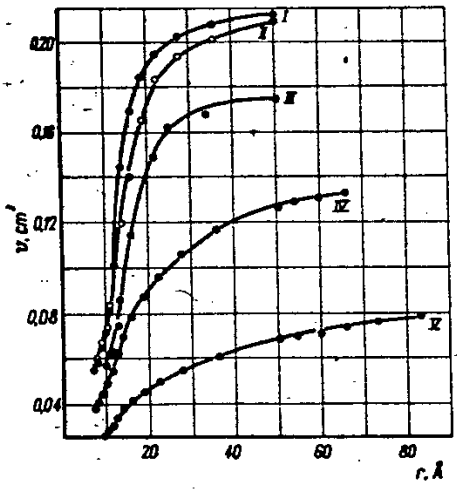

Fig. 5. The volume of capillaries as the function of the capillary radius. Curve I - pure Al_2O_3; curve II - 1.74% Cr, non-calcined; curve III - 8% Cr, calcined at 500°C; curve IV - 6.4% Cr, non-calcined; curve V - 8% Cr, non-calcined.

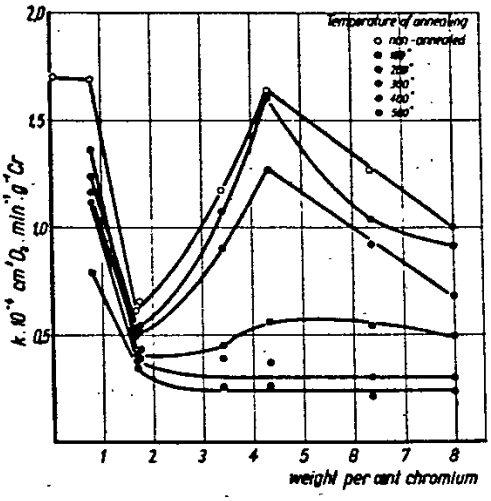

Fig. 6. Specific rate constant of hydrogen peroxide decomposition as the function of chromium concentration. Temperature of the reaction 30°C.

of the space within capillaries as the function of pore radius for several catalysts of various composition. It was calculated from the desorption branches of the hysteresis loops by applying the Kelvin equation

$$\ln\frac{p}{p_0} = -\frac{2V}{rRT}\cos\theta$$

and assuming that $\theta = 90^{\circ}$. The value for the surface tension of argon at -194° used in these calculations was 14.9 dynes/cm and the density value of the liquefied gas was 1.42 [12].

From the saturation value of the adsorption as p approaches p_0 one can estimate the volume of gas, necessary to fill the capillaries on condensation to liquid and thus calculate the total volume of the space within capillaries. The results of these calculations are summarized in column 4 of table 1.

Table 1
Calculations of pore volume and pore radius from adsorption isotherms.

Chromium concentration wt%	Temperature of calcination °C	Specific surface area m^2/g	Adsorption caled as volume of liquid per gram cm^3	Average pore radius Å
1	2	3	4	5
pure Al_2O_3	0	82.6	0.226	54.8
1.74	0	81.1	0.224	55.2
6.40	0	49.3	0.139	58.1
6.40	500	67.1	0.195	56.4
8.00	0	28.4	0.088	62.0
8.00	500	67.5	0.195	57.8

Assuming in the first approximation the tube-like shape of the capillaries one is able to calculate the average radius of the capillary, which equals 2 times the volume-to-surface ratio. The values of r so obtained are given in column 5 of table 1.

The curves represented in fig. 5 clearly indicate that CrO_3 deposited on the surface of alumina plugs at first small capillaries. As its amount increases, capillaries of greater and greater radii are closed and in the preparation, containing 8% of chromium large capillaries dominate. On annealing such samples at 500° larger capillaries re-open and the surface area increases. These processes reflect in the changes of the average radius (cf. table 1) which increases on increasing chromium concentration in the non-calcined samples, and decreases when a sample of high chromium concentration is calcined at high temperature.

We would like here to point out that differentiation of curves represented in fig. 5 leads to the conclusion that greatest values should be ascribed to capillaries whose radius amounts to 12-15 Å. This is in sharp disagreement with the value of the order of 50 Å, calculated from the volume-to-surface ratio. The latter value was however computed on the assumption

that capillaries have the tube-like shape. The discrepancy would be obvious if the capillaries have large bodies but narrow outlets as visualized in the bottle-neck theory of McBain [13]. It must be however emphasized that whatever is the absolute value of the pore radius it does not bear upon the validity of conclusions concerning the changes of the pore radius distribution on depositing CrO_3.

Fig. 6 shows the rate constant of the hydrogen peroxide decomposition, calculated per gram of chromium (for simplicity it will be called specific rate constant) plotted as the function of the concentration of chromium for samples annealed at various temperatures. Samples non-calcined and calcined below the temperature, at which considerable decomposition of CrO_3 begins, differ in their catalytic behaviour from samples calcined at higher temperatures. At first the specific rate constant remains practically constant, decreases sharply at concentrations higher than about 1% and then passes through a maximum at the concentration of about 4%. These two inflection points correspond to the above mentioned two characteristic concentrations of chromium, at which the state of aggregation of CrO_3 changes. It has been found in our previous research [8] that the rate constant of hydrogen peroxide decomposition on chromia catalysts may be related to the concentration of Cr^{+6} ions acting as acceptor centers. It must be emphasized that here the concentration of Cr^{+6} ions remains practically constant, so that in the case of CrO_3-Al_2O_3 catalysts there is no direct proportionality between the rate constant and the concentration of Cr^{+6} ions in contradiction to the results of Matsunaga [2]. The origin of the changes of specific rate constant must be looked for rather in the changes of the state of aggregation of CrO_3. At concentrations lower than about 1% chromium ions occur in the state of atomic dispersion. Each chromium ion may act as an active center of the reaction. Although their concentration changes and so does the absolute activity (cf. fig. 7) the rate constant per gram chromium remains practically constant. At the concentration of about 1% crystal nuclei begin to form. The absolute activity remains now constant but the specific rate constant sharply decreases. It seems more difficult to explain the increase of the absolute activity and of the specific rate constant in the range of 1.5-4% of chromium. Absolute activity may rise because more and more of the surface is covered by crystallites of CrO_3. To account for the increase of specific rate constant the assumption must be made that the activity of Cr^{+6} acceptor centers increases. This conclusion is supported by the decrease of the activation energy of the reaction, beginning at about 1.5%, as shown in fig. 8. The reason of the decrease of activation energy however is not yet clear. At the concentration of about 4% the crystallites begin to grow thicker. The absolute activity attains a constant level, whereas the specific rate constant decreases. The decrease of the activation energy may be compensated by the decrease of the surface area of CrO_3 accessible to the reactants, due to the closing of larger capillaries by growing CrO_3 crystallites.

In the case of samples annealed at higher temperatures the plots of specific rate constant versus concentration show at first a similar pattern to that observed with samples annealed at low temperatures. At concentrations higher than about 1.5% the specific rate constant assumes a low value,

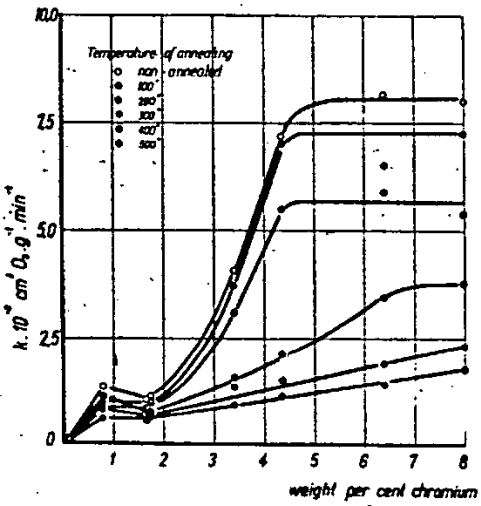

Fig. 7. Rate constant of hydrogen peroxide decomposition as the function of chromium concentration. Temperature of the reaction 30°C.

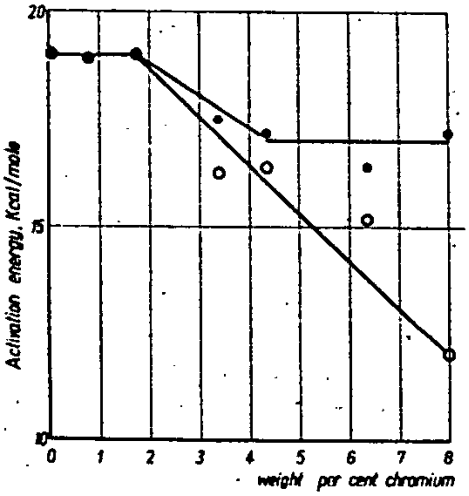

Fig. 8. The activation energy of hydrogen peroxide decomposition as the function of chromium concentration.
○ – non-calcined samples and samples calcined at 100°C and 200°C,
● – samples calcined at 300, 400 and 500°C.

practically independent of the concentration. As discussed above (cf. fig. 2) CrO_3 decomposes at higher temperatures into lower chromium oxides. Apparently chromium ions of lower valency are inactive in hydrogen peroxide decomposition. Certain amount of Cr^{+6} ions appear however on the surface of the crystallites as the result of the surface oxidation and act as active centers of the reaction. It is interesting to mention that the activation energy of about 17 kcal per mole observed for these catalysts is the same as that found for Cr_2O_3 catalysts [8].

Topchiev et al. [6] investigated the behaviour of chromia-alumina catalysts in the polymerization of ethylene and concluded that Cr^{+5} ions are responsible for the catalytic activity. Their catalysts correspond to the range of chromium concentration, wherein the catalysts show only a low activity in hydrogen peroxide decomposition. This indicates to the important role of Cr^{+6}/Cr^{+5} concentration ratio in the selectivity of chromia-alumina catalysts. This problem will be discussed in more detail after completing the investigation of the activity of our catalysts in dehydrogenation of cyclohexane together with measurements of magnetic properties and EPR spectra, which are now being studied.

REFERENCES

1) R.P.Eischens and P.W.Selwood, J. Am. Chem. Soc. 69 (1947) 1590, 2698.
2) Y.Matsunaga, Bull. Chem. Soc. Japan 30 (1957) 868, 984; 31 (1958) 745.
3) V.B.Kazansky, Iu.I.Pietcherskaia and V.V.Voevodsky. Kinetika i Kataliz 1 (1960) 257; 2 (1961) 454; Actes Deuxième Congres Intern. Catalyse, Paris (1960) p. 2121.
4) P.Cossee and L.L Van Reijen, Actes Deuxième Congres Intern. Catalyse, Paris (1960) p. 1679.
5) D.E.O'Reilly, Adv. in Catalysis 12 (1960) 100.
6) K.W.Topchieva, O.K.Sharaiev, A.I.Perelman and A.W.Topchiev, Neftechimia 1 (1961) 780; 2 (1962) 18, 187.
7) R.Fricke and K.Jockers, Z. anorg. allg. Chem. 262 (1950) 3.
8) J.Deren, J.Haber, A.Podgórecka and J.Burzyk, J. Catalysis, in print.
9) J.Deren, J.Haber and J.Sloczyński, Chemia Analit. 6 (1961) 659.
10) B.Kubota, J. Am. Ceram. Soc. 44 (1961) 239.
11) O.Glemser, U.Hauschild and F.Trüpel, Z. anorg. allg. Chem. 277 (1954) 113.
12) P.H.Emmett and T.W.DeWitt, J. Am. Chem. Soc. 65 (1943) 1253.
13) J.W.McBain, J. Am. Chem. Soc. 57 (1935) 699.

Declassified in Part - Sanitized Copy Approved for Release 2014/03/04 : CIA-RDP80-00247A004200070001-6

REGULARITIES OF CATALYSIS ON CHELATE POLYMERS

N. P. KEIER

Institute of Catalysis, Novosibirsk, USSR

Abstract: An investigation was made of the catalytic activity of chelate polymers differing in the ligand. The chelate polymers of transition metals were shown to posses a high catalytic activity, which changes by some orders depending on the chemical nature of the ligand bound with the metal (the donor atoms bound directly with the metal in the chelate group and the organic redical in the polymer chain). It was shown that the influence of the ligand on the catalytic activity is related to the change of the electronic state of the metal. No relation was found between catalytic properties and bulk electrical properties of chelate polymers.

1. INTRODUCTION

Until recently a narrow range of inorganic substances as heterogeneous catalyst were studied: such as metals, oxides and sulfides of metals. Only in the past years, in connection with the development of the electronic theory of catalysis, began the study of organic polymers possessing semiconductor properties (polyacrylonitrill and other) [1, 2].

The synthesis of chelate polymers is one of the new trends in the preparation of polymer materials with a set of specific chemical and physical properties [3, 4]. These substances have a high chemical and thermal stability, their conductivity varies over a wide range depending on their composition [5]. The presence of the metal bound with the donor atoms in the chelate group of the polymer with coordinate bonds makes these substances of particular interest for investigating their catalytic properties. In the same way the metal is bound with active groups of protein in enzymes of oxidation - reduction type. The search for new types of heterogeneous catalysts intermediate between inorganic catalysts and enzymes led us to the study of the catalytic activity of chelate polymers. The first results obtained by us proved that the use of these substances as heterogeneous catalysts might be very promising.

2. CATALYTIC PROPERTIES OF CHELATE POLYMERS

We undertook an investigation of the catalytic activity of chelate polymers which have a doubly charged metal ion in the chelate group. Their general structure may be represented by the following formula:

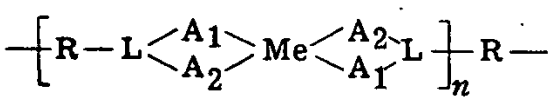

were A_1 and A_2 are the donor atoms entering into the composition of the chelateforming compound (ligard $\begin{matrix}A_1\\A_2\end{matrix}$L-R-L$\begin{matrix}A_1\\A_2\end{matrix}$). A small number of elements may be used as donor atoms: oxygen, sulphur, nitrogen and their combinations. We studied the catalytic properties of chelate polymers presented in table 1, polychelates of various metals: copper, nickel, cobalt, iron, manganese, zinc and cadmium, were used.

Table 1
The list of the chelate polymers studied.

Symbol chelate polymer	The organic combination from which the chelate polymer was synthesed	Symbol chelate polymer	The organic combination from which the chelate polymer was synthesed
I(R)Me	bis-di-tia sodium carbamate	3b(r)Me	Shiff's bases of diacetyl-resorcin
2a(R_ir)Me	bis-tia-amides-α-picolin and 2,6-lutidin	3c(r)Me	Shiff's bases of 55 diasodiphenyl bis salicylic aldehyde
2b(R)Me	poly 44'-bis α tia-amides 2,6-lutidin	4aMe	5,5-methylene bis salicylic aldehyde
2cMe	rubeanic acid	4bMe	dinitroresorcin
3a(r)Me	Shiff's bases of 55'methylene bis salicylic aldehyde	4cMe	trinitroresorcin

An investigation was carried out of the decomposition of hydrazine in the gaseous phase; this reaction gives the possibility of tracing the change in the catalytic activity of the various polychelates and their influence on the selectivity of the process because the decomposition may proceed in two ways.

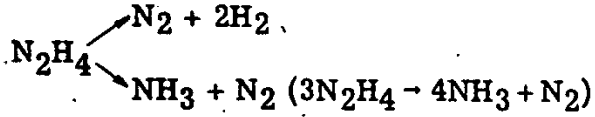

The decompositon reaction of hydrogen peroxide was investigated in the liquid phase. This reaction was of interest as it served as model for the action of the enzyme of catalase.

2.1. *Decomposition of hydrazine*

The investigation of chelate polymers of identical chemical composition and structure differing only in the metal atom of the chelategroup showed that the catalytic activity is determined primarily by the metal atom of the group [6].

All zinc and cadmium polychelates were catalytically inactive. The activity of polychelates of copper, nickel, iron and cobalt depended on the ligand bound with the metal in the polymer and varied over a wide range from zero upwards. Besides, for the group of polymers 2a(R, r)Me the catalytic activity was investigated before the introduction of the metal. There was no catalytic activity. For hydrazine decomposition it was shown that the catalytic activity and selectivity of the catalytic action was determined for polychelates of a given metal by the nature of donor atoms bound with the metal of the chelate group [11, 12]. The nature of the organic radical in the polymer chain exercised a decisive influence on the catalytic properties of the polymer.

On all catalytically active polychelates hydrazine decomposition starts with its irreversible chemisorption. Hydrazine desorption proceeds only with its decompositon to the products of the reaction. For polychelates, which provide hydrazine decomposition to ammonia and nitrogen chemical, adsorption of ammonia is observed. For the polychelate $I(R_3)Co$ chemisorption of ammonia is more than 50% coverage, calculated on the metal located in the chelate groups on the surface, considering that one center adsorbs one molecule. This ammonia is strongly chemisorbed and is removed only partially by evacuation at 110°C. The decomposition reaction of hydrazine is stopped by adsorbed ammonia, which shows that hydrazine adsorption and its decomposition occur at the same centers where there is strong adsorption of ammonia. Outgassing occurring at 130° restores the activity of the sample in the decomposition reaction of hydrazine. The reaction proceeds almost to 100% in the direction of the formation of ammonia.

2.2. *Decomposition of hydrogen peroxide*

Many polychelates had a high catalytic activity in this process. There was observed partial dissolving of some polychelates, undissolved in water, during the reaction apparently under the influence of hydrogen peroxide.

For the elucidation of regularities of the heterogeneous reaction in these cases the rates of heterogeneous and homogeneous reactions were determined separately. Many polychelates could not be dissolved and behaved in a process only as heterogenous catalysts. The non-radical-chain nature of hydrogen peroxide decomposition was established by means of adding the strongest inhibitor of the chain process of hydrogen peroxide decomposition-phenol-into the reaction solution. According to the literature data phenol in 0.01 mol/l concentration inhibits the process of hydrogen peroxide decomposition completely [15]. For some of the most catalytically active catalysts the control showed the absence of inhibition of hydrogen peroxide decomposition after adding phenol in the 0.022 mol/l concentration and higher ones. The influence of phenol in the concentration of 0.0245 mol/l on the rate of the process was also tested at high *p*H equal to 11.8 in the samples 4bCu, $I(R_3)Cu$, $I(R_3)Co$ when the rate of heterogenous process of hydrogen peroxide decomposition reaches 10^3 mole/seccentr. In this case, also the addition of phenol did not influence the decomposition rate showing the absence of the participation of the radical-chain mechanism of the decomposition in the process of heterogenous catalytic dissociation of hydro-

gen peroxide on the polychelates of copper and cobalt. For reactions of hydrogen peroxide decomposition in the presence of polychelates of various metals bound with various ligands 3 main dependences, similar to those found out earlier for hydrazine decompositing, were elucidated:

1) The catalytic activity is defined by the metal entering into the chelate group. The activity of polychelates of a definite metal depends on the chemical composition of the ligand bound with it:

2) Atoms of ligands directly bound with the metal in the chelate group.

3) The organic radical entering into the main or side chain of the polymer.

The study of the dependence of the rate of hydrogen peroxide decomposition on the concentration of peroxide and the *p*H of solution has showed that various polychelates behave differently. For example, for polymer 3a(r,)Cu the order close to the first was found for the dependence of the rate on the concentrations of hydrogen peroxide (see equations 1). For the sample 4bCu and I(R_2)Cu the dependence of the decomposition rate on the concentration of hydrogen peroxide corresponded to the second order (of equations 2)

$$1.\ W = K_1 [H_2O_2]^{1.2}$$

$$2.\ W = K_2 [H_2O_2]^2$$

By the nature of the influence of the *p*H of the solution on the rate of hydrogen peroxide decomposition one can judge the stage mechanism of hydrogen peroxide decomposition. In fig.1 the dependence is given of the decomposition rate on *p*H of the solution for the polychelates studied. In the presence of the polychelate 4bCu the decomposition rate increases linearly with the increase in *p*H from 1 to 9. For the polymer 3a(r,)Cu the dependence on *p*H has maximum in the region *p*H equal to 4-6. The increase of the decomposition rate with the increase of *p*H medium indicates the participation of dissociation ions HOO^- in the reaction. The participation of HOO^- ions in homogeneous catalytic process of hydrogen peroxide decomposition was postulated by many authors, in particular, by Nikolaev for hydrogen peroxide decomposition of copper ammonium [16]. When investigating hydrogen peroxide decomposition in the presence of iron ions in the solution, the intermediate complexes of iron ions with ion HOO^- were observed by spectroscopic methods [17, 18].

The mechanism of heterogenous decomposition of hydrogen peroxide in the presence of polychelates may be presented by the following steps [16, 18].

$$1.\ H_2O_2 \rightleftharpoons H^+ + HOO^-$$
$$2.\ \Pi + HOO^- \rightleftharpoons [\Pi HOO^-]$$
$$3.\ [\Pi HOO^-] + H_2O_2 \rightarrow H_2O + O_2 + OH^- + \Pi$$
$$4.\ OH^- + H^+ \rightleftharpoons H_2O$$

Assuming that equillibrium value of chemisorption on the polymer catalyst surface is in conformity with the equilibrium isotherm of Lengmuir for the equilibrium concentration of adsorbed ion OOH^- on the surface, we get the equation:

$$[\Pi\,OOH^-] = \frac{V_m\, b[HOO^-]}{1 + b[HOO^-]} \qquad (1)$$

we suppose that we may neglect adsorption of H_2O and OH^- compared with the adsorption of the ion (HOO^-) in the presence of measurable concentrations of HOO^- ions. If the adsorption of HOO^- ions is great and reaches saturation then the equation of equilibrium adsorption takes the form:

$$[\Pi\,OOH^-] = V_m \qquad (2)$$

since the value in $b[HOO^-] > 1$ V_m- the value corresponding to coverage of all adsorption centres on the surface, and equal to the number of chelate groups with a metal on the polymer surface is designated by us N_{sme}. In this case the rate of the decomposition reaction is defined by the third stage of interaction of a surface sample with hydrogen peroxide molecule according to the equation

$$W = K_3\, N_{sme}\, [H_2O_2]\,. \qquad (3)$$

In the region where adsorption is small $b[HOO^-] < 1$

$$[\Pi\,HOO^-] = V_m\, b[HOO^-]\,. \qquad (4)$$

In this case, the equation for hydrogen peroxide decomposition is

$$W = \frac{d[H_2O_2]}{dt} = K_3\, N_{sme}\, b[HOO^-]\,[H_2O_2] \qquad (5)$$

substituting

$$[HOO^-] = \frac{K_{diss}[H_2O_2]}{[H^+]} = K'[H_2O_2]$$

we get the equation for the decomposition rate

$$W = K_3\, N_{sme}\, b\, K'[H_2O_2]^2 = K_6[H_2O_2]^2\,. \qquad (6)$$

From the equations 3 and 6 we have the kinetic equation for hydrogen peroxide decomposition 3' and 6'

$$\ln[H_2O_2]_t = K_3\, t + \ln C_o \qquad (3')$$

$$C_o = [H_2O_2]_{t=0}\ \frac{1}{[H_2O_2]_t} = K_6\, t + \frac{1}{C_o} \qquad (6')$$

The course of the reaction measured in the process of hydrogen peroxide decomposition by the volume of liberated oxygen on the samples 3a(r,)Cu and 4bCU as it is seen from figs. 2 and 3 corresponds to the equation (3' and 6'). For the sample 4bCu where there is the first order of dependence of the reaction rate on the concentration of hydrogen peroxide due to strong adsorption of HOO^- ion the dependence of the reaction rate on the *p*H medium is weak. The reaction rate, in this case, is defined by the stage of interaction of intermediate complex with hydrogen peroxide. Apparently, in this case too the mechanism is the same from which we may judge by the dependence of the decomposition rate *p*H within the ranges *p*H below 5. Some decrease in the rate in the region above 6 may be associated with the decrease in the concentration of non-dissociated hydrogen peroxide, the in-

teraction which defines the reaction rate in accordance with eq. 3.

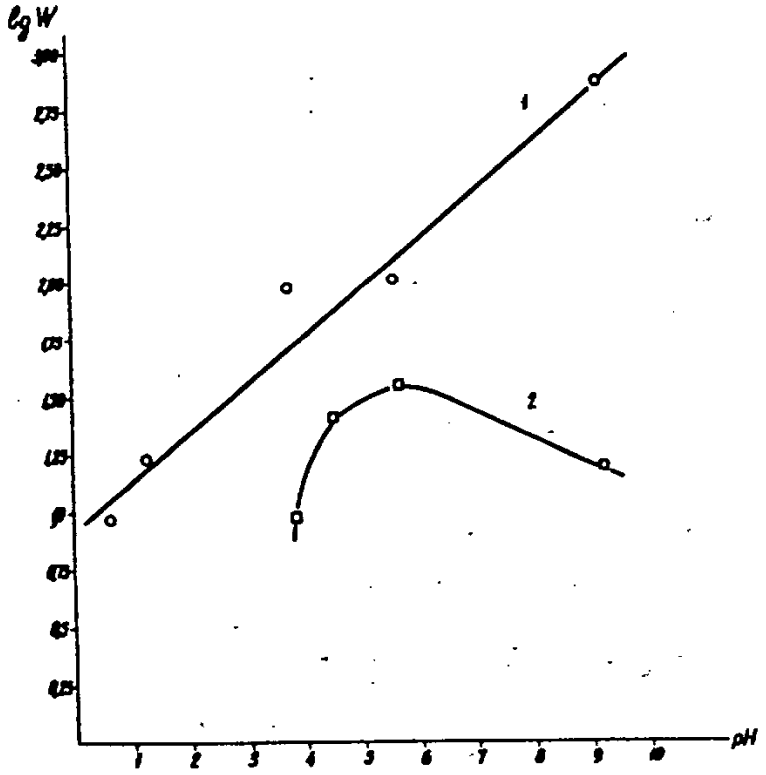

Fig. 1. Rate dependence of heterogeneous decomposition of hydrogen peroxide on *p*H solutions of the samples:
1. 4bCu 2. 3a(r_1)Cu
T = 60° $[H_2O_2]_o$ = 3.3 mol/l

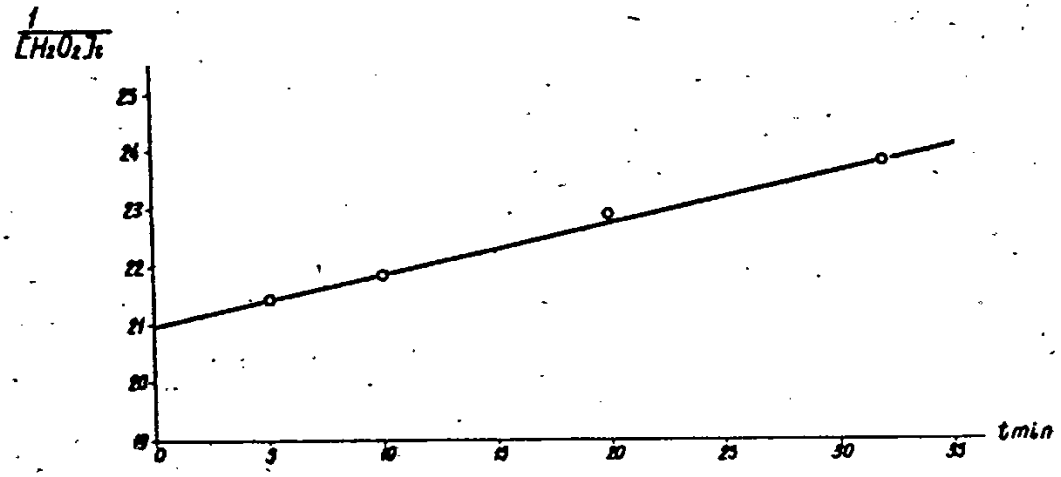

Fig. 2. Kinetics of hydrogen peroxide decomposition for the polymer 3a(r_1)Cu according to eq. (3)
T = 60° $\log [H_2O_2]_t = kt + \log C_o$; $[H_2O_2]_o = C_o$ = 4.7 mol/l

For the sample 4bCu the increase of reaction rate with an increase in *p*H in the whole region investigated shows the absence of saturation of adsorption for HOO^- ion, adsorption of which defines apparently, the reaction rate.

Evidently the rate of the 3d stage of interaction of intermediate adsorption complex with the molecule H_2O_2 proceeds fast in this case and doesn't define the rate of the process. The process of decomposition as a whole on this polymer proceeds with a higher rate.

It should be noted that catalytically inactive samples remained inactive even at high *p*H. Apparently, adsorption of OOH^- ion on the metal of the chelate group was absent in this case.

It is of interest to trace the activity of chelate polymers of various metals in this reaction. The most active catalysts were copper polychelates which in accordance with the composition of donor atoms in the chelate group yield the series Cu2(OO) > Cu2(NS) > Cu2(NO) > Cu(SS).

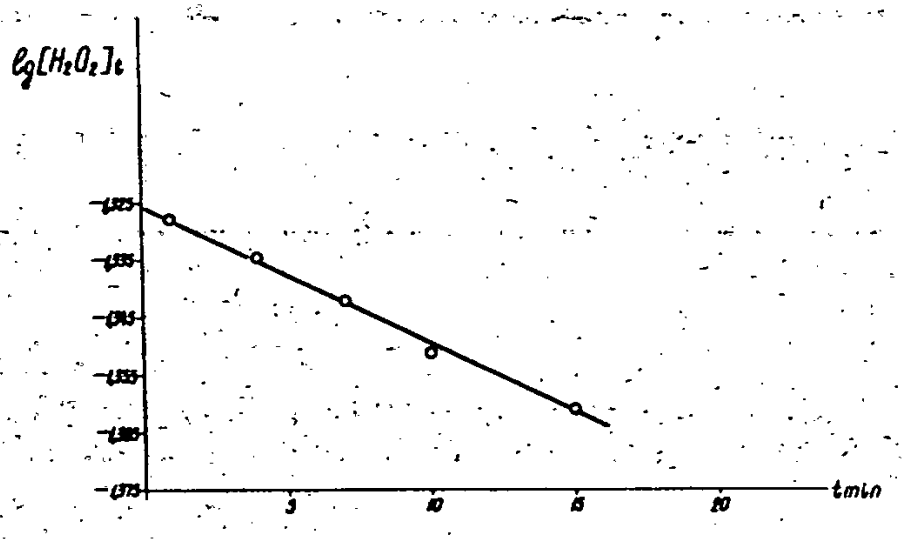

Fig. 3. Kinetics of the process of hydrogen peroxide decomposition for the polychelate 4bCu according to eq. (6).

$$\frac{1}{[H_2O_2]_t} = kt + \frac{1}{C_o} \qquad T = 60^o$$

$[H_2O_2]_o = C_o = 4.7$ mol/l

$[H_2O_2]_t$ = mol/l $\times 10^{-2}$

Then iron polychelates being the next Fe2(NO) > Fe2(OO) and the polychelates Fe2(NS) are inactive. Among cobalt polychelates Co2(SS) > Co2(NS) are active, nickel polychelates are active only in the structure. Ni2(OO). Nickel polychelates in the structures Ni2(NO) and Ni2(NS) and Ni2(SS) - are catalitically inactive. More active polychelates of various metals yield the series Cu2(OO) > Fe2(NO) > Co2(SS) ~ Mn2(NO) > Ni2(OO).

Various metals have the highest possible catalytic activity in the structures of polymers differing by donor atoms in the chelate group and organic radicals in main and side chains of the polymer.

3. DISCUSSION OF RESULTS

Comparison of catalytic activity of copper polychelates of different chemical composition and structure and catalytic activity of polychelates of various metals with their electrical conductivity shows the absence of any correlation between them. This fact prevents relating the mechanism of catalytic effect of chelate polymers to the type of "semiconductor" catalysis [19-22] widely discussed in literature.

The latter is associated with chemisorption of the reacting substances with the formation of bonds which are more ionic in character.

The non ionic nature of bonds of the chemisorbed molecule of hydrazine with the metal in the chelate group of the polymer formed during hydrazine on the copper polychelates of the group 1(R)Cu is not accompanied by a considerable change of resistance of the sample. Only in one case for the polychelate $1(R_5)Cu$ a weak decrease of resistance is revealed within the range of 5% in comparison with the initial resistance of the sample, 10^7 ohm. Generally chemisorption accompanied by electron transfer leading to the formation of an ionic bond of the sorbed molecule on contact with the oxide semiconductor causes a great change in the resistance value by 1-2 and more orders. The increase or decrease proceeds according to the direction of electron transfer and the type of conductivity of the semiconductor contact. A slight change of the resistance observed during hydrazine chemisorption may be a second rate factor due to hydrazine chemisorption with the formation of coordination ore covalent bond. Strong influence of the ligand: donor atoms bound with the metal in the chelate group and the organic radical in the polymer chain shows the dependence of the catalytic properties on the electronic state of the metal.

For experimental elucidation of this topic the study of polychelates by physical methods was made. The magnetic properties of polychelates of the group $2a(R_1r)Cu$ were studied by the electron paramagnetic resonance (EPR) methods and by the measurements of magnetic susceptibility. The X-ray spectroscopy method was used as well. According to the data of Anufrienko a great change of band width in the EPR spectrum from 15 to 60 Oe is observed when investigating copper polychelates of the structure $2a(R_1r)Cu$ differing by the organic radical R in the main polymer chain. The change of the band width justifies the influence of the organic radical on the intensity of electron exchange between copper ions possessing an unpaired electron located in the chelate groups of the polymer. In recently published investigation by Eation, Josey, Phillips and Benson[23] of nickel chelate complexes by the nuclear magnetic resonance method (NMR), the influence of the chemical composition of the organic radical on the transfer and distribution of electron density of an unpaired electron of nickel ion (spindensity) on the ligand was shown.

Appearantly a similar phenomenon occurs, to a greater extent, in chelate polymers with a change in the ligand: donor atoms in the chelate group and with a change in the organic radical. The first results obtained for the influence of the organic radical on the EPR spectrum completely confirm this supposition.

An investigation was made of the fine structure of X-ray k-absorption spectrum of copper in polychelates obtained on the base of sodium bis-dithiocarbamate with the chelate group Cu(SS) by us. Polychelates contained in the main chain of the polymer organic radicals of aliphatic or aromatic composition were studied. As radicals of aliphatic species dimethyl (R_2) and hexamethylen (R_3), and for aromatic species phenyl (R_4) and diphenyl (R_5) were used.

Replacement of the organic radical in the chain of the polymer with a constant composition of the surroundings immediate to the atom of copper was found to change the X-ray k-absorption spectrum of copper in the chelate group. Fig.4 gives the spectra measured for the above mentioned polychelates. For comparison, in the same figure the spectrum of metallic

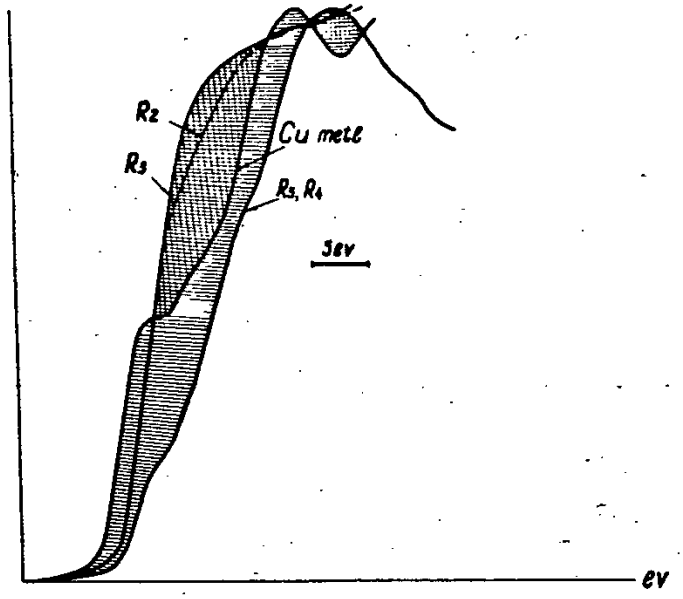

Fig. 4. Comparison of the original region of the X-ray spectrum of absorption of copper in metal and in polychelates of I(R)Cu structure with various organic radicals in the polymer chain.

copper is shown. Great differences in the intensity of X-ray k-absorption edge in the initial and middle regions for polymers containing aliphatic and aromatic radicals can be seen. The introduction of the aliphatic radicals R_2 and R_3 causes intensification of absorption of copper in the chelate group in the initial and middle region. The radicals of aromatic composition have an opposite effect, weakening the absorption of copper in the initial and middle region. Moreover in both cases the point of bending on the curve of the absorption edge (which is usually identified with the Fermi level) is displaced by 1.5 eV to the side of short waves in comparison with that of metallic copper. Analogous displacement by 1.2 eV takes place for cuprous oxide containing copper with the charge Cu^+. So the charge of copper in polychelates is close to unity Cu^+, which correlates with the data of the chemical analysis.

The curves of the k-absorption edge for the aromatic radicals R_4 and R_5 nearly coincide. For the aliphatic radicals, R_2 and R_3, some increase of the effect with the growth of chain length takes place. When the transition

from the radical R_2 to R_3 takes place the intensity of the k-absorption edge of copper increases slightly.

The initial long wave region of absorption according to modern concepts, appears when the transition of the electron in absorbing the atom into 3d, 4s, 4p free states, takes place.

Transition into 3d and 4s levels are forbidden by the selection rules. For free atoms this causes the appearance of bands of very weak intensity differing by 2 or more orders compared with that of bands corresponding to the transitions allowed by the selection rules. In solids and molecules these selection rules become less strict, very often due to the presence of hybridization of electron states of various symmetry in the crystal field or ligand-field (in the case of complexes). This leads to a comparative increase of the intensity of the initial region of X-ray k-absorption and the rise of dependence of the structure of the X-ray k-absorption edge on the degree of hybridization of wave functions of variable symmetry appearing in the process of interatom interaction. Using these concepts for explaining the results obtained we arrive at the conclusion that the presence of organic radicals of aromatic composition R_4 and R_5 in the polymer chain leads to the decrease of intensity of 1s electron transition into 4p states and for the aliphatic radicals R_2 and R_3 the intensity of this transition increases. Such a result may be explained by the difference in the degree of hybridization 4s and 4p of electron states leading to the growth of absorption intensity in unoccupied hybrid orbits in the case of aliphatic radicals. Another possible explanation is that the change of radicals influences the π-bonds of the ligand with hybrid Sp electron states of the metal, and that may also cause the change of intensity of k-edge X-ray absorption.

However, in both cases, quite apart from the interpretation of the spectrum, the electron state of the central copper ion in the chelate group changes.

The differences in effect of aromatic and aliphatic radicals in the polymer chain, the nature of interaction of copper with addendum atoms in the polychelates, as is clearly seen in the structure of X-ray k-absorption spectra of copper, are all reflected in the change of the catalytical activity of the above mentioned polychelates. For the decomposition of hydrazine the radical affects the direction and velocity of the decomposition of hydrazine.

For polychelates with the aromatic radicals R_4 and R_5 in the polymer chain strong decomposition of hydrazine to hydrogen and nitrogen without the formation of ammonia takes place. For polychelates with the radicals R_2 and R_3 the decomposition proceeds to 50 and 12% respectively with the formation of ammonia.

For the decomposition reaction of hydrogen peroxide the given preparations differ in activity too. Polychelates containing the aromatic radicals R_4 and R_5 in the polymer chain have a specific catalytic activity which exceeds the activity of the polymer with the aliphatic radical R_2 by more than an order.

It is possible that the nature of hybridisation has an effect on the strength of the bond of intermediate adsorbing complex of the reacting molecule on

the copper centre. As intensive chemical adsorption of hydrazine is not accompanied by the change of electrical conductivity it may be carried out as a donor, coordination bond using unfilled hybrid orbitals of the copper centre. The character of the bond of the complex with a reacting molecule must effect the direction of decomposition- that is the selection of the process and the rate of the reaction as well. For a more detailed elucidation of the observed correlations a further investigation is required.

Thus the data first obtained confirm the hypothesis made in 1961 that the catalytic activity is defined by the electronic state of a metal in the chelate group depending on the donor atoms and the radicals in the polymer chain bound with it.

REFERENCES

1) A.V.Topchiev, M.A.Geiderikh, B.E.Davydov, V.A.Kargin, B.A.Krentsel, Y.M.Kustanovich and L.S.Polak, Dokl. Akad. Nauk SSSR 128 (1959) 312.
2) E.S.Dokukina, S.Z.Roginskii, M.M.Sakharov, A.V.Topchiev, M.A.Geiderikh, B.E.Davydov and B.A.Krentsel, Dokl. Akad. Nauk SSSR 137 (1961) 893.
3) A.A.Berlin and N.G.Matveev, Usp. Khim. 3 (1960) 777.
4) A.P.Terent'ev, V.V.Rode and E.G.Rukhadze, Vysokomolek.soed. 2 (1960) 1557.
5) A.P.Terent'ev, V.V.Rode, E.G.Rukhadze, V.M.Vozzhennikov, Z.V.Zvonkova and L.Y.Badzhadze, Dokl. Akad. Nauk SSSR 140 (1960) 1093.
6) N.P.Keier, G.K.Boreskov, V.V.Rode, A.P.Terent'ev and E.G.Rukhadze, Kinetika i Kataliz 2 (1960) 509.
7) A.P.Terent'ev, E.G.Rukhadze, G.V.Panova and I.G.Mochaliva, Vysokomolek. soed. 5 (1963) 842.
8) A.P.Terent'ev, V.V.Rode and E.G.Rukhadze, Vysokomolek. soed. 4 (1962) 91.
9) G.K.Boreskov, N.P.Keier, L.F.Rubzova and E.G.Rukhadze, Dokl. Akad. Nauk SSSR 144 (1962) 1069.
10) N.P.Keier, G.K.Boreskov, L.F.Rubzova and E.G.Rukhadze, Kinetika i Kataliz 3 (1962) 680.
11) N.P.Keier, M.G.Troizkaya and E.G.Rukhadze, Kinetika i Kataliz 3 (1962) 69.
12) N.P.Keier and M.G.Troizkaya, Kinetika i Kataliz (1963), in press.
13) N.N.Semenov, Zepnyc reakcii. Gost. Khimizdat. Leningrad.
14) V.J.Vedeneev, G.N.Gerasimof and A.P.Purmal, Zhur. Fiz. Khim. 31 (1957) 1216.
15) M.G.Evans, P.Georg and N.Uri, Trans. Faraday Soc. 45 (1949) 230.
16) L.A.Nikolaev, Zhur. Fiz. Khim. 25 (1951) 712; J. chim. phys. 51 (1954) 1, 752.
17) M.L.Haggett, P.Jones and W.F.K.Wynne-Jones, Disc. Faraday Soc. 29 (1960) 153.
18) Kremer and Stein, Trans. Faraday Soc. 55 (1959) 953.
19) F.F.Volkenstein, Zhur. Fiz. Khim. 23 (1949) 917.
20) F.F.Volkenstein, Electron theory catalysis of the semiconductors, (Moscow, 1960).
21) S.Z.Roginskii, Kinetika i Kataliz 1 (1960) 15.
22) H.G.Hauffe, Angew. Chem. 67 (1955) 189.
23) D.R.Eaton, A.D.Josey, W.D.Phillips and R.E.Benson, Disc. Faraday Soc. 34 (1962) 77.
24) R.G.Akopdjanov, E.E.Vajnstein, N.P.Keier and L.M.Kefeli, Kinetika i Kataliz (1963) in press.

ELEMENTARY MECHANISM OF HETEROGENEOUS CATALYTIC POLYMERIZATION OF ETHYLENE OXIDE

O. V. KRYLOV, M. J. KUSHNEREV, Z. A. MARKOVA and E. A. FOKINA

Abstract: Polymerization of ethylene oxide on the surface of a number of solid oxides, hydroxides and carbonates has been studied. Catalysts having cations of high e^2/r value are most active. Compounds of Fe^{3+} are most active among transition metal compounds. The study of modification of the surface of Al_2O_3 by different groups demonstrated that they affect mainly the value of k_o but not the activation energy of chain growth. Infrared spectroscopic study demonstrated that during adsorption and polymerization of C_2H_4O the surface groups are not disturbed and no hydrogen bonds formed.
From these and other data it has been assumed that surface unscreened cations are active centres of polymerization. The number of active centres on Al_2O_3 and MgO have been estimated from adsorption data and from molecular weight measurements. Mechanism of the process is given. Initiation of the polymerization process takes place at the free valencies on the partly dehydrated catalyst surface. As the chain grows, monomer molecule forms a coordination bond with the surface cation and after that enters the polymer chain. Chain termination is more often due to the action of the substances containing the hydroxyl.

1. INTRODUCTION

Polymerization reaction of ethylene oxide on the surface of solid oxides, hydroxides and metal carbonates is one of the few polymerization reactions resulting in the formation of polymers of a molecular of 10^{-4} - 10^{-7} weight on common (noncomplex) catalysts. As modelling is rather simple in this case its study can furnish valuable data not only on the mechanism of heterogeneous polymerization but on the nature of the catalytic surface of oxide and hydroxides.

High molecular polymers of ethylene oxide were originally obtained in the research [1] when solid strontium carbonate was used as a catalyst. Since then Japanese scientists have carried out a large number of experiments with solid polymerization catalysts (see ref. [2] for example). The authors of the present paper and Sinyak in a number of papers [3,4] have proved that ethylene oxide polymerization can take place on a large number of various oxides, hydroxides and metal carbonates. The rate of polymerization on the most active of them, namely BeO, MgO, Fe_2O_3 at 90 - 100° was nearly the same as that of reaction [1] on $SrCO_3$, but unlike the latter these oxides catalyzed the reaction to a considerable rate even at room temperature due to lower energy of activation (9-14 kcal/mole^{-1} instead of 20-22 kcal/mole^{-1} for $SrCO_3$).

2. REGULARITIES IN THE CATALYTIC ACTIVITIES

Some available data on the mechanism of the reaction can be of value when considering regularities in the selection of catalysts. According to our data the regularities in the selection can be explained by the fact that monomer activation takes place as a result of its linkage with the catalyst cation. Compounds of metals whose ions have higher value of e^2/r, namely Be^{2+}, Mg^{2+}, Fe^{3+}, Al^{3+} are most active. In the range of $Be(OH)_2$, $Mg(OH)_2$, $Ca(OH)_2$, $Sr(OH)_2$, $Ba(OH)_2$, the rate of polymerization at low temperatures decreased due to the increase in the energy of activation of polymer chain growth and the decrease in the activity of unit centre. The same variations in the activity have been found in the range of BeO → BaO.

Of considerable interest were the regularities in the activities of hydroxides of transition metals (see fig. 1). The most active catalysts among

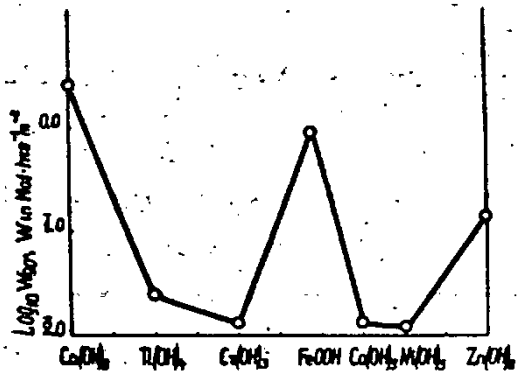

Fig. 1. The change of specific catalytic activity in a series of metal hydroxides of IV period.

them were FeOOH, $Zr(OH)_4$, $Th(OH)_4$, i.e., compounds of cations with electronic states d^0 and d^5. Dowden and Wells [7] have noted that in a number of redox reactions cation configurations d^0, d^5, d^{10} show very low catalytic activity in the range of transition metal compounds. They attributed that fact to the absence of stabilization energy of the crystal field. In our case, crystal field stabilization is likely to be a factor unfavourable for catalysis. Structures d^0 and d^5 as regards their activity in the redox reactions were in the same group as the non-transition metal compounds but were found to possess not minimum but maximum of catalytic activity. Manganous oxide of electronic structure d^5 exhibited, however, low activity. The studied sample obtained by decomposing $MnCO_3$ showed activation energy of 9.7 kcal/mole^{-1} which was nearly equal to that of the most active catalysts, but its value for k_0 (~ 10 min^{-1}m^{-2}) was very low.

3. EFFECT OF VARIOUS SURFACE GROUPS ON CATALYTIC ACTIVITY

On decomposing hydroxides and carbonates as for example when converting $Be(OH)_2$ → BeO, $MgCO_3$ → MgO catalytic activity increases continuously. The calculation [5] shows that the number of active polymerization

centres is approximately equal to the number of surface unscreened metal ions, i.e., to the number of metal ions which become free from OH or CO_3 groups.

The effect of modifying the surface of Al_2O_3 by other groups on its catalytic activity has also been studied. Reaction kinetics have been studied on the basis of the catalyst overweight on the pan of MacBain quartz balance at constant ethylene oxide pressure (from 2 to 100 mm Hg). Such techniques of studying kinetics avoids chain termination in the course of the polymerization. Chain growth constant k_g does not differ much from the k_g in the liquid-phase polymerization.

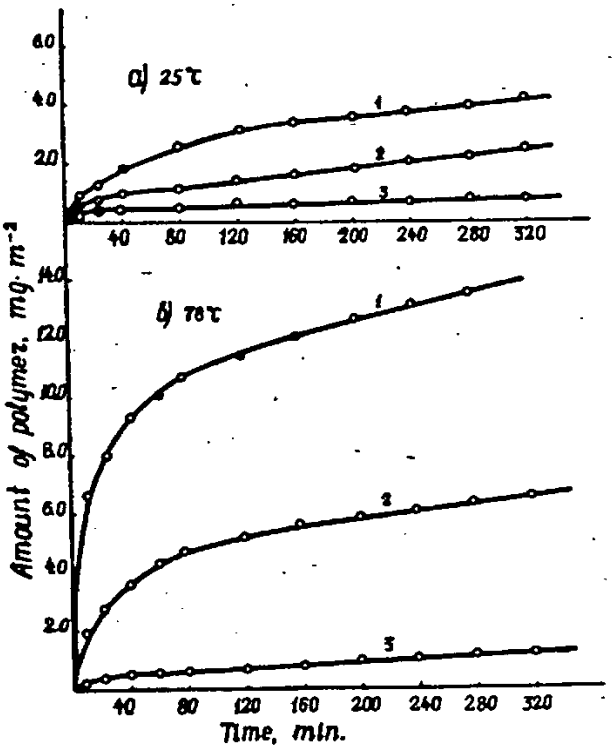

Fig. 2. Kinetic curves of ethylene oxide polymerization (a) at 25°, (b) at 78° on catalysts (1) Al_2O_3, (2) Al_2O_3·HCl, (3) Al_2O_3:BF_3.

Fig. 2 shows kinetic curves of adsorption (polymerization) of ethylene oxide at 25°C (fig. 2a) and 78°C (fig. 2b) on the three samples of aluminium oxide: (1) Al_2O_3 activated in an air stream at 500°C for 10 hours with a surface of 180 m^2, (2) The same Al_2O_3 treated with HCl (0.6 millimoles per 1 g of catalyst) and (3) the same Al_2O_3 treated with BF_3 at pressure of 15 mm for 20 minutes*. In the experiments shown in fig. 2 the pressure of ethylene oxide was kept constant and was equal to 10 mm. A study of the pressure effect showed that the rate of reaction increases linearly with the pressure increase up to 20 - 30 mm Hg (Henry region) and becomes inde-.

* The authors are much obliged to prof. K. V. Topchieva and T. V. Antipina for furnishing these samples.

pendent from pressure at 70 - 100 mm Hg. As stated in the research [5], the decrease in the rate at the beginning of the process was due on the one hand to the fact that the total rate of adsorption and polymerization was measured first and on the other hand due to the formation of solid polymer film on the catalyst. When the formation of that solid film is completed the rate becomes constant at P = const.

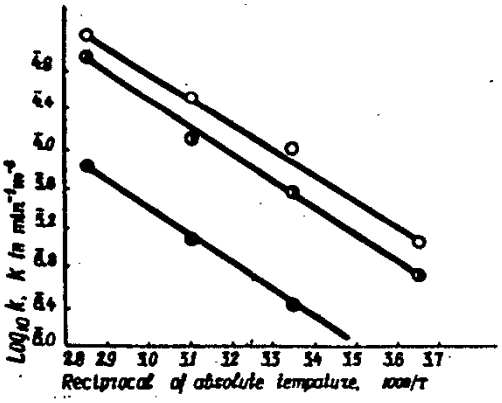

Fig. 3. The change of rate constant logarithm with reciprocal temperature on (1) Al_2O_3, (2) Al_2O_3·HCl, (3) Al_2O_3·BF_3.

Fig. 3 shows the dependance of the logarithm of rate constant of the first order calculated for the first state of the process (when there is no solid film) on the inverse temperature. From these data it has been calculated (1) for Al_2O_3·HCl E_1 = 11.3 kcal/mole^{-1}, lg k_0 = 3.8; (2) for Al_2O_3·HCl E_1 = 11.9 kcal/mole^{-1}, lg k_0 = 3.5; (3) for Al_2O_3·BF_3 E_1 = 11.6 kcal/mole^{-1}, lg k_0 = 2.3. For the second stage of the process (diffusion through the film) the value E_2 is 6.1; 7.3; 4.1 kcal/mole^{-1} respectively. It has been demonstrated [5] that the decrease of the activation energy during the formation of the solid film of the polymer was not caused by the conversion into the diffusion region but by the decrease of equilibrium concentration of monomer over the catalyst. The difference $E_1 - E_2$ = 4 - 7.5 kcal/mole^{-1} should be equal to the heat of solution of the monomer in polymer Q_s. Measurement of temperature dependance of the solubility of the monomer in polymer produced Q_s, being equal to 7 kilocalories per mole.

When modifying Al_2O_3 under the action of BF_3, protonic acidity of the catalyst [8] increases owing to the formation of the surface compound Al - O^{H} : BF_3. The mobility of the proton in the surface OH - group increases in this compound. Proton-acid centres can be formed also when HCl acts on Al_2O_3. From the data obtained by us it can be seen that the energy of activation of polymerization of ethylene oxide, when modifying the surface of Al_2O_3, does not change but the activity decreases owing to the decrease in k_0. Evidently, the proton-acid centres are not active polymerization centres. The decrease in activity noted, when treating the surface of Al_2O_3 with HCl and BF_3, is due to the screening of active centres which is greater in the case of the larger molecule BF_3.

Fig. 4 shows kinetic curves for polymerization which was carried out under similar conditions at 25°C and at ethylene oxide pressure of 10 mm Hg

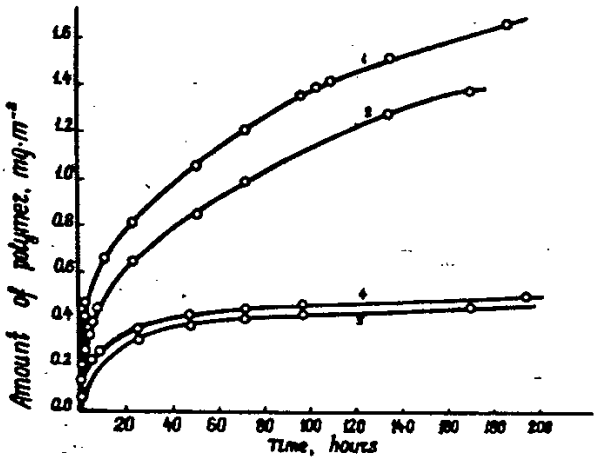

Fig. 4. Kinetic curves of ethylene oxide polymerization at 25° and 10 mm Hg on (1) Al_2O_3, (2) silica-alumina, (3) silica gel, (4) methylated silica gel.

on Al_2O_3 (curve 1), silica-alumina (curve 2), silica gel (curve 3) and methylated silica gel (curve 4). The latter sample was kindly furnished by prof. I. E. Neumark (the technique of its preparation is described in [9]). The quantity of the polymer formed has been calculated in all cases in per 1 m^2 of surface. From these data it will be seen that silica-alumina is somewhat less active than Al_2O_3. Silica gel is much less active. Methylating of silica gel did not deteriorate its catalytic properties. Thus, these data indicate that it is not the HO-group that is an active centre but rather the surface cation.

Molecular weight of a polymer is determined from the viscosity of aqueous solutions (see [5]). As practically there was no termination of the chain in the experiments on polymerization from the gaseous phase, these experiments allow us to determine the number of active centres by dividing the weight of the polymer by its molecular weight. In polymerization on Al_2O_3 the number of active centres found in that way was equal in the experiments at 0°C to 2.7×10^{14} cm^{-2}, at 22°C to 3.9×10^{14} cm^{-2}, at 50°C to 1.5×10^{14} cm^{-2}, at 80°C to 1.7×10^{14} cm^{-2}, on the average it equalled about 2×10^{14} centres per 1 cm^2 of Al_2O_3. The number of active centres does not depend upon temperature.

It is of interest to compare the found values of E and k_0 on previously found catalysts. On $Be(OH)_2$ E = 9.0 kcal/mole^{-1}, lg k_0 = 3.9; on FeOOH E = 8.5 kcal/mole^{-1}, lg k_0 = 3.1. Thus, altering the metal cation affects mainly the energy of activation. Variations of k_0 can be explained by the variations in the number of active centres.

Higher values of E(16 - 22 kcal/mole^{-1}) and higher values of k_0 (by 2-3 orders higher) have been obtained on base catalysts: BaO, SiO, CaO, $Ca(OH)_2$, $CaCO_3$. The number of active centres calculated from the data on molecular weight was even somewhat less than on Be-, Mg-, Fe-, Al-catalysts and was in the neighbourhood of 2×10^{13} cm^{-2}. The reasons for this have not been understood yet. It is probable that the number of active centres on the solid base increases as the temperature increases too. It is

also probable that the polymerization proceeds on them according to some different mechanism.

4. SPECTROSCOPIC AND X-RAY STUDY

Infrared studies carried out previously [6] demonstrated that adsorption of a molecule of ethylene oxide without breaking the ring precedes its addition to the polymer chain. A study of the change of state of surface groups of the catalyst itself in the course of adsorption and polymerization of ethylene oxide was of particular interest. The technique of carrying out infrared spectra in the process of adsorption from the gaseous phase on the solid adsorbent by means of spectrometer IKC-12 was described earlier [6]. The object of the study, the same as in the paper mentioned above, was partly dehydrated Mg(OH).

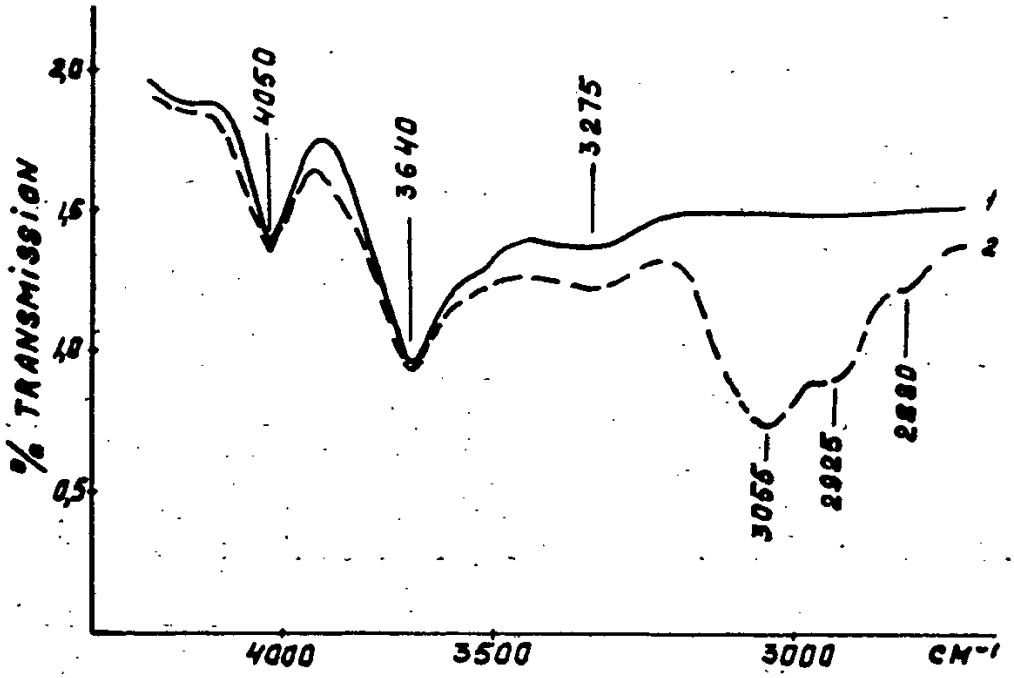

Fig. 5. The change of $Mg(OH)_2$ absorption spectrum during adsorption and polymerization of ethylene oxide: (1) initial sample after evacuation at room temperature, (2) after 2 days in ethylene oxide.

Fig. 5 shows the change of the spectrum of Mg(OH) in the region of valent OH-vibrations in the process of adsorption and polymerization of ethylene oxide. In the spectrogram of the initial sample of $Mg(OH)_2$ (curve 1) are absorption bands 4050 cm^{-1}, 3640 cm^{-1} and 3275 cm^{-1} characteristic of brucite structure [10] and a wide band with a maximum 3400 cm^{-1}. The band 3400 cm^{-1} disappears on heating the sample for a short time up to 150-200°C. The adsorption and the polymerization of ethylene oxide causes the appearance of absorption bands 3055, 2925 and 2880 cm^{-1} (curve 2), indicating the presence on the surface of physically adsorbed ethylene oxide and polymer molecules [6].

According to our estimations the adsorption of ethylene oxide molecules upon OH surface groups should decrease the intensity of their absorption bands by 0.2% which is distinctly registered by the method used in this work. However, as is shown by the comparison of curves 1 and 2 ethylene oxide adsorption and polymerization are accompanied neither by an intensity change of bands at 4050 and 3640 cm^{-1}, nor by a change of their position. Thus, the OH-groups of magnesium hydroxide are not active centres in the catalytic ethylene oxide polymerization.

On the surface of some samples used by us there were also present carbonate groups CO_3^{2-}. Fig. 6 shows the spectrum of the catalyst

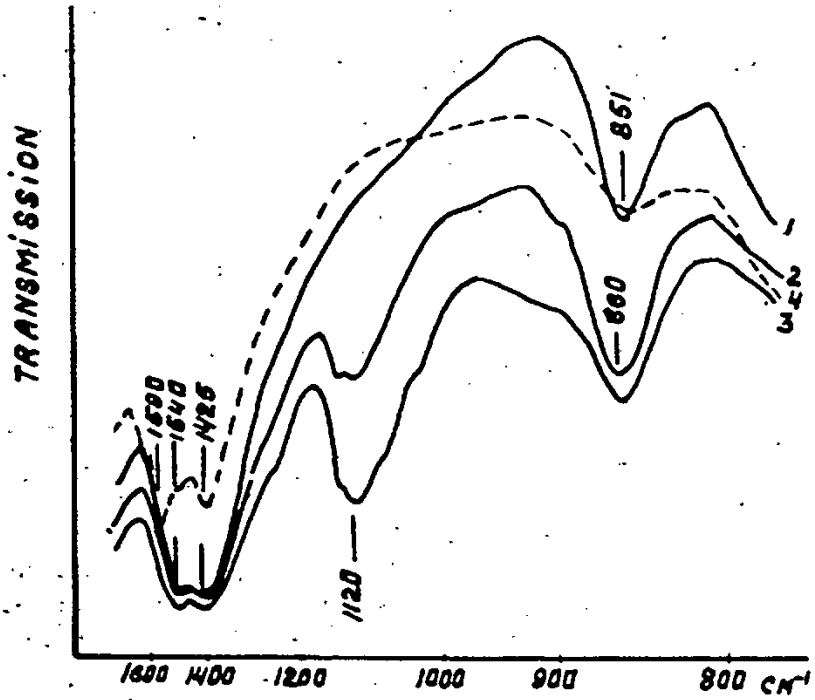

Fig. 6. Absorption spectrum of $xMg(OH)_2 \cdot yMgCO_3$ during adsorption and polymerization of ethylene oxide; (a) initial sample, (2) after 2 hours in ethylene oxide, (3) after 2 days in ethylene oxide, (4) after heating in vacuum for 6 hours at 180-200°C.

$xMG(OH)_2 \cdot yMgCO_3$ in the long-wave region when ethylene oxide is adsorbed and polymerized on it. Curve 1 is the spectrum of the catalyst. Bands 1540 cm^{-1}, 1425 cm^{-1} and 851 cm^{-1} should be attributed to the ion of CO_3^{2-} (see for example [11]). In the subsequent curves the band 1120 cm^{-2} represents the vibrations in the chain of -C-O-C polymer. The band 870 cm^{-1} belonging to the ring C - C superimposes on the catalyst band 851 cm^{-1}

O

gives absorbtion maximum of 860 cm^{-1}. With the passage of time the intensity of the band at 1120 cm^{-1} increases but the intensity of the bands at 1540 and 1425 cm^{-1} practically does not change. It is evident from this that carbonate ion does not take part in adsorption and polymerization of ethylene oxide.

After heating the catalyst together with the polymer for 6 hours at

180 - 200°C (curve 4) bands 851 cm^{-1} and 1540 cm^{-1} appreciably decrease in intensity which might be attributed to the effect of interaction of ions of CO_3^{2-} with fragments of polymer molecules lying on the surface of the catalyst.

Thus, infrared spectroscopic study shows that neither OH-groups nor CO_3-groups of the surface are active centres for ethylene oxide polymerization. Only ions of metal Me^{n+} or of oxygen O^{2-} on the surface may be those centres.

X-ray study of the catalyst system plus growing polymer has been carried out by means of the apparatus YPC-50-I. It has been found out that with a smaller amount of coating (less than 5 layers) of the dehydrated MgO with the polymer the latter exhibits the texture corresponding to a deformation of the polymer film along the plane (100) MgO. This is an indirect reason in favour of much higher catalytic activity of planes of higher concentration of Mg^{2+}. On Al_2O_3 the film stretches along the faces with high indexes.

5. ADSORPTION STUDY

Interest was shown for the estimation of the number of coordination-unsaturated metal ions on the surface of catalysts by means of independent adsorption measurements. For this purpose we studied adsorption and desorption of dioxan which is often used for the determination of Lewis acidity. Dioxan adsorption has been studied by gravimetric methods at initial pressures of from 2 to 10 mm Hg and at temperatures of ranging from 0 to 80°C. The greater part of dioxan on Al_2O_3 and MgO is adsorbed with heat of adsorption of 5-7 $kcal/mole^{-1}$ (determined from adsorption isobars). Its smaller part is adsorbed irreversibly and is removed after the elevation of temperature up to 100 - 200°C. The heat of adsorption of this part of dioxan determined according to Polanyi equation from the rates of desorption is 18 - 20 kilocalories on MgO and 20 - 25 kilocalories on Al_2O_3. The number of active centres on which dioxan adsorbs irreversibly $3 - 7 \times 10^{13}$ cm^{-2} on Al_2O_3 and $1 - 3 \times 10^{13}$ cm^{-2} on MgO is less than that of active centres found from the measurements of molecular weight (see above). This discrepancy can be made smaller if we assume that a molecule of dioxan occupies two active centres.

It is rather more difficult to study adsorption of ethylene oxide itself because the ring is cleaved and polymerization starts simultaneously with adsorption. If we interrupt the experiment and pump out the catalyst during the polymerization on MacBain balance pan its weight will decrease due to the desorption of ethylene oxide. The decrease in weight is likely to correspond to the amount of ethylene oxide adsorbed without bond scission. This amount equals 1.4×10^{14} molecules per 1 cm^2 for Al_2O_3, to 0.4×10^{14} molecules per 1 cm^2 for MgO (pressure of C_2H_4O prior to pumping out is 10 mm Hg).

Thus, the determination of the number of polymerization active centres by different methode gives similar results - about 10^{14} cm^{-2}. These figures

are close to the number of coordination unsaturated metal ions on the surface of the studied catalysts [5].

Water adsorbed at room temperature on the surface of OH-groups of oxide has evidently little effect on the rate of polymerization [5]. Adsorption of water at 200° results in strong poisoning of MgO and BeO due to rehydration of the surface. CO_2 poisons the catalyst already at room temperature probably due to screening of the active centre - the cation during adsorption on the neighbouring O^{2-} ion.

6. STUDY OF CHAIN INITIATION AND OF CHAIN TERMINATION

The data above demonstrate that the process of polymerization of ethylene oxide takes place on the surface cation. The experiments at polymerization in solutions of benzene, chlorobenzene, ethylene dichloride, ethyl alcohol, in monomer mass and also in normal hexane (in which polymer is insoluble) revealed no effects due to dielectric constant of the solvent on the rate constant of chain growth. Thus, in the process of polymerization no separation of charges occurs as observed in the case of free-ion mechanism of chain growth. At the same time the rate constant of chain termination, i.e., the polymer molecular weight, is strongly affected by the solvent. The molecular weight in solvents containing hydroxyl-groups, for example in ethyl alcohol is considerably reduced. General equation for the molecular weight, confirmed by the experimental data reads as follows:

$$M = A\frac{C_0 - C}{S_1 + \int w_t dt} = \frac{Ak_g t}{1 + k_t' S_2 b' t\,(C_0 - \frac{1}{2}k_t S_1 t) + k_t'' S_2 b''\, C_{solv}\, t}$$

Here A = factor of proportionality taking into account the volume of the system, k_g = rate constant of chain growth, k'_{term} and k''_{term} = rate constants of chain termination under the action of monomer and solvent, S_1 = number of active centres of polymerization, S_2 = number of centres of the second kind on which monomer or solvent terminating the chain are adsorbed, b' and b'' = adsorption coefficients of monomer and solvent (or of impurities) on those centres, C_0 = initial, C = present concentration of ethylene oxide, t = time. In polymerization experiments on MacBain balance the last two terms in the denominator are absent and the chain termination takes place only during the latest treatment of the polymer + catalyst system. In experiments with very pure nonhydroxyl solvents some part is played by the second term in the denominator. But in a great number of solvents the third term in the denominator is considerably greater than the second one and the second term can be neglected.

If the second and the third terms in the denominator are small and $M = Ak_g t$, distribution of polymer fraction according to molecular weights is, as Flory [12] demonstrated, very narrow and the average-weight molecular weight M_w at sufficiently high degrees of polymerization is close to average numerical M_n. The value M_n for low molecular weights can be determined on the basis of analysis of end groups. For this purpose we

prepared polymers with specially reduced molecular weight on the catalyst Al_2O_3 in the mixture of ethylene oxide with ethylene glycol. In this case ethylene glycol is a polymerization initiator. The content of OH-groups was determined by treating polymer with 10% solution of phtalic anhydride in pyridine and by back titration with 0.5 N solution of NaOH. In one of the experiments it has been found (assuming that 1 OH-group exists in 1 molecule of polymer) that $M_n = 220$, $M_w = 560$, in another experiment where initiation was performed by means of alcohol, $M_n = 1380$, $M_w = 1560$. In all cases M_n is considerably lower than M_w.

Experiments carried out on Al_2O_3 under normal conditions (without initiating by solvents containing hydroxyl) showed very low values of M_n but the accuracy of determination or M_n was low. To check up distribution in this case, molecules of the polymer were fractionated by dissolving it in ethylene dichloride and by subsequent precipitation with hexane. The results we obtained indicate that in spite of a considerable degree of polymerization (for the polymer received on Al_2O_3 in the benzene solution with M_w being 11500) the distribution was wide and did not corresponded to the Flory distribution. The calculation of average numerical molecular weight on the basis of these data shows $M_n = 2200$ which is considerably lower than M_w and is close to the value of M_w found from the analysis of end groups. This points to the significant part played by the chain termination reactions in accordance with the above equation. The chain termination is due to the effect of impurities in benzene and in the monomer.

As stated above, substances containing hydroxyl can participate in initiating the chain. OH-groups on the surface of catalysts may apparently be initiators of the chain. The rate of such initiation is small, however, and on hydroxide and carbonate catalysts the reaction is usually preceded by a long period of induction [4]. On the contrary, on oxide catalysts having no OH-groups initiation proceeds quickly with no period of induction.

We may consider this case as "quasi-radical" mechanism of initiation as partly dehydrated oxides have on some surface ions of metal excess positive and on ions of oxygen excess negative free valencies which are not intercompensated. In such a mechanism unsaturated C=C or C=O bonds may be found at the end of the polymer chain. Unsaturated C=C bonds were determined by the addition of the solution of Br and then KJ and by back titration with thiosulfate. The content of carbonyl groups was determined by titration with hydroxylamine hydrochloride. The experiments indicated the presence of C=C bonds and the absence of C=O bonds (with an accuracy of up to 5% of the number of end groups) in terms of 1 group per molecule.

7. PROCESS STAGE SCHEME

We can propose the following stage diagram of polymerization of ethylene oxide and oxide catalysts on the basis of the above experiments

a) Chain initiation

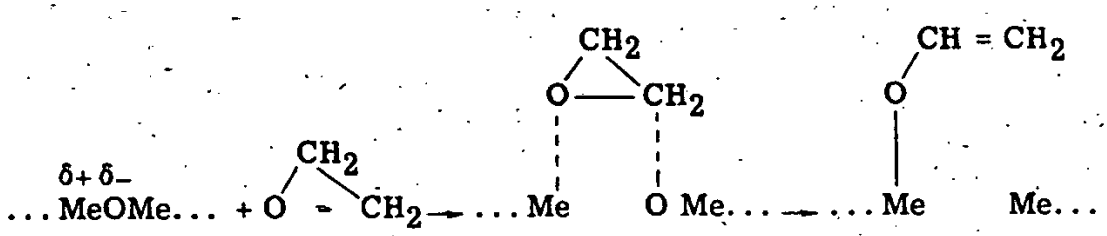

The formation of small number of additional OH-groups in this process may be not traceable in the spectrogram if their number is not more than 1×10^{13} cm^{-2} (maximum 5% of total number of OH-groups).

b) Chain growth

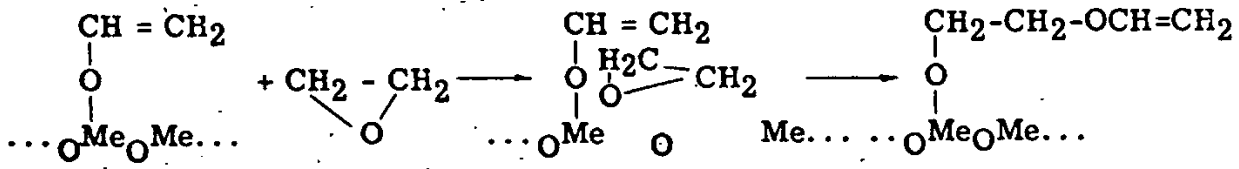

and so on. The surface metal ion bonded with the polymer chain by the principal link and by coordination valence with a free pair of electrons of oxygen in the ethylene oxide ring. Scission of coordination bond and the entry of the molecule of the monomer into the polymer chain is a limiting stage of the reaction. The crystal field stabilization energy makes the coordination bond stronger and retards this stage.

Furukawa [13] suggested that in stereospecific polymerization of propylene oxide the monomer adds on to two metal atoms of the catalyst. Analogously for ethylene oxide one might admit the formation of the complex on solid oxides

The following facts, however, do not speak in favour of this mechanism: 1) in polymerization of propylene oxide on solid oxides we obtained amorphous but not crystalline polymers; 2) bands in the infrared spectrogram belonging to the ring C - C, in adsorption practically remain unchanged;

3) calculation of k_o in the chain growth reaction according to the theory of absolute reaction rates (about 10^5 min^{-1} under reaction conditions) revealed that a part of rotational degrees of freedom is retained in the adsorption of C_2H_4O.

c) Chain termination

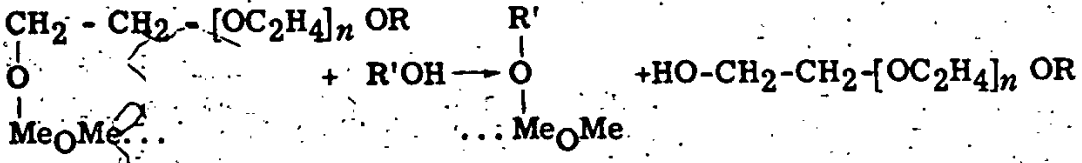

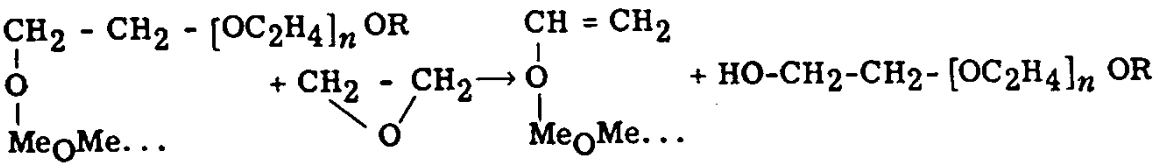

The first version of termination by means of solvent or impurities as said above is more probable than the second version, i.e., termination by polymer.

Kinetic data obtained earlier [3-5] corroborate the proposed scheme.

REFERENCES

1) F. N. Hill, F. E. Bailey and J. T. Fitzpatrick, Ind. Eng. chem. 50 (1958) 5.
2) J. Furukawa, T. Saegusa, T. Tsuruta and G. Kakogawa, Makromolek. Chem. 36 (1959) 25.
3) O. V. Krylov and Y. E. Sinyak, Vysokomolek. sojedinenija 3 (1961) 898.
4) O. V. Krylov and Y. E. Sinyak, Neftechimija 2 (1962) 688.
5) O. V. Krylov, M. J. Kushnerev and E. A. Fokina, Neftechimija 2 (1962) 697.
6) Z. A. Markova, Kinetyka i kataliz 3 (1962) 366.
7) D. A. Dowden and D. Wells, Actes 2e Congr. intern. catalyse, Paris, 2 (1961) 1499.
8) T. V. Antipina and G. N. Avdonina, Zhurnal fisitcheskoi chimii 31 (1959) 192.
9) I. E. Neumark and I. B. Slinyakova, Ukrainskii chimitcheskii zhurnal 27 (1961) 196.
10) R. M. Hexter, J. Opt. Soc. Am. 48 (1958) 770.
11) I. M. Hunt, M. P. Wishard and L. C. Bonham, Analyt. Chem. 22 (1950) 1478,
12) P. J. Flory, J. Am. Chem. Soc. 62 (1940) 1561.
13) J. Furukawa, Polymer 3 (1962) 487.

THE STRUCTURE OF POWDER CATALYSTS, MADE OF Ni-Co ALLOYS, AND THEIR CATALYTIC ACTIVITY AND KINETICS OF REAGENTS ADSORPTION IN THE PROCESS OF BENZENE HYDROGENATION

Zdzislaw SOKALSKI and Józef PODKOWKA
Physico-Chemical Department of the Silesian Institute of Technology, Gliwice, Poland

1. INTRODUCTION

Powder catalysts, made of Ni-Co alloys, have been investigated by Lihl, Wagner and Zemsch [1], as well as by Hund [2]. This type of contact catalysts is of special importance in investigations, the aim of which is to determine the dependency between the catalytical properties and the crystal structures of the catalysts. They offer much possibility of choosing such a series of catalysts, which are characterized by continual changes of their structural properties. The method of preparing these catalysts is based on the reduction of suitable salts of mixed crystals.

According to Grim's theory [3], two metals can form a continuous series of mixed crystals, if the difference of their ionic radii does not exceed 7% (in cases when the electrical load and their chemical nature is the same). The ionic radii of Ni and Co amount to 0.78 and 0.82 A respectively. Thus the difference is only 5%. Because the ionic radii of both metals, founding the structural lattice of the catalyst are so very similar, there exists a rather broad range of concentrations of aqueous solutions of salts, which may be used for the production of catalysts. In this case one cation of the metal A is to be wedged into the crystal lattice of the metal B. This case in the interchangeability of the cations forms the basis for a wide series of experiments, the more so, because when suitable proportions of the initial components are used, there may be produced crystals of various crystalline phases. The above mentioned authors [1, 2] have limited their investigations to the examination of the catalytical properties and cristalline structure of powder catalysts, made up of Ni-Co alloys. Today it is well-known that the chemisorption of the reagents of a catalic reaction is one of the elementary processes of contact analysis, so that the investigations into the kinetics of chemisorption render it possible to describe the heterogeneity of the catalyst surface quantitatively and it seems to be worth-while to supplement both the kinetic and structural investigations with measurements of the adsorption kinetics of the reagents of benzene hydrogenation in conjunction with the activity of the contacts is such a reaction.

2. EXPERIMENTAL PART

2.1. *The preparation of the catalysts*

For the experiments there were used powder catalysts, which had been produced by means of a thermal decomposition of mixed crystals composed of Ni and Co formates. In such a way, too, catalysts have been produced by Hund, Lihl and Wagner [1, 2]. The initial reagents were Ni and Co formates, got by means of electrolysis; they have been dissolved in suitable proportions in a 10%-HCOOH. Then this solution was evaporated at its boiling temperature until a saturated solution has been received. After that the solution was cooled down by means of water at a temperature of 14°C. The crystals prepared in this way, were dried at a temperature of 110°C.

2.2. *Catalytical investigations*

The reduction of the catalysts and the catalytical reaction of C_6H_6-hydrogenation have been carried out in an apparatus which is shown in fig. 1.

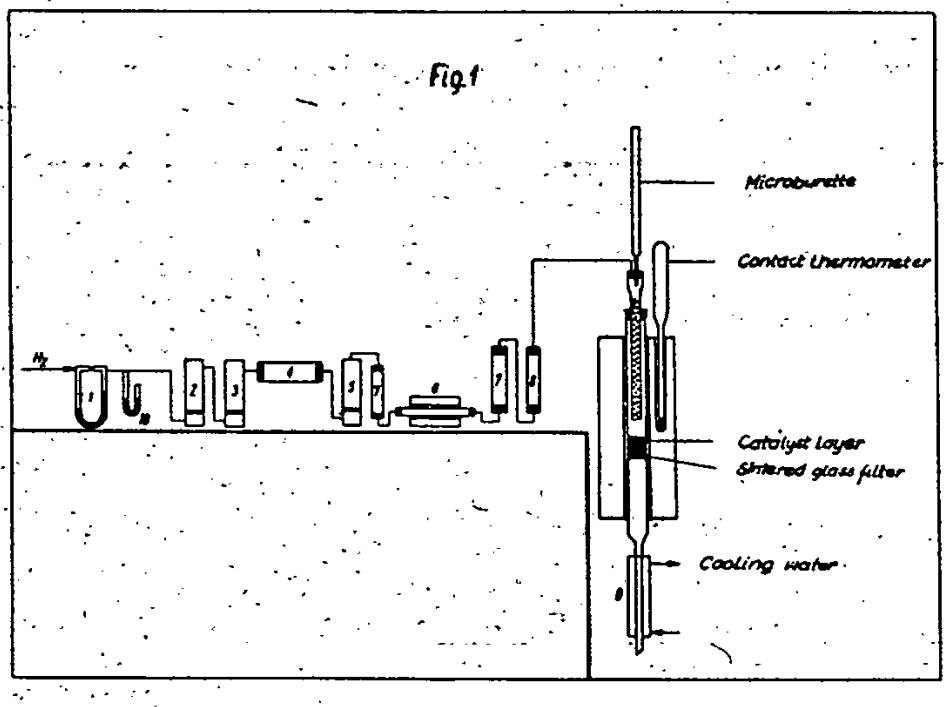

Fig. 1. Apparatus for reduction and catalytical hydrogenation of C_6H_6.

The electrolytical hydrogen, taken from a pressure bottle, has been passing successively through a fleometer [1], then through absorbers with H_2SO_4 [2] and with KOH [3], through a filter with active carbon [4], an absorber with pyrogallol solved in KOH [5], next through an oven containing the catalysts for removing the last traces of oxygen [6], and finally through pipes filled with anhydrous $CaCl_2$ and $Mg(ClO_4)_2$ [7]. The reduction of all the catalysts has been executed at a temperature of 330°C with hydrogen flowing past at a rate of 40 l/h. The time of reduction amounted to 2 hours. Afterwards the

oven was cooled down to reaction temperature, while the hydrogen flow was kept low. The cooling time was the same in all the experiments. The amount of Ni in the catalysts, which have been prepared in this way, increased successively from 0 to 10, 30, 70 and up to 100%. The nickel content was determined by precipitating α-dimethyloglyoxime and weighing it.

The reduction value was determined by solving the weighed amount of the reduced catalyst in 20% H_2SO_4 and by measuring the volume of the evolved H_2. The reduction values of various catalysts are presented in table 1.

Table 1
Reduction values of catalysts with various Ni-contents.

Ni-content in weight %	0	10	30	70	100
Reduction value	97.5	99.0	98.1	96.5	98.5

It follows from this table that the reduction values for all catalysts amount nearly up to 100%.

Having set up the temperature, benzene was dropped down from a microburette at a rate of 0.1 ml/min, while the hydrogen was flowing at 6 l/h. This makes a 20% excess of a stoichiometric proportion. In this way the benzene was dropping down for 10 minutes, after which for 5 minutes pure hydrogen was passed through in order to remove from the catalyst all C_6H_6 and C_6H_{12}. Then again benzene was dropped in for 10 minutes (after Lihl and Wagner). For each catalyst six experiments have been carried out in order to get reliable information as to the activity changes during the process. The reaction products were being cooled down in a water condenser [8], the liquid products being investigated by using a refractometer for their C_6H_6- and C_6H_{12}-content. For this purpose a calibration curve was designed determining in this way the content of C_6H_6 and C_6H_{12}. Experiments have also been carried out, the aim of which was to show whether C_6H_6 can be hydrogenated by using simply a pure glass pumice. It has been proved, that in such conditions no hydrogenation does occur. The kinetics of hydrogenation has been examined at temperatures of 140° and 180° using catalysts with 0, 10, 30, 70 and 100% Ni content. The dependence of the yield (in %) of the hydrogenation of C_6H_6 to C_6H_{12} upon the temperature is represented in fig. 2, whereas figs. 3 and 4 show the dependence of the yield upon the duration of the experiment at temperatures of 140 and 180°C respectively.

For these same catalysts the kinetics of the dehydrogenation of C_6H_6 have been carried out at temperatures of 215, 260, 290 and 310°C. The results of those experiments are set up in table 2.

2.3. *Survey of the adsorption kinetics*

It is much easier to interprete quantitatively the results of the measurements in the kinetics of adsorption, if these measurements are taken under isobaric conditions. In these conditions the constants of the equation,

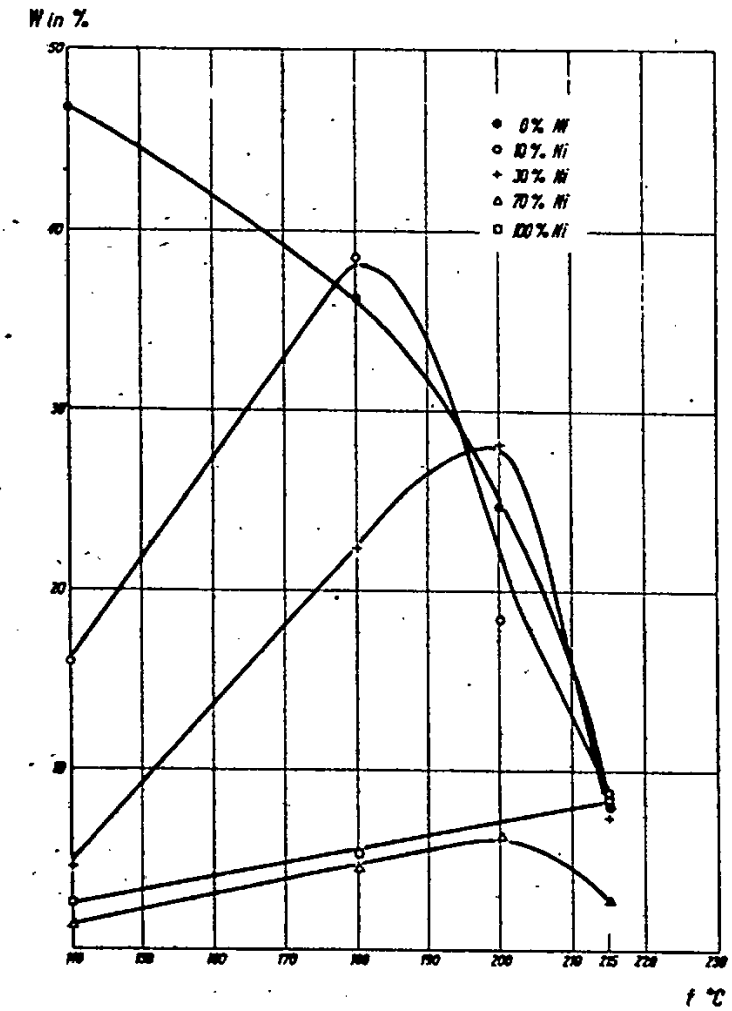

Fig. 2. The dependence of the yield of a C_6H_6 to C_6H_{12}-reaction upon the temperature.

Table 2

Ni-content in the catalyst in %	Yield of the reaction $C_6H_{12} \rightarrow C_6H_6$ at temp.			
	215	260	290	310
0	0	4.3	5.2	-
10	0	6.0	6.4	7.1
30	0	6.5	8.4	9.8
70	0	6.4	7.6	9.5
100	-	9.3	14.4	16.3

concerning the distribution function of the active spots according to the activation energy, e.g. in the equation

$$\rho(E) = \exp\left[- k_0 t \exp\left(- E/RT\right)\right],$$

the constant k_0 is independent of the pressure, so that a less complicated equation can be used.

To avoid such difficulties, the apparatus, measuring the adsorption kinetics, has been equipped with a manostat and thus the isobaric conditions

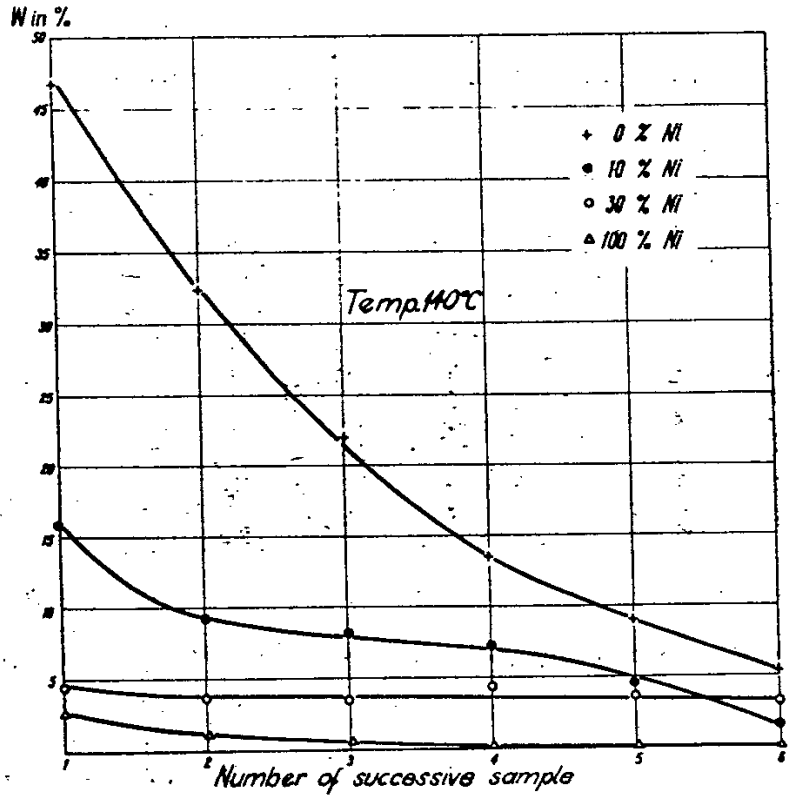

Fig. 3. The dependence of the yield of a C_6H_6 to C_6H_{12}-reaction at 140°C upon the duration of the experiment.

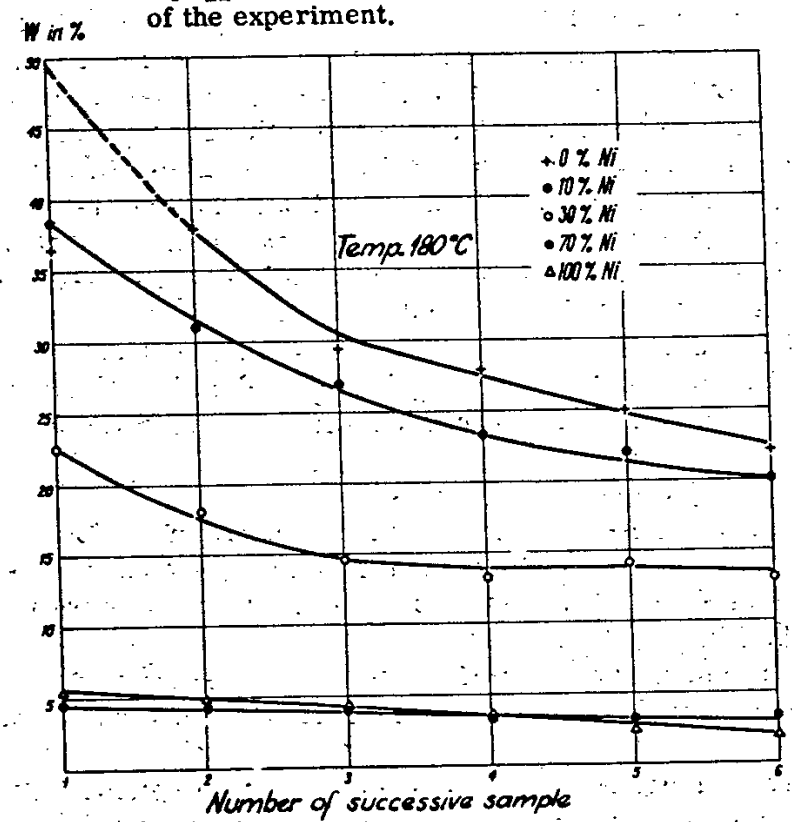

Fig. 4. The dependence of the yield of a C_6H_6 to C_6H_{12}-reaction at 180°C upon the duration of the experiment.

are fulfilled. The scheme of a modified apparatus, developed by Taylor and Strother [4] for taking measurements of adsorption kinetics is shown in fig. 5.

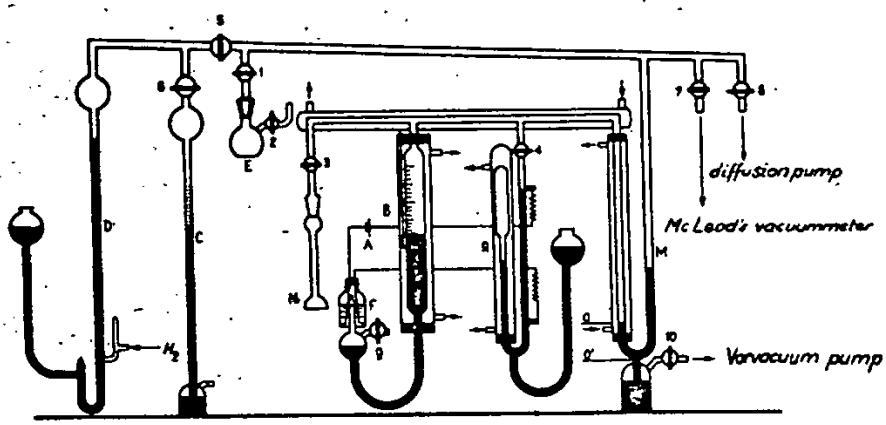

Fig. 5. Apparatus for measuring the adsorption kinetic by p = const.

The samples were degased at a temperature of 350°C; in this operation a vacuum was used of about 10 mm Hg during 4 hours. The hydrogen was developed in an electrolyser, as shown in fig. 5, and introduced into the apparatus through the mercury lock D. Liquid benzen and cyclohexane was passed into the vessel E, where a high vacuum was formed, and from there brought into the main apparatus.

All measurements were performed under a pressure of 25 mm Hg. The first measurement was taken 1 minute after the cock 3 has been opened. As inmediate measurement is impossible because of the aerodynamical perturbances, occurring when the gas is passed into the adsorption vessel, and because of the initial instability in working of the manostat. The last measurement was performed after 90 minutes. Roginski has stated in his paper [5] - basing on an analysis of a great number of experiments - that between the first measurement and the last one there should be observed that $t_2 > 40\ t_1$, what in our case is fulfilled as $t_2 = 90\ t_1$.

Kinetical measurements have been carried through at temperatures of 140° and 180°C, using catalysts of 0, 10, 30, 70 and 100% Ni-content. The results of those experiments are represented in figs. 6 to 10.

2.4. *Roentgenographic measurements*

The roentgenographs were made with cameras of the Debye and Scherrer type. The experimental results of these measurements are to be seen in table 3 as well as in fig. 11. The roentgenographs of the investigated catalyst are given in the plates 1 - 5.

Basing on the analysis of Ni-Co systems, the appearance of two lattice phases has been proved. They are the hexagonal α -phase and the cubic β -phase.

In standard conditions for 0% of Ni content the α -phase is stable. The appearance of the β -phase in these conditions in a quantitative prevailance can be ascribed to the stabilizing properties of dissolved atomic hydrogen into a cristalline lattice of Co.

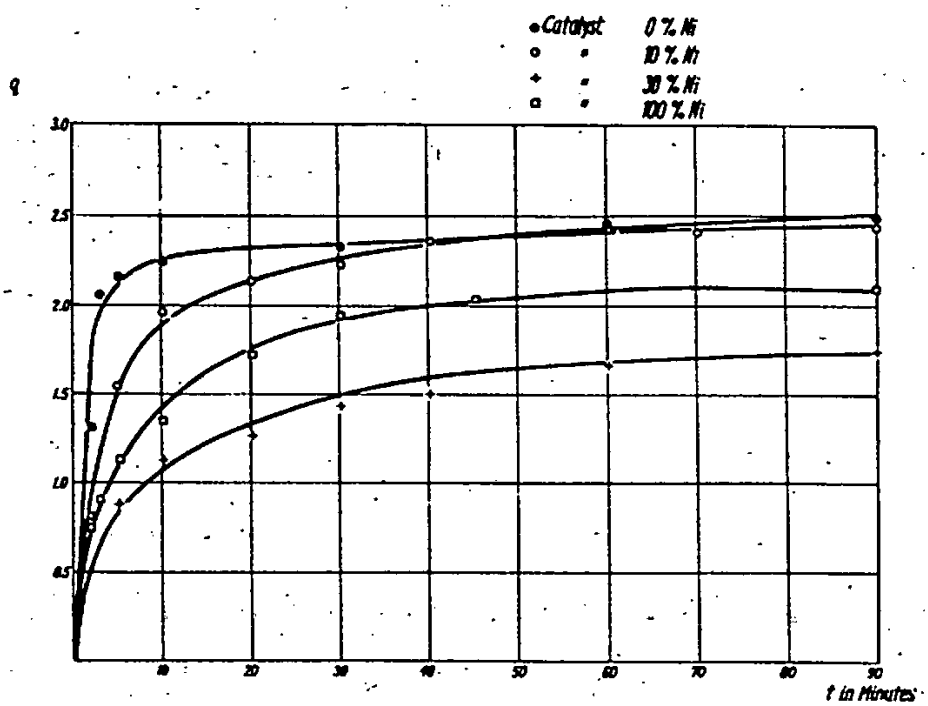

Fig. 6. Kinetic-adsorption isotherms of H_2 at 140°C.

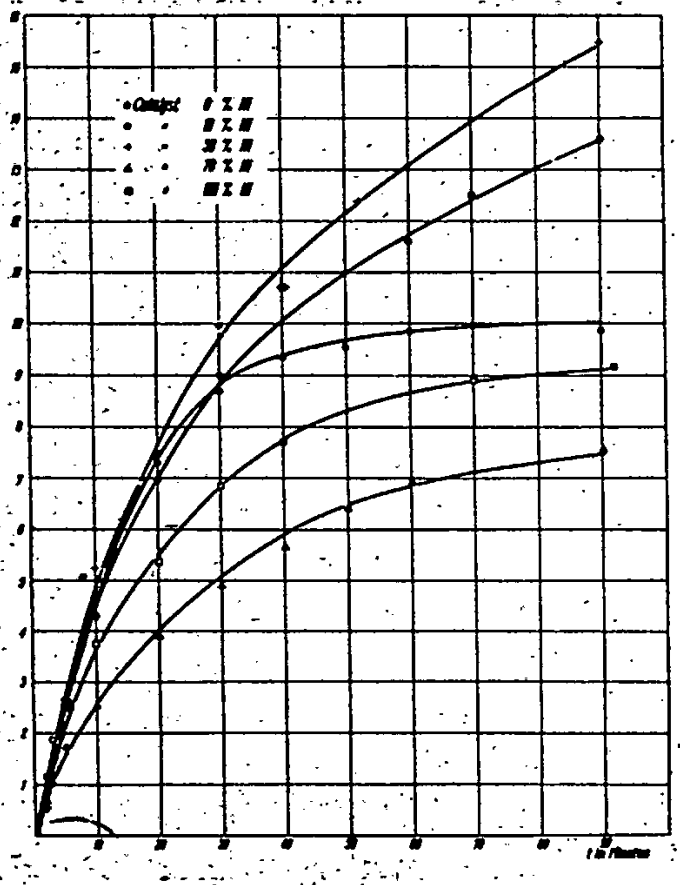

Fig. 7. Kinetic-adsorption isotherms of C_6H_6 at 140°C.

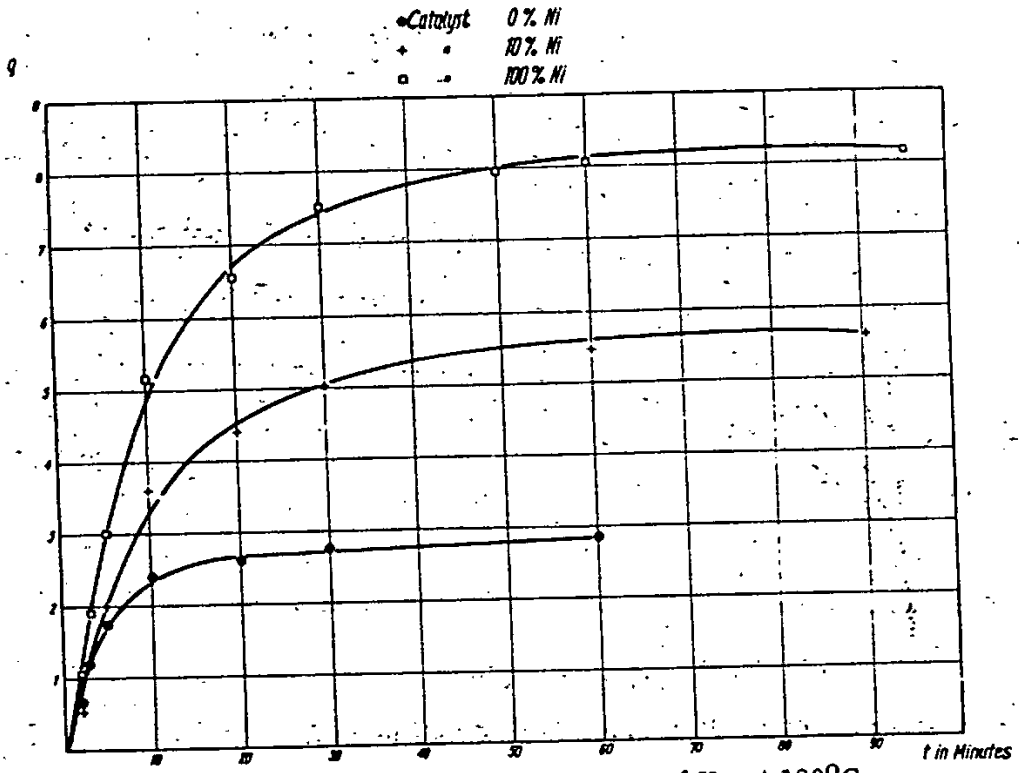

Fig. 8. Kinetic-adsorption isotherms of H_2 at 180°C.

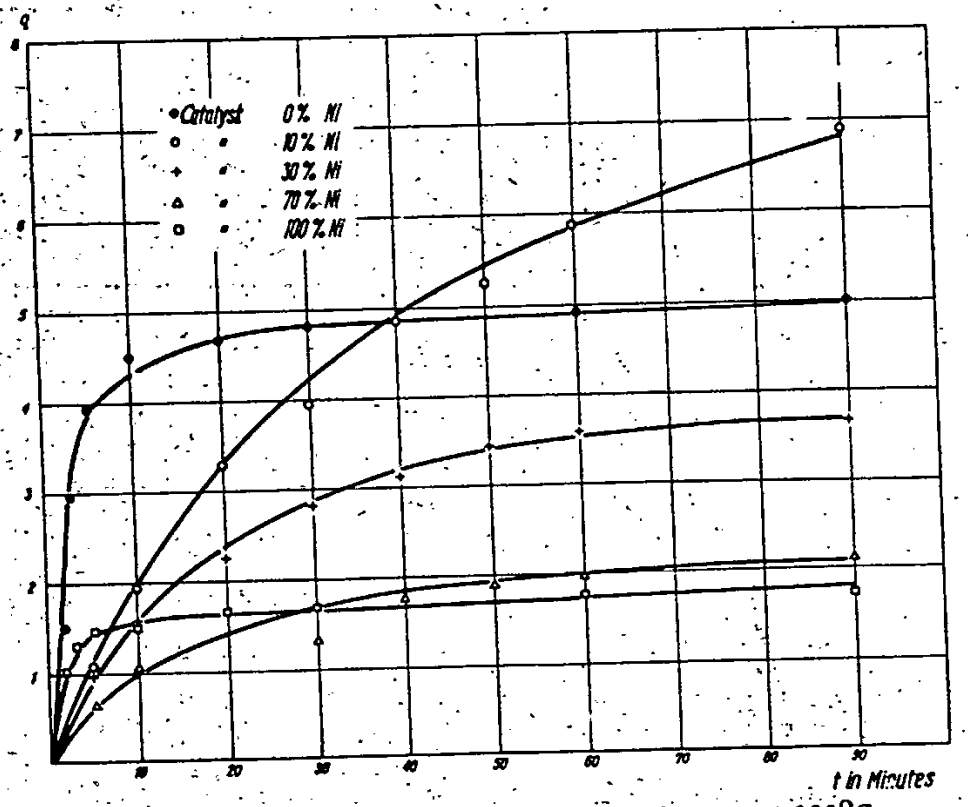

Fig. 9. Kinetic-adsorption isotherms of C_6H_6 at 180°C.

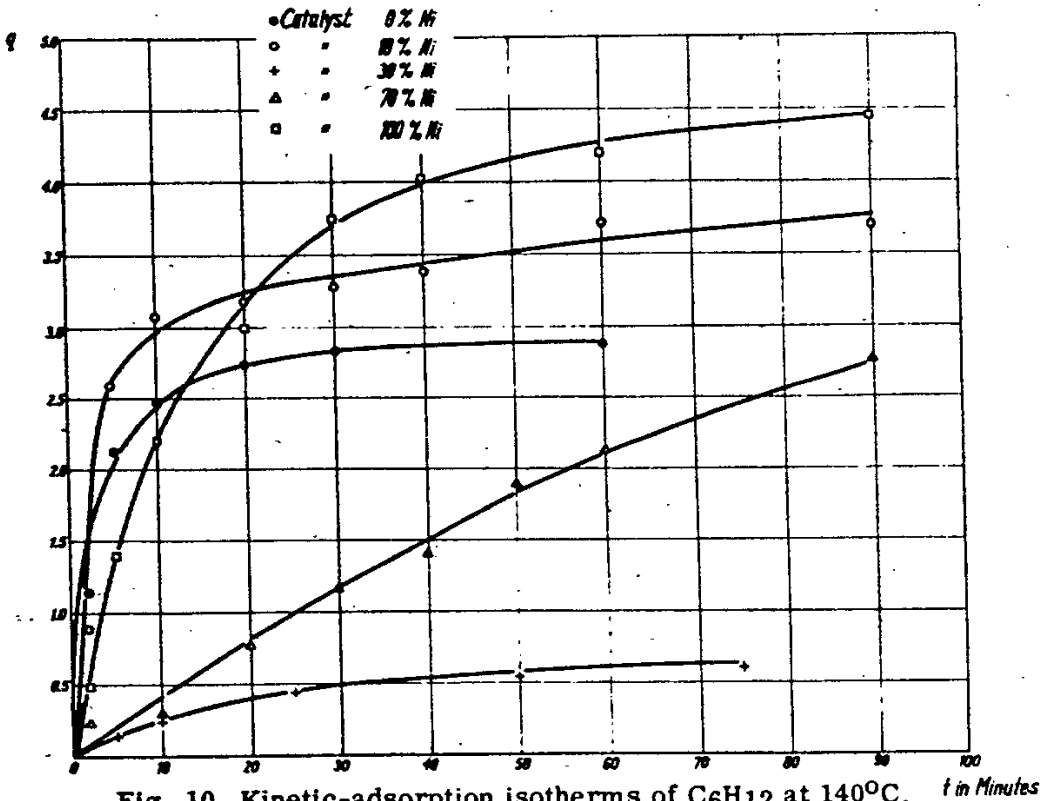

Fig. 10. Kinetic-adsorption isotherms of C_6H_{12} at 140°C.

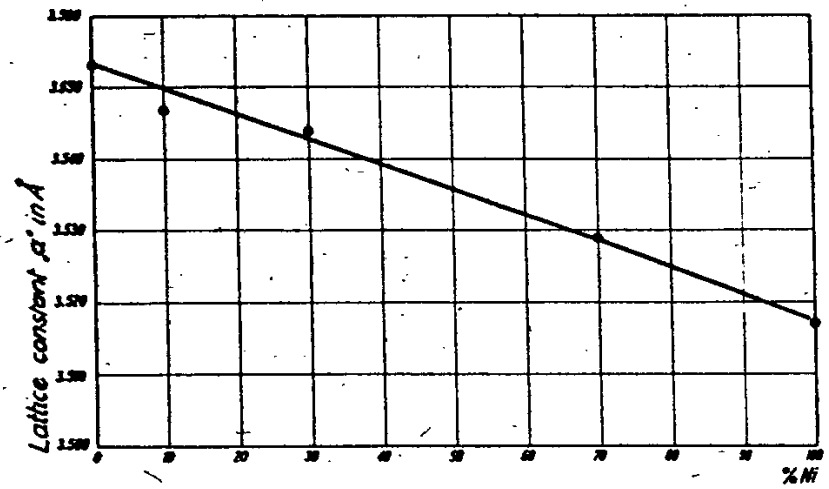

Fig. 11. Dependence of the lattic constant g on the composition of the catalysts.

A catalyst with 10% nickel content develops a higher amount of the β-phase. This is caused by building into the Co-lattice some amount of nickel atoms (there appears a greater ability of dissolving Ni-atoms). Together with this there has been observed a decrease of the lattice constant a. (cf. fig. 11) and a deviation from the additive properties of the lattice constants in regard to its chemical consistance. (The deviation from Vegard's rule in caused by lattice contraction.)

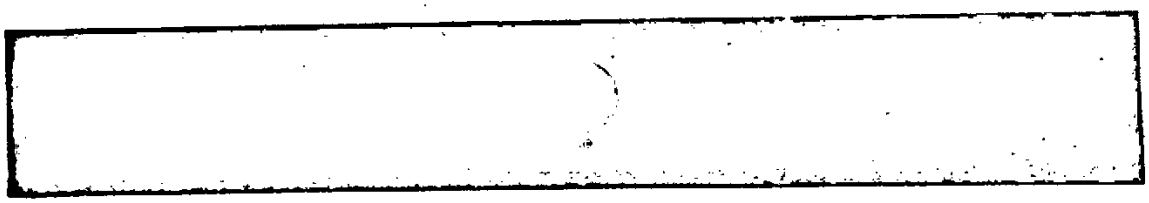

Plate 1. Roentgenograph of a contact with 0% Ni-content.

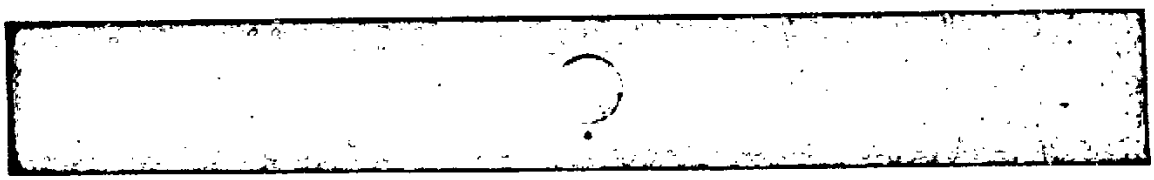

Plate 2. Roentgenograph of a contact with 10% Ni-content.

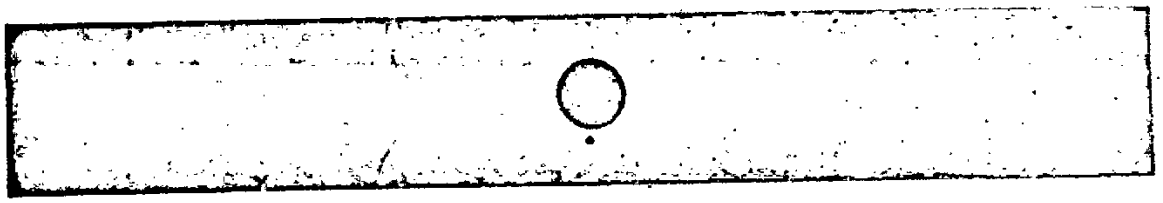

Plate 3. Roentgenograph of a contact with 30% Ni-content.

Plate 4. Roentgenograph of a contact with 70% Ni-content.

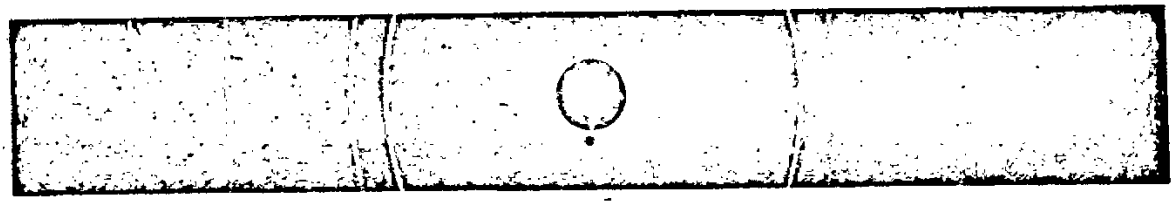

Plate 5. Roentgenograph of a contact with 100% Ni-content.

Table 3
Roentgenographic-structure investigation results for Ni-Co powder-catalysts

Ni - content in % of weight	Phase composition	Dispersivity of the system		Morfological structure of the crystalits	
		Phase β	Phase α	Phase β	Phase α
0	α and β, phase β prevailing	average size of the crystalits, range 0.1μ	non isometric shape of the crystalits: thickness 0.01μ width: 0.1μ	has an isometric shape of the crystalits	appears in form of extremely thin sheets, arranged in layer packets
10	phase composition as above mixed crystals	as above	as above	as above	as above
30	Gradual decay of phase α mixed crystals	slight increase of the average size of the crystalits in phase β	as above	as above	as above
70	phase β mixed crystals	as above	as above	as above	as above
100	phase β mixed crystals	0.1μ		as above	as above

The roentgenograph of a catalyst with 30% Ni-content is characteristic for its further decrease of the lattice constant of the β-phase, for the decay of the α-phase and the sharpening of the bands (reflexions). This phenomenon may be attributed to the increase of the regularity in the lattice structure.

Catalysts with 70% and 100% nickel content are made only of the β-phase, which is in standard conditions the only stable structural form of nickel. Very sharp bands of the catalysts with 100% Ni-content prove that the system is characteristic for its well-formed structure of the crystal lattice.

The investigated series of powder catalysts [4] has been assumed to be structurally modified by forming a solid solution of two substitutive metals, viz. Ni and Co. As it is shown in fig. 11, in this series there is maintained a continuity of changes of the crystal lattice constant, this continuity being dependent upon the chemical composition of the catalysts.

According to Wolkensteijn's theory of catalysis, the contact catalysts are modified due to their contact with the reagents of the catalytic reaction. If those reagents are gases, the contact modification is called a gaseous modification [5]. The contacts are submitted to such a gaseous modification even while the reagents of the investigated reaction are being absorbed. Especially the initial period of adsorption, characteristic for its larger numerical values of the adsorption potentials, exerts a dominant influence upon the modification. In this case both the catalyst and the adsorbed reagents are treated as being one quantum mechanic system [5]. The process of the gaseous modification may be forwarded on the basis of the following assump-

tion. The priority of covering the adsorbed molecules belongs to those surface elements, which expose the highest potentials of adsorption, characterizing the investigated system by stronger binding forces between the atoms of the reagents and the catalyst surface. The covering of these surface elements is executed during the initial stages of the adsorption time t_x, the degree of covering the reagent x being equal to θ_x. The remaining fraction of the surface, not covered by any reagents, i.e. $(1 - \theta_x)$, the surface elements of which are characteristic for their medium or low values of adsorption potentials, is being covered at later stages of the adsorption time t'_x.

In result of the surface reaction the products, formed within the range of active surface concentrations, are being desorbed and the substrats again adsorbed.

It may be assumed that the covered surface θ is constantly blockaded throughout the whole time t_x. Thus the surface $(1 - \theta_x)$, which has been covered during the time interval t'_x, possesses active surface elements, allowing in the case of a dynamic adsorption to achieve a continuous repetition of the reaction cycles, viz. the adsorption of the reagents, the surface reaction and the desorption of the products. In this case on the surface fraction $(1 - \theta_x)$, covered within the period of time t'_x, there are gathered the adsorbed reagents with an active surface concentration. For the purpose of a quantitative, comparative comprehension of the kinetics of the adsorption processes, taking place for the investigated series of catalysts, it is desirable to distinguish between the two time intervals t_x and t'_x. Such a distinction is made rather easy in cases when the transfer from the extent θ to the extent $(1 - \theta_x)$ is characterized by a discontinuity of the function. It has been assumed that the longest times of all the possible times of initial adsorption is in the case of our series of contacts the time of modification, after which the process kinetics for all the contacts follows the functional dependency $y = a \ln t$, this dependency remaining constant. The position of the straight lines representing a nickel content of 30% and 70% proves that according to the above-mentioned assumptions it is impossible to choose a shorter period of time than 10 minutes, i.e. $\log t = 1$. The straight lines represented in figs. 1 - 5 may be expressed by means of the equation $y = a \log x + b$. They are practically continual functions from $\log t = 1$ upwards, whereas the quantity b is characteristic for the initial period of adsorption, which is a period of spontaneous gaseous modification. The time t_x, extending from 0 to 10 minutes, is assumed to be the time of the spontaneous gaseous modification, while $t'_x > 10$ minutes is assumed to be the time of adsorption taking place at the surface fraction $(1 - \theta_x)$. In this time there occurs the covering of the adsorption places with active concentrations. If the straight lines in figs. 13-17 cut the axis of $\log t_x = 1$, the contact surface is not modified (gaseous modification).

Basing on these principles there have been received straight lines in the coordinates system $q = f(\log t)$, as shown in figs. 13-17.

In order to determine the characteristic coefficients as being a quantitative expression of the adsorption process we may take up the following considerations, basing upon the kinetics of adsorption:

The adsorption rate constant k is determined by means of eq. (1).

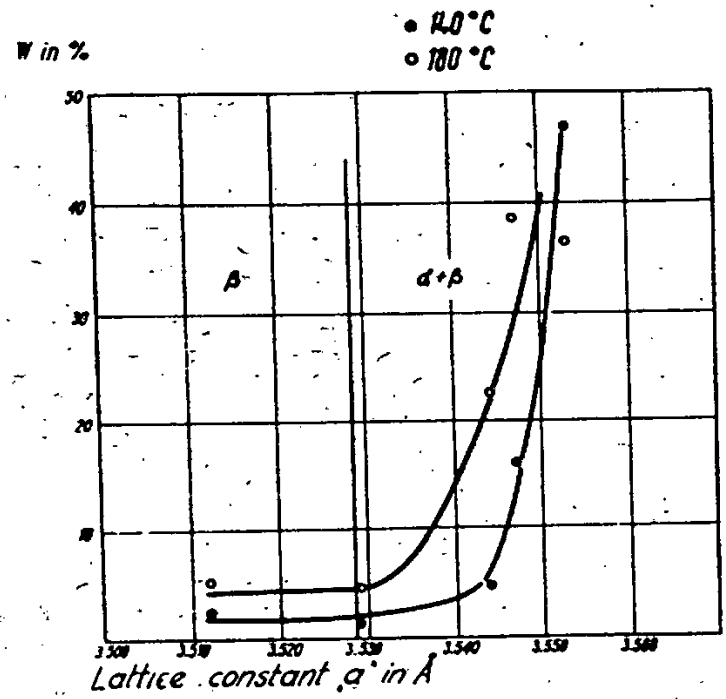

Fig. 12. Dependence of the reaction efficience of the hydrogenation of C_6H_6 on the lattice constant *a*.

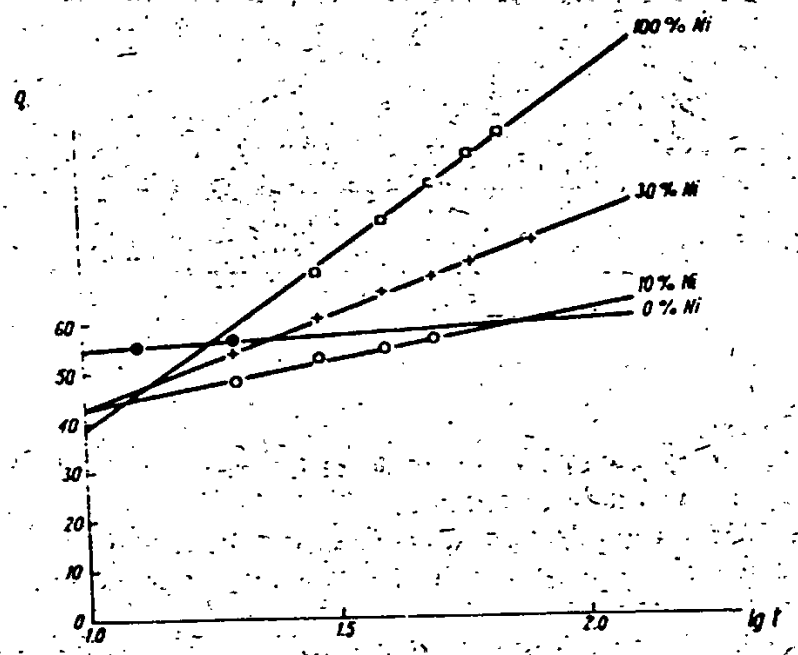

Fig. 13. Diagram $q = f(\log t)$ of H_2 adsorption at 140°C.

STAT

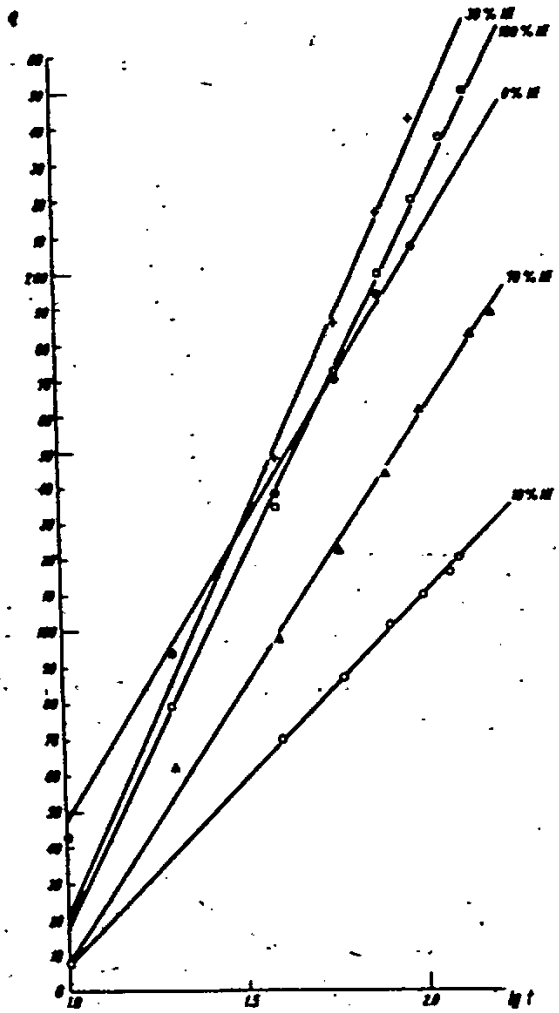

Fig. 14. Diagram $q = f(\log t)$ of C_6H_6-adsorption at 140°C.

$$\frac{1}{S_x} \frac{dq_x}{dt \cdot n_{o(x)}} = k_x \qquad (1)$$

where:
dq_x - differential of the adsorbed molecule of the reagent x,
dt - differential of the adsorption time,
S_x - surface at which the adsorption process is taking place,
$n_{o(x)}$ - concentration of the reagent x in the gaseous phase. For isobaric conditions $n_{o(x)}$ = const.

On the other hand the rate of the adsorption constant can be represented by means of Arrhenius' equation

$$k_x = A_x \exp\left(-\frac{E_x}{RT}\right) \qquad (2)$$

where:

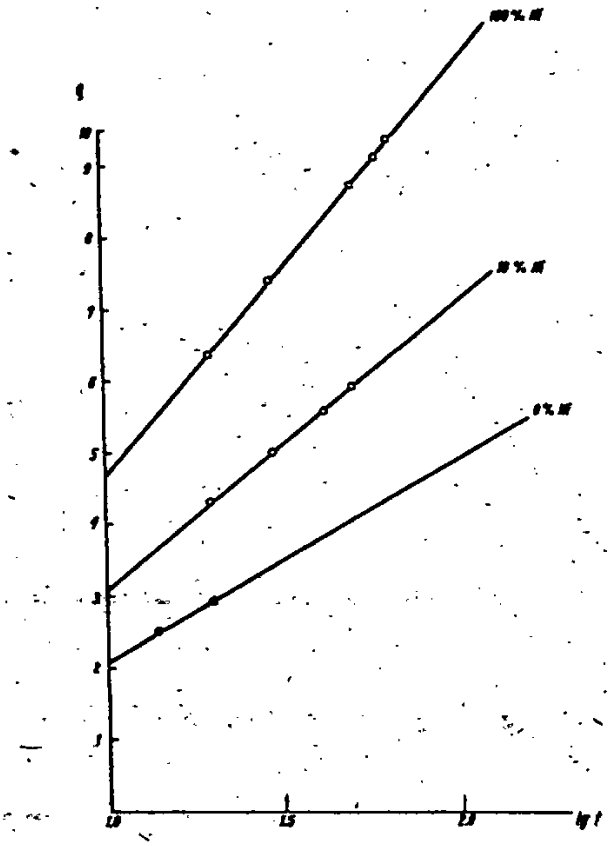

Fig. 15. Diagram $q = f(\log t)$ of H_2-adsorption at 180°C.

A_x - coefficient referring to the reagent x,
E_x - activation energy of adsorption of the reagent x,
R - molar gas constant,
T - absolute temperature.

The coefficient A_x depends upon the number of collisions of the gaseous molecules occuring at one unit of the surface S_x per second. Thus

$$A_x = \frac{Z_x}{S_x} p_x \tag{3}$$

where Z_x/S_x represents the number of molecules striking against the surface unit within the period of one unit of time. p_x is a quantity dependent on the arrangement of the adsorbed gas molecules and their orientation in respect to the lattice parameters at the surface of the adsorbent. Comparing k_x in both equations (1) and (2) we get a new dependency (4):

$$\frac{dq_x}{dt \cdot n_{ox}} = Z_x p_x \exp\left(-\frac{E_x}{RT}\right). \tag{4}$$

For our particular case, where hydrogen and benzen are the reagents, eq. (4) may be written in the following form:

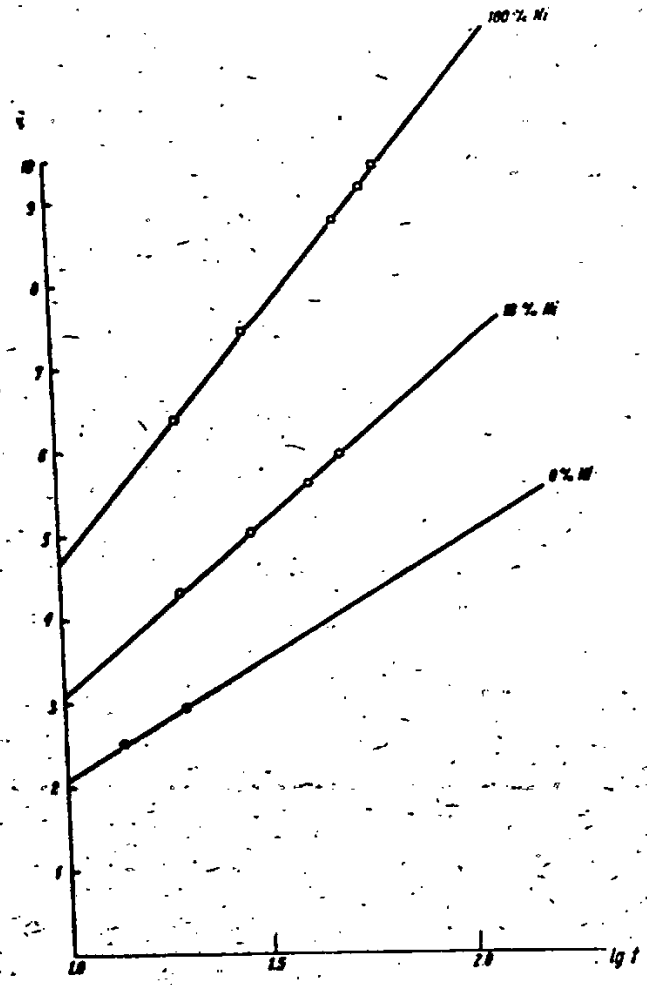

Fig. 16. Diagram $q = f(\log t)$ of C_6H_{12}-adsorption at 140°C.

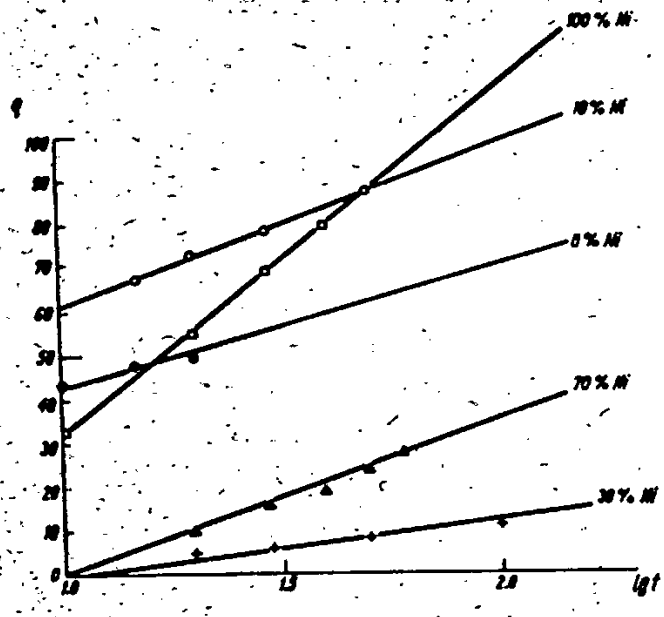

Fig. 17. Diagram $q = f(\log t)$ of C_6H_6-adsorption at 180°C.

$$\frac{dq(H_2)}{dt \cdot n_{oH_2}} = Z_{H_2} p_{H_2} \exp\left(-\frac{E_{H_2}}{RT}\right) \tag{5}$$

and

$$\frac{dq_{C_6H_6}}{dt \cdot n_{oC_6H_6}} = Z_{C_6H_6} p_{C_6H_6} \exp\left(-\frac{E_{C_6H_6}}{RT}\right) \tag{6}$$

The empirical eq. (7) expresses the adsorption kinetics of the reagents of the catalytical hydrogenation process of benzen to cyclohexane:

$$q_x = a_x \ln t_x + b_x . \tag{7}$$

To this process corresponds the heterogenetic distribution function [6]

$$\rho(E)_x = H_x \tag{8}$$

whereas

$$\rho(E)_x = \frac{1}{dE_x} \frac{dN_{E_x}}{N_x} \tag{8a}$$

in which N_E denotes the number of adsorption spots at one surface unit with an activation energy of E_x, while N_x is the general number of all adsorption spots at the surface unit. The expression dN_{E_x}/N_x represents the probability that at one surface unit there occur dN_{E_x} adsorption spots with an activation energy of E_x.

Differentiating eq. (7) against the time we obtain:

$$V_{H_2} = \frac{dq_{H_2}}{dt} = \frac{a_{H_2}}{t}$$

and

$$V_{C_6H_6} = \frac{dq_{C_6H_6}}{dt} = \frac{a_{C_6H_6}}{t} \tag{9}$$

Hence for equal adsorption times we shall get the following equation:

$$\frac{V_{H_2}}{V_{C_6H_6}} = \frac{a_{H_2}}{a_{C_6H_6}} \tag{10}$$

where V_x is the adsorption rate of the reagent x.

Inserting into eqs. (5) and (6) the corresponding expressions from eqs. (9) and (10) we get to another dependency, viz.:

$$\frac{a_{H_2}}{t\, n_{oH_2}} = Z_{H_2} p_{H_2} \exp\left(-\frac{E_{H_2}}{RT}\right) \tag{11}$$

$$\frac{a_{C_6H_6}}{t\, n_{oC_6H_6}} = Z_{C_6H_6} p_{C_6H_6} \exp\left(-\frac{E_{C_6H_6}}{RT}\right). \tag{12}$$

Dividing both these latter equations by sides we obtain:

$$\frac{a_{H_2}}{a_{C_6H_6}} = \beta \frac{Z_{H_2}\ p_{H_2}}{Z_{C_6H_6}\ p_{C_6H_6}} \exp\left(-\frac{E_{H_2} + E_{C_6H_6}}{RT}\right) \qquad (13)$$

where $\beta = \frac{n_{oH_2}}{n_{oC_6H_6}} \times \text{const.}$

Equation (13) is valid for equal times of adsorption of the reagents i. e. for such theoretical conditions which form the basis for expressing the adsorption by the name of a quasiconsecutive adsorption of two reagents. In our case they are hydrogen and benzene.

Making use of eq. (13) we can set up the algebraic sum $E_x - E_y$, if only the respective numerical values of a_x and a_y are known. The latter values can be evaluated from the kinetical equation of adsorption $\rho = f(\ln t)$ where for our experimental measurements $a = \text{tg } \alpha$.

Setting up a respective equation of type (13) for the reagents C_6H_6, H_2, C_6H_{12} by multiplying both sides of the equations by the coefficients $a_{C_6H_6}$, a_{H_2} and then dividing both sides of the equations by another equation with the coefficient $a_{C_6H_{12}}$, we come to the following dependency:

$$RT \ln \frac{a_{C_6H_6}\ a_{H_2}}{a_{C_6H_{12}}} = RT \ln \beta' \frac{Z_{C_6H_6}\ p_{C_6H_6}\ Z_{H_2}\ p_{H_2}}{Z_{C_6H_{12}}\ p_{C_6H_{12}}} + \qquad (14)$$

$$+ E_{C_6H_{12}} - E_{C_6H_6} - E_{H_2} .$$

This equation is valid for equal times of adsorption of the reagents C_6H_6, and C_6H_{12} in case when the adsorption takes place for each reagent seperately.

The algebraic sum of activation energies of adsorption of the respective reagents in a catalytical reaction may be measured in a similar way, if only $\ln (a_x/a_y)$ is known. We base in this case, of course, on experimental investigations.

In fig. 18 we find represented the efficiency of the reaction of hydrogenizing benzene into cyclohexane at a temperature of 180°C; it is drawn in form of the function $\ln (a_x/a_y)$:

$$w = \varphi\left(\frac{a_x}{a_y}\right) . \qquad (14a)$$

The appearance of two parallel straight lines in fig. 18 may be explained when basing on fig. 17.

The straight lines appearing in fig. 17 and concerning the content of 30% and 70% Ni refer to the adsorption of benzene steams, for which, as we see from the drawing, there is no preliminary adsorption procoess. In our case this is synonymous with depriving the catalyst surfaces of their gaseous modification.

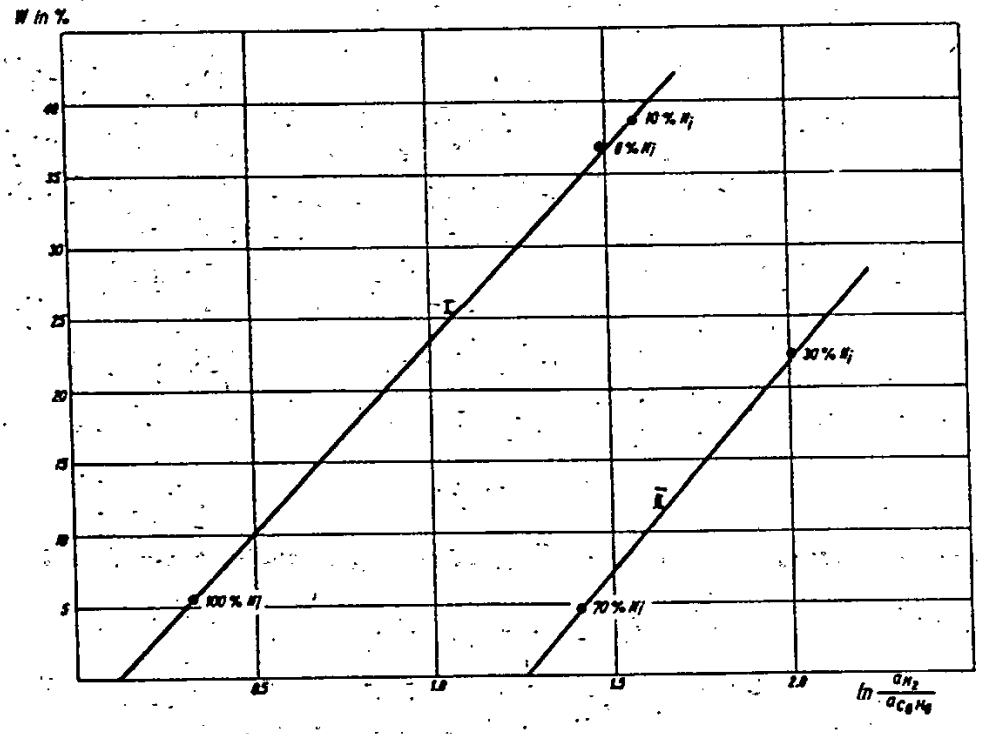

Fig. 18. Diagram $w = f(\log \frac{a_{H_2}}{a_{C_6H_6}})$ for the kinetics of adsorption at 180°C.

As the parallel straight lines I and II may be displaced with regard to one another, it must be concluded, basing on eq. (14), that the multiplier occuring in front of the exponent, as given in eq. (14) is larger for straight line II then for straight line I. Hence the mathematical product $Z_{H_2}\, p_{H_2}$ for 30% and 70% catalysts, the surfaces of which have not been modified by benzene steams, is larger than in case of modified surfaces.

As a temperature of 140°C the diagrams in fig. 19 comprising the characteristic value $dw/d(\ln a_x/a_y) = \Phi$, have a negative slope, whereas for a temperature of 180°C the slope is a positive one.

In the stationary state of a catalytical process there establishes at the catalyst surface a simultaneous adsorption process of the substrates, as well as a process of desorption of the reaction products. In such conditions the simultaneous adsorption must agree with the kinetics of the catalytical process.

For the stationary state we apply the following equation:

$$\frac{a^x_{C_6H_6}\, a^x_{H_2}}{a^x_{C_6H_{12}}} = \frac{Z^x_{H_2}\, Z^x_{C_6H_6}}{Z_{C_6H_{12}}} \cdot \frac{p_{H_2}\, p_{C_6H_6}}{p_{C_6H_{12}}} \beta' \exp\left(\frac{E^x_{C_6H_6} - E^x_{C_6H_6} - E_{H_2}}{RT}\right) \qquad (15)$$

where both values $a^x_{C_6H_6}$ and $a^x_{H_2}$ refer to the adsorption ratio at the active

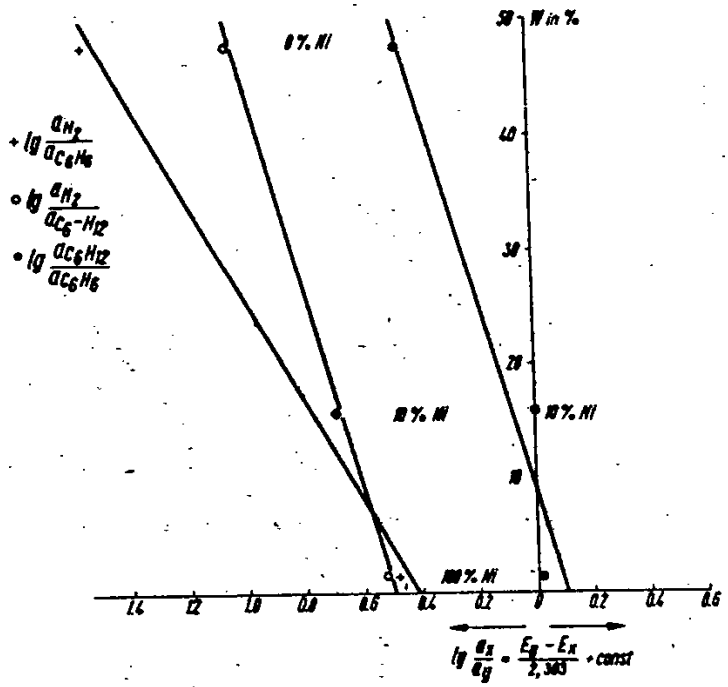

Fig. 19. Diagram $w = f(\log \frac{a_{H_2}}{a_{C_6H_6}})$ for the kinetics of adsorption at 140°C.

spots, whereas $a^{x}_{C_6H_{12}}$ expresses the ratio of desorption in cases when t_x = const. E_x are the values of the activation energy in a real desorption, connected with the active spots of adsorption, in contract to the value E_x denoting the apparent activation energy of the process. In such conditions the value expressed by static parameters equals to 1. The right hand side of the expression in eq. (15) bases on the conception of Van 't Hoff's box, the box being replaced by a porous catalyst. In order not to obscure the mechanism of this process, in which the cycles of adsorption and desorption occur again and again one after the other on various, so called "mosaical" areas of the catalyst surface, this successive occurence depending on the activation energy of these areas, we have confined our observations to stating the most general form of these phenomena.

Equation (15) may be expressed in the following way:

$$\frac{a_{C_6H_6}\,\gamma_{C_6H_6}\,a_{H_2}\,\gamma_{H_2}}{a_{C_6H_{12}}\,\gamma_{C_6H_{12}}} = \text{const.}^{x}\ \exp\left(\frac{E^{x}_{C_6H_{12}} - E^{x}_{C_6H_6} - E^{x}_{H_2}}{RT}\right) \qquad (16)$$

The values γ_x denote the coefficients, by which the numerical values of a_x, resulting from the measurements of a separate adsorption process, are to be multiplied in order to obtain the expression a_x. Thus eq. (16) expresses the stationary state of a catalytic process in case of a quasi-simultaneous adsorption, i. e. in case of an adsorption (on active spots) determined on the basis of kinetical measurements of a separate adsorption.

Because of the fact that for the stationary state the condition must be fulfilled, demanding that

$$\frac{a_{C_6H_{12}}\,\gamma_{C_6H_6}}{a_{C_6H_{12}}\,\gamma_{C_6H_{12}}} = 1\ , \tag{17}$$

hence

$$a_{H_2}\,\gamma_{H_2} = \text{const.}^{x}\ \exp\left(\frac{-\epsilon_{H_2}\,E_{H_2}}{RT}\right) \tag{18}$$

where $\epsilon_{H_2}\,E_{H_2} = E^{*}_{H_2}$.

In case when the selectivity of the hydrogenization process of benzene to cyclohexane for a stationary state amounts to 100%, then

$$w = \frac{-d_{H_2}}{dt} = \frac{dg^{x}_{H_2}}{dt} = \frac{a^{x}_{H_2}}{\text{const.}} = \frac{a_{H_2}\,\gamma_{H_2}}{\text{const.}}\ . \tag{19}$$

where w denotes the efficiency of a detailed process and $-(dH_2/dt)$ the hydrogen consumption during the catalytic process.

Taking into consideration eq. (19) as well as eq. (18) we obtain the following formula:

$$w = \text{const.}^{x}\ \exp\left(\frac{-\epsilon_{H_2}\,E_{H_2}}{RT}\right). \tag{20}$$

The experimental data for w, obtained for a series of catalysts, which have been modified at a temperature of 140°C, are presented in form of a function $\log a_{H_2}$ in fig. 20 (curve I).

This curve I fulfills the following equation:

$$w = \text{const.}\ \exp\left(-k\ \ln a_{H_2}\right) \tag{21}$$

where k is the negative directivity index.

Because the quantity w is connected with the adsorption of the active spots, eq. (21) may be expressed thus:

$$a^{x}_{H_2} = \text{const} \cdot \exp\left(-k\ \ln a_{H_2}\right)\ . \tag{22}$$

It results from this equation, that on the surface of catalysts with rising values of $(dg^{x}_{H_2}/dt) = a_{H_2}$ of a separate adsorption, there appears in a quasi-simultaneous adsorption for the stationary state a decrease of active spots. These facts correspond to the comparative results of the efficiency of the catalytical process, as we may see from the experimental curve presented in fig. 20. The efficiency of the process shrinks with the decrease of the number of active adsorption spots.

Dividing both sides of eqs. (20) and (21) we get:

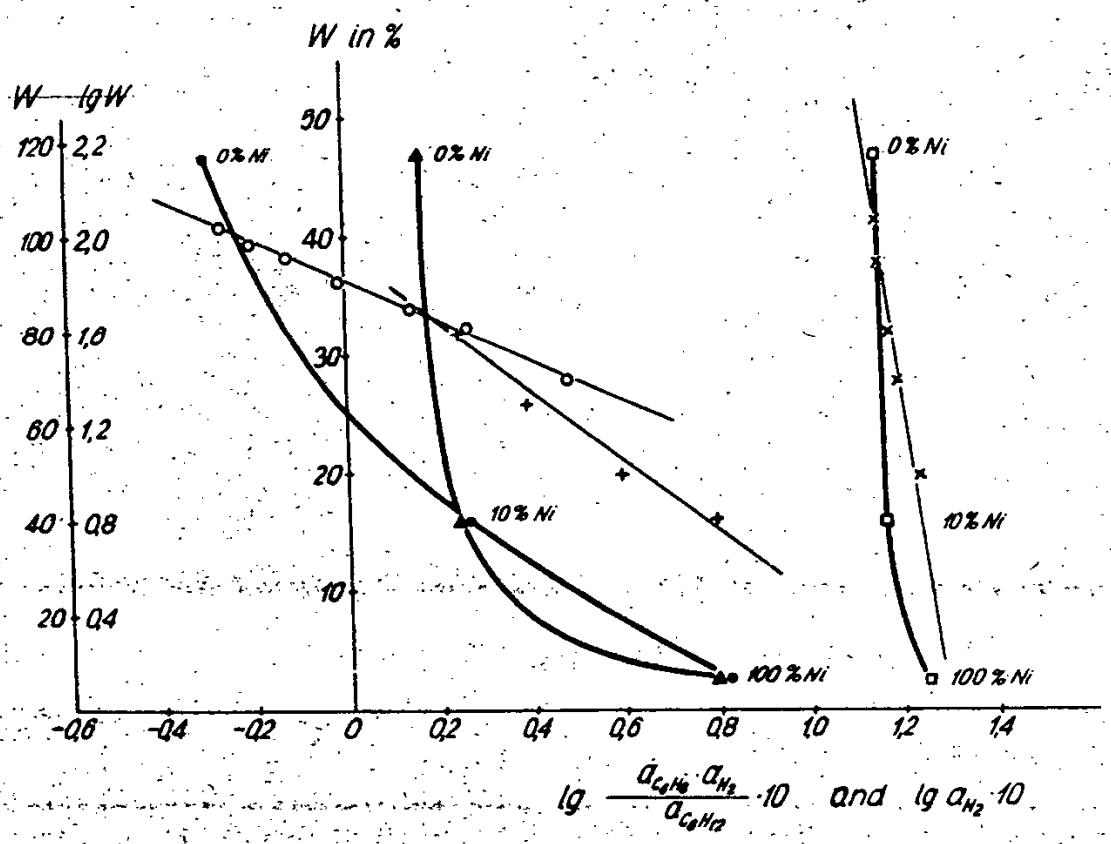

Fig. 20. Diagram $w = f\left(\frac{a_{C_6H_6} \cdot a_{H_2}}{a_{C_6H_{12}}} \times 10\right)$ and $w = f(\log a_{H_2} \times 10)$.

$$1 = \frac{\text{const.}^{x}}{\text{const.}} \exp\left(\frac{\epsilon_{H_2} E_{H_2}}{RT}\right) + k \ln a_{H_2}. \qquad (23)$$

It results from eq. (23) that function w has only one meaning if

$$\frac{\text{const.}^{x}}{\text{const.}} = 1 .$$

In such a case

$$\frac{\epsilon_{H_2} E_{H_2}}{RT} = k \ln a_{H_2} .$$

Knowing, then, from the diagram the value of k (according to eq. (21), and from the experiments the value of a_{H_2}, we can thus determine $\epsilon_{H_2} E_{H_2} = E^{*}_{H_2}$ for a quasi-simultaneous process.

The curve in fig. 20 corresponding to the temperature of 140°C and to $\ln a_{H_2}$, quite fulfills the experimental equation

$$w = \text{const} \cdot \exp\left(-k \ln a_{H_2}\right) .$$

For the sake of comparison, curve III(140°C) has been plotted in the coordinate system, too, viz.:

$$w = \varphi\left(\ln \frac{a_{C_6H_6}\, a_{H_2}}{a_{C_6H_{12}}}\right) .$$

It is easy to make out, that the curve in the latter case does not correspond to eq. (21). This is proved by the scatter of points of the straight line presented in this system:

$$\log w = \varphi\left(\log \frac{a_{C_6H_6}\, a_{H_2}}{a_{C_6H_{12}}}\right) .$$

The failure of curve II is a result of the lack of the coefficients γ_x; taking into account these coefficients, we should obtain the relation:

$$\frac{a_{C_6H_6}\, \gamma_{C_6H_6}}{a_{C_6H_{12}}\, \gamma_{C_6H_{12}}} = 1 .$$

The experimental curve II for a temperature of 180°C in the coordinate system $w = \varphi(\ln a_{H_2})$ fulfills eq. (21) quite well.

According to the results of structural investigations, the increase of nickel in the contact series of 0, 30 and 100% of Ni-content causes the appearance of a more regular structure of the crystals. The more regular structure of the crystal lattice comes forth in the kinetics of hydrogen adsorption, and the expressions $a^x_{H_2}$ and a_{H_2} represent the quantitative expressions of its kinetics. The numerical value of $a^x_{H_2}$ decreases as the amount of nickel content in the catalysts increases, in spite of the fact that a_{H_2} increases, too.

The quantity $-\mathrm{tg}\,\alpha = (da^x_{H_2}/da_{H_2})$ on the other hand, is a constant value, which proves that the changes of the structural properties of the investigated catalysts are continuous ones.

REFERENCES

1) F. Lihl, H. Wagner and P. Zemsch, Z. Elektrochem. 56 (1952) 612, 56 (1952) 619.
2) F. Hund, Z. Elektrochem. 56 (1952) 609.
3) W. Langenbeck, Angew. Chem. 68 (1956) 453.
4) S. Strother and H. Taylor, J. Am. Chem. Soc. 56 (1934) 586.
5) S. Z. Roginski, Problemy kinetiki i kataliza, Vol. VI (Moskwa - Leningrad, 1948).
6) S. T. Roginski, Adsorpcja i kataliz na nieodnorodnych powierchnostiach (Moskwa, 1948).

ABOUT MECHANISM OF CATALYTIC CONVERSIONS AND STRONG ADSORPTION OF UNSATURATED CYCLIC HYDROCARBONS ON PLATINUM AND PALLADIUM

V. M. GRYAZNOV, V. I. SHIMULIS, V. D. YAGODOVSKII
Peoples' Friendship University,
named after Patrice Lumumba, Moscow, USSR

Abstract: The mass-spectrometric investigation of the gaseous products of benzene vapour adsorption on platinum film at room temperature has shown the formation of hydrogen and methane. In the uncondensable at -196°C products of cyclohexene conversion on palladium film there has been found only hydrogen. These results confirm the idea that the redistribution of hydrogen in the unsaturated hydrocarbons is the combination of the dehydrogenation and hydrogenation reactions. Besides these data reveal some peculiarities of the strong adsorption of benzene on metal films.

1. INTRODUCTION

The investigations of cyclohexene, cyclohexadiene, benzene and cyclohexane conversions on platinum and palladium films [1-12] have shown that catalytic redistribution of hydrogen at room temperature and pressures less than 10^{-2} torr may occur as the combination of the dehydrogenation and hydrogenation reactions of the original hydrocarbon. In the course of these catalytic processes there has been observed the educing of gas which did not condense at the temperature of liquid nitrogen and contained hydrogen. The hydrogen is also splitted at the strong adsorption which takes place during the first contact of any studied hydrocarbon with fresh platinum or palladium film. The splitting of hydrogen at the adsorption of benzene on the films of nickel, iron and platinum was observed earlier [13] but the data of gas analysis are not presented in that paper. For further elucidation of the interactions between hydrocarbons and metal surfaces the mass-spectrometric investigation of the forming gases was carried out.

2. EXPERIMENTAL

The gaseous products of the strong adsorption of benzene vapour on the platinum film were analysed with the help of radio frequency mass spectrometer (omegatron) which had the glass bulb *. The benzene vapour introduced into the adsorption bulb and omegatron by molecular flow through the capil-

* These experiments were made with participation of T. N. Ovchinnikova.

lary cut off with gallium valve. The pressure of residual gases before the experiment was about 2×10^{-7} torr on the air scale of ionisation gauge. The peaks of residual gases, methane, benzene and krypton for calibrating of the omegatron have been measured. It has been found that the relation M/e = const/f between the M/e-mass-to-charge ratio of resonance ions and the radio frequency f is fulfilled satisfactorily till M/e = 84.

The mass-spectrum of benzene has been recorded at radio frequency voltage 2 V which was used in the work [14]. This spectrum had peaks M/e = 74, 52, 39 except molecular ion peak. The decrease of radio frequency voltage to 0.8 V allowed to observe the peaks 51 and 50 too. Peaks 74, 52, 51, 50 and 39 are the most intensive ones according to data [15], but the relative intensity of each of these peaks respective to the molecular peak is much more in the experiments with the omegatron (see table 1). It seems likely that peak 77 was not separated from peak 78. The relative intensities of the peaks of methane mass spectrum have been found close to the data [15] (see table 2). The intensity of peak 14 has not been estimated because of the presence of nitrogen admixture in methane.

The mass spectra of benzene and methane have been recorded during the pumping of analysed vapour out of omegatron and adsorption bulb. How-

Table 1
The most intensive peaks of the benzene mass spectrum.

M/e	Relative intensities		
	Roberts and Johnsen [15]	This work	
		immediately after admission	10 min after admission
78	100.0	100	100
77	18.4	-	-
74	3.79	8	170
52	17.5	70	-
51	14.7	80	460
50	12.0	63	-
39	11.3	60	428

Table 2
The intensities of the methane mass spectrum.

M/e	Relative intensities	
	Roberts and Johnsen [15]	This work
16	100.0	100
15	80.1	83
14	8.28	-
13	2.90	2

ever, it was desirable to make the analyses of small quantities of gaseous products of benzene chemisorption without pumping out the omegatron. In this connection experiments have been carried out with introduction of the definite quantities of benzene and methane in the omegatron.

The necessary quantity of vapour was introduced with a help of capillary. The speed of molecular flow through the capillary was measured for krypton whose adsorption on the glass walls of the apparatus at room temperature was negligible. The corresponding data for benzene and methane have been calculated as $W = W_{Kr}\sqrt{M/M_{Kr}}$.

It has been found that the intensities of peaks 16 and 15 rise up linearly with the quantity of methane admitted in omegatron. The other result has been obtained by letting in benzene vapour in the omegatron out off from the pump. Peak 78 dropped swiftly and peaks 1, 2, 14, 15, 16 rose. This indicated the decomposition of benzene probably caused by the contact with hot metal parts of the working omegatron. This undesirable effect was diminished by freezing the benzene in front of the omegatron at temperature of liquid nitrogen. The introduction of benzene vapour into uncooled adsorption bulb without platinum film brought about the appearance of peaks 15 and 16 in the mass spectrum of uncondensable gases. Special conditions for cooling the low part of the adsorption bulb have been selected, and they prevent the appearance of peaks 15 and 16 in the mass spectrum. Under these conditions the opening of the magnet operated non-greased glass valve between the omegatron and the adsorption bulb with benzene vapour increased the intensity of peak I alone. Therefore this procedure is good for revealing methane if it appeared at the chemisorption of benzene on platinum film.

The platinum film was sublimed into the adsorption bulb by electric heating of platinum wire. The bulb walls had the room temperature, the pressure during the sublimation was about 5×10^{-7} torr and dropped to 2×10^{-7} torr after cooling the wire. The platinum film was transparent as the ones used in previous works [5-9], its geometrical surface was equal to 100 cm^2. The benzene vapour was introduced into the adsorption bulb immediately after the film sublimation. During the benzene introduction and 5 min after that the adsorption bulb had the room temperature. For the next 40 min the low part of the bulb was cooled by liquid nitrogen. The cooled part of the bulb was not covered with platinum film. The cooling continued for 27 min more after opening non-greased glass valve between the adsorption bulb and omegatron for freezing the benzene vapour which could penetrate into omegatron through the glass valve.

The mass spectrum of uncondensable at -196°C gaseous products of benzene adsorption on platinum film is presented in table 3. The pressure in the system was 1.5×10^{-7} torr. Peaks 15 and 16 indicate the formation of methane. It is interesting to note that peak 15 is somewhat higher than peak 16 in spite of reverse intensity correlation in the methane mass spectrum (see table 2). The following records of mass spectra of the benzene adsorption products have shown the regular change of some peak intensities (see fig. 1). The extrapolation of straight lines for M/e = 15 and 16 in fig. 1 with the help of the data of table 1 permit to evaluate the amount of methane which has been formed before switching on the omegatron as 10^{14} molecules.

Table 3
The mass spectrum of uncondensable at -196°C gaseous products of benzene adsorption on the platinum film.

M/e	Intensity (mV)	M/e	Intensity (mV)	M/e	Intensity (mV)
1	64	8	12	16.5	7
2	23	12	2	17	6
6	1	14	42	18	2
6.5	3	15	37	28	48
7	15	15.5	6	29	15
7.5	16	16	33	40	2

The detection of methane in gaseous products of strong benzene adsorption on platinum film made us verify whether methane formed during the catalytic redistribution of hydrogen in cyclohexene and cyclohexadiene. Palladium is a better catalyst for these reactions than platinum and the mirror palladium film was used in the experiments with cyclohexene. The procedure of film sublimation was similar to the described above, the reaction bulb had the same size as the adsorption bulb used in the experiments with platinum film and benzene. The cyclohexene vapour was admitted in the reaction bulb with fresh palladium film till the pressure was about 0.1 torr and was heated during 15 min at 50°C. In accordance with the previous data [6, 9] the uncondensable at -196° gas was found in the reaction bulb. The pressure of that gas was close to 3.5×10^{-3} torr. The gas was introduced into the ionisation region of MX-1302 mass spectrometer through the needle valve. The speed of gas introduction was permanent in all the analyses and in the course of calibration on hydrogen before sublimation on the palladium film on the walls of reaction bulb. Mass spectrum of uncondensable products of cyclohexene conversion coincided with the hydrogen mass spectrum, the pressure dependence of peak 2 intensity (black circles on fig. 2) was very close to that for pure hydrogen (light circles). Thus methane has not been found in the gaseous products of cyclohexene conversion on palladium film.

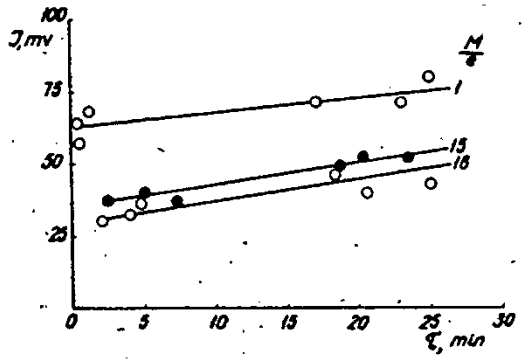

Fig. 1. The dependence of peaks intensities of mass spectrum of gaseous products of benzene adsorption on platinum film on the time after this products admission into omegatron.

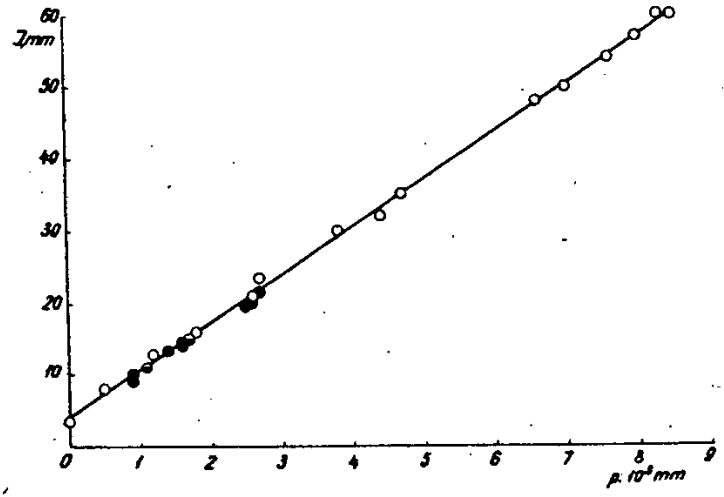

Fig. 2. The pressure dependence of peak 2 intensity for gaseous products of cyclohexene conversion on palladium film (black circles) and for hydrogen (light circles).

3. DISCUSSION

The detection of methane in products of benzene adsorption on fresh platinum film throws light upon the mechanism of interaction between benzene molecules and metal surface. There are some data [16] about formation of methane at high temperature hydrocracking of hydrocarbons on iron, cobalt and nickel catalysts. For high temperature the mechanism of methane formation from the elements was proposed in paper [17]. The main role in that mechanism was ascribed to the external C atoms of graphite cristal lattice. It was supposed that the hydrogenation of double bonds between such atoms led to breaking these bonds and forming of pairs of CH_3 groups linked to neighbouring "benzene" elements of graphite net. This scheme was used [18] for explanation of kinetics of methane formation from the elements.

The strong adsorption of benzene molecules on platinum with partial splitting of H atoms is probably connected with appearance on the metal surface of peculiar radicals which are bound with metal atoms. The hydrogen being released may join adsorbed benzene molecules. As a result of such redistribution of hydrogen among adsorbed molecules there appears a whole series of products, and it is quite possible that tensions occurring in rings, connected, in situ of splitted H atoms, with several metal atoms, condition a deep destruction. Among the products of this destruction one may expect methane and CH_3 radicals. The last assumption conforms with reverse intensity correlation of lines 15 and 16 than the usual one for the methane mass-spectrum.

The increase of methane and hydrogen formation with contact time of benzene and platinum film may be caused by displacement of the adsorbed benzene molecules along the metal surface. The molecules previously adsorbed in the places of low adsorption potential pass to the strong adsorption centres where the destruction can occur. Such displacement of benzene molecules takes about 10 min at room temperature [4]. The cooling of the

low part of the adsorption vessel by liquid nitrogen may decrease the temperature of platinum film under 20°C and therefore moderate the mobility of adsorbed benzene molecules. This explanation is not the only possible one.

The question about the methane formation at the strong adsorption of cyclohexene is to be solved by special investigation. In the above experments the cyclohexene pressure was comparatively high and the catalytic dehydrogenation could make the detection of strong adsorption products difficult.

In considering the mechanism of catalytic redistribution of hydrogen in unsaturated hydrocarbons on carbons [9,11 12] the essential point was the evaluation of quantities of uncondensable at -196°C gas which was taken for hydrogen. This assumption is confirmed in this paper. It is a new argument in favour of the idea that the hydrogen redistribution in hydrocarbons on metal catalysts is the combination of dehydrogenation and hydrogenation reactions but not a one-stage process.

REFERENCES

1) V.M.Grjaznov and V.D.Yagodovskii, Doklady Akad.Nauk SSSR 116 (1957) 81.
2) V.M.Grajznov, V.D.Yagodovskii and A.M.Bogomolnii, Ho Dju ok, Doklady Akad. Nauk SSSR 121 (1958) 499.
3) V.M.Grajznov, V.D.Yagodovskii and M.K.Charkviani, Vestnik Moskovsk. Univers.Ser II, Chemistry (1960) no.1, p.11.
4) V.M.Grajznov, V.I.Shimulis and V.D.Yagodovskii, Doklady Akad.Nauk SSSR 132 (1960) 1132.
5) V.M.Grajznov and V.I.Shimulis, Kinetika Kataliz 2 (1961) 534.
6) V.M.Grajznov and V.I.Shimulis, Kinetika Kataliz 2 (1961) 894.
7) V.M.Grajznov and V.I.Shimulis, Vestnik Moskovsk.Univers. Ser.II, Chemistry (1961) no.6, p.25.
8) V.M.Grajznov, V.I.Shimulis and T.V.Dillingerova, Vestnik Moskovsk.Univers. Ser.II, Chemistry (1962) no.2, p.26.
9) V.M.Grajznov and V.I.Shimulis, Doklady Akad.Nauk SSSR 139 (1961) 870.
10) V.M.Grajznov, V.D.Yagodovskii, E.A.Savel'eva and V.I.Shimulis, Kinetika Kataliz 3 (1962) 99.
11) V.M.Grajznov, Investigation of Kinetics and Mechanism of Conversions of Some Hydrocarbons on Metals, D.Sci.Thesis Moscow (1962).
12) V.M.Grajznov, Uspekhi Khim.32 (1963) 433.
13) R.Suhrman, B.Hahn and G.Wedler, Naturwissenschaften 44 (1957) 60.
14) A.P.Averina, Pribori Technika Eksperim.(1962) no.3, p.123.
15) R.H.Roberts and S.E.J.Johnsen, Analyt.Chem.20 (1948) 1225.
16) H.Koelbel, H.B.Ludwig and H.Hammer, J.Catalysis 1 (1962) 156.
17) C.W.Zielke and E.Gorin, Ind.Eng.Chem.47 (1955) 820.
18) K.Hedden, Z.Elektrochem.66 (1962) 652.

SYSTEMATIC STUDY OF FACTORS INFLUENCING THE SELECTIVITY OF DECOMPOSITION REACTIONS OF ALCOHOLS ON PURE AND SUPPORTED MIXED OXIDES

I. BATTA, S. BÖRCSÖK, F. SOLYMOSI and Z. G. SZABÓ
Institute of Inorganic and Analytical Chemistry,
University of Szeged, Szeged, Hungary

Abstract: To contribute to the problem of selectivity, kinetical parameters of the decomposition reactions of isopropyl alcohol, depending on the procedure of preparation and the poisoning of the catalyst, were measured as accurately as possible. The poisoning was achieved not only with cations, but with anions, too. A very marked change in selectivity was caused already by a relatively small amount of sulphate ions, since in their presence the dehydration reaction became dominating. Special care was taken to establish a correlation between the electric properties and catalytic activity. Considering the other experimental data also it can be stated as a rule that the more ionic a character a catalyst oxide possesses, the more it dehydrogenates, and the nearer the oxide approaches the covalent character, the greater is the dehydration.

1. INTRODUCTION

In this paper we summarize the results of experiments on the catalytic decomposition of isopropyl alcohol on zinc oxide. The catalytic decomposition of isopropyl alcohol may be twofold: dehydrogenation and dehydration. The process - as we shall see - goes under certain conditions in both directions on zinc oxide, too. Thus the study of this catalytic reaction renders a suitable model for the investigation of the problem of selectivity. The reaction belongs to type II of Wheeler's classification.

Literature contains numerous experimental data on the catalytic decomposition of alcohols on zinc oxide. The overwhelming majority of authors regards zinc oxide as a dehydrogenating catalyst. However, there are diverse opinions concerning the mechanism of dehydrogenation and selectivity, respectively. None of these have so far rendered a generally accepted theory. The mechanism as suggested by Eucken [1] and Wicke [2] is based on geometrical viewpoints and really a great many of the experimental facts are in accordance with the deductions drawn from this view. For example, the deuterium content of water formed in the dehydration of alcohols increased when the surface of the oxide was covered with deuterium [3]. Further the geometrical view is supported by the experimental facts, too, referred to by Marsh [4], namely that with several oxide catalysts, whether previously preheated or not, the same selectivity factor has been found in the catalytic decomposition of alcohols and of formic acid.

Another standpoint is taken by Schwab [5]. According to him catalysts treated at high temperatures are dehydrogenating while those treated at low temperatures dehydrating. The difference comes from the surface conditions. Catalysts formed at high temperatures are dense, have smooth surfaces and dehydrogenation takes place on them in one-point adsorption, while catalysts prepared at low temperatures have large surfaces and dehydration occurs in the pores according to a two-point adsorption. Wheeler [6] has given considerable support to Schwab's theory when pointing out theoretically the correlation between the pore structure and the activity of the catalyst, what influences the temperature coefficient, the kinetic order and the poisoning characteristics, and hence the selectivity of the catalyst. For selectivity type II, studied by us, the rule is generally valid that reactions taking place at low pressures are accelerated by catalysts with small pores, those operating at high pressures by catalysts with large pores.

However, since Wheeler in his theory considers geometrical factors only, such as pore size, his results, though being very interesting and valuable for experimental purposes, do not give satisfactory solution concerning the mechanism, i. e., the sequence of elementary processes of the chemical conversion. Namely, it is not substantiated how the reaction is influenced by the material of the catalyst (supposing the same surface characteristics).

Another possible interpretation of selectivity is rendered by Hauffe's [7] theory when discussing the role of the electronic factor in the alterations of selectivity, so successfully applied in the theory of catalytic processes on metals and semiconductors.

In our own experiments we have started from the observation that the selectivity of Al_2O_3, applied widely in the dehydrogenation of alcohols, is different in the case of oxides prepared from nitrate and from sulphate by precipitation. Our experiments were aimed at studying how the activity of pure *n*-conductor zinc oxide, a dehydrogenating catalyst, can be altered so that it also operates as a dehydrating agent.

2. EXPERIMENTAL

2.1. *Apparatus*

Catalytic decomposition reactions were carried out in the so called open Schwab reactor modified by us [8]. The evaporation of alcohol at a constant rate, i. e., the constant feed concentration was assured by constant temperature adjusted by an ultrathermostate. Catalysts were applied in the form of small grains of pellets. The stream of alcohol vapour penetrates the catalyst layer from top downwards. The rate of the catalysed reaction was controlled by soap-bubble flow-meters after condensing the products boiling above 0°C in a water cooler. The first flow-meter controlled the total amount of gas. Thereafter propylene was frozen out by liquid air, thus the second flow-meter indicated only the amount of hydrogen, i. e.,

the rate of the dehydrogenation reaction.

2.2. *Preparation of catalysts*

Catalysts used in our experiments were all prepared from the same sample of zinc oxide. Zinc oxide was dissolved in either c.p. nitric acid or in a mixture of c.p. nitric acid and c.p. sulphuric acid of various ratios. Then the complex $[Zn(NH_3)_6]^{2+}$ salt was formed with excess ammonium hydroxide. Zinc hydroxide was separated by boiling this solution and by expelling the ammonia. The precipitate was dried, decomposed at 400°C while slowly raising the temperature, and tempered for five hours at 500 or 800°C, respectively. These were the catalysts prepared by coprecipitation. In case of catalysts prepared by suspension, zinc oxide was suspended in a solution of certain amount of zinc sulphate, phosphorus pentoxide, boric acid and zinc chloride, then dried and treated at 500 or 800°C, respectively.

The sintered catalysts were powdered and compressed into pellets. The surface of the ready catalysts was determined by BET method from the adsorption measured at the temperature of liquid nitrogen. Electric resistance was measured on tablets pressed between platinum plates, in a vacuum apparatus at different temperatures, first in oxygen, then in vacuo, in hydrogen and in oxygen again.

3. RESULTS

Our experimental data do not allow us to make a decision between the two points of view referred to in the Introduction as they support both considerations in certain aspects.

The poisoning with cations of higher or lower valency, and this is what increases or decreases the electron conductivity, only influences the dehydrogenation reactions so that it changes the energies of activation but not the selectivity [9]. When different amounts of sulphate ions were added to zinc oxide and the catalyst and treated exactly in the same manner as in case of pure zinc oxide, catalysed the dehydration reaction to a marked extent. This experimental result may give rise to the problem of poisoning with anions. To this end we attempted to poison zinc oxide with other anions. In the case of phosphate and borate, although a slight decrease of the selectivity factor was observable (by selectivity factor we mean the ratio of conversion towards dehydrogenation and of total conversion) the effect was far weaker than that due to the sulphate. No effect was observed when silicic acid and chloride ions were added. The latter can be ascribed to the fact that at the temperature of the experiment zinc chloride is too volatile and so the chloride content diminishes appreciably during pre-treatment. Table 1 shows that by increasing the SO_3 content the energy of activation of the total conversion changes considerably, the energy of activation of the dehydrogenation reaction increases, while that of the dehydration reaction decreases.

BET measurements showed that by the addition of sulphates the surface of zinc oxide is markedly enlarged. The compact catalyst changes into one

Table 1

Values of catalytic activity, surface area and resistivity for various specimens.

No.	catalyst	analysis, mole% of poisoning	total activity $V_{(H_2+Pr)}$ ml min^{-1} g^{-1} at 300° C	surface m^2/g	specific activity $V_{(H_2+Pr)}$ ml min^{-1} m^{-2}	selectivity V_{H_2} / $V_{(H_2+Pr)}$: 100	E_{total} kcal $mole^{-1}$	kcal $mole^{-1}$	E_{H_2} kcal $mole^{-1}$	ρ(ohm cm)^x at 340° C	$E\rho$ kcal $mole^{-1}$
			coprecipitated, treatment at 500° C for 5h.								
4	ZnO	-	1.08	7.6	0.14	93-97	22.2	22.4	-	$8.5 \cdot 10^6$(O_2)	17.1
8	ZnO+SO_3	0.2% SO_3	0.32	6.0	0.065	36-45	34.0	33.6	33.4	3.9 (H_2)	
146	ZnO+SO_3	2.2% SO_3	0.85	25.9	0.034	29-50	31.9	27.6	32.6		
5	ZnO+SO_3	3.8% SO_3	1.99	21.1	0.094	8-15	31.1	-	21.2	$3.1 \cdot 10^6$(O_2) 193 (H_2)	20.4
			coprecipitated, treatment at 800° C for 5h.								
6	ZnO	-	1.27	6.2	0.21	90-98	21.0	21.4	29.2	$0.63 \cdot 10^6$(O_2) 19.3(H_2)	11.2
12	ZnO+SO_3	0.2% SO_3	0.57	5.9	0.097	80-92	24.3	25.4	28.3		
147	ZnO+SO_3	1.9% SO_3	0.38	27.8	0.014	33-50	37.0	30.2	44.7		
145	ZnO+SO_3	3.3% SO_3	0.26	18.6	0.014	20-28	41.6	36.6	37.4	$52.9 \cdot 10^6$(O_2) 365 (H_2)	21.8
			suspended, treatment at 500° C for 5 h								
152	ZnO	-	3.57	12.9	0.28	89-96	26.0	23.8	-		
3	ZnO+SO_3	0.1% SO_3	0.88			20-30	37.4	24.5	41.2		
1	ZnO+SO_3	1.0% SO_3	1.17	10.4	0.11	8-10	31.7	-	31.7		
9	ZnO+B_2O_3	1.0% B_2O_3	3.85			89-94	27.9	29.5	-		
13	ZnO+B_2O_3	5.0% B_2O_3	3.58	16.4	0.22	93-99	21.3	24.0	-		
11	ZnO+Cl	0.24% Cl	3.2			88-92	30.7	31.5	-		
150	ZnO+P_2O_5	1.0% P_2O_5	1.37			94-98	32.5	31.3	-		
			suspended, treatment at 800° C for 5 h.								
10	ZnO+B_2O_3	1.0% B_2O_3	2.81			95-100	-	-	-		
151	ZnO+P_2O_5	1.0% P_2O_5	1.01			86-96	34.1	28.0	-		
154	ZnO+P_2O_5	5.0% P_2O_5	1.64			92-100	28.6	27.3	-		
153	ZnO+SiO_2	2.0% SiO_2	2.31			96-100	29.8	29.3	-		
54	MgO (500° C)	-	0.20			96-100	27.0	26.6	-		
15	MgO+SO_3(500° C)	0.6% SO_3	0.23			91-94	27.4	26.6	-		
155	$Zn_2P_2O_7$ (400° C)	-	1.0			0	-	-	53.4		
17	$Zn_2P_2O_7$ (800° C)	-	0.19	17.0	0.011	0	-	-	37.0		
16	$ZnSO_4$ (400° C)	-	9.3			0	-	-	41.0		

x determined in 100 mm Hg oxygen or hydrogen, resp.
xx determined in 100 mm Hg oxygen
Pr - propylene

STAT

the rate of the dehydrogenation reaction.

2.2. *Preparation of catalysts*

Catalysts used in our experiments were all prepared from the same sample of zinc oxide. Zinc oxide was dissolved in either c.p. nitric acid or in a mixture of c.p. nitric acid and c.p. sulphuric acid of various ratios. Then the complex $[Zn(NH_3)_6]^{2+}$ salt was formed with excess ammonium hydroxide. Zinc hydroxide was separated by boiling this solution and by expelling the ammonia. The precipitate was dried, decomposed at 400°C while slowly raising the temperature, and tempered for five hours at 500 or 800°C, respectively. These were the catalysts prepared by coprecipitation. In case of catalysts prepared by suspension, zinc oxide was suspended in a solution of certain amount of zinc sulphate, phosphorus pentoxide, boric acid and zinc chlroride, then dried and treated at 500 or 800°C, respectively.

The sintered catalysts were powdered and compressed into pellets. The surface of the ready catalysts was determined by BET method from the adsorption measured at the temperature of liquid nitrogen. Electric resistance was measured on tablets pressed between platinum plates, in a vacuum apparatus at different temperatures, first in oxygen, then in vacuo, in hydrogen and in oxygen again.

3. RESULTS

Our experimental data do not allow us to make a decision between the two points of view referred to in the Introduction as they support both considerations in certain aspects.

The poisoning with cations of higher or lower valency, and this is what increases or decreases the electron conductivity, only influences the dehydrogenation reactions so that it changes the energies of activation but not the selectivity [9]. When different amounts of sulphate ions were added to zinc oxide and the catalyst and treated exactly in the same manner as in case of pure zinc oxide, catalysed the dehydration reaction to a marked extent. This experimental result may give rise to the problem of poisoning with anions. To this end we attempted to poison zinc oxide with other anions. In the case of phosphate and borate, although a slight decrease of the selectivity factor was observable (by selectivity factor we mean the ratio of conversion towards dehydrogenation and of total conversion) the effect was far weaker than that due to the sulphate. No effect was observed when silicic acid and chloride ions were added. The latter can be ascribed to the fact that at the temperature of the experiment zinc chloride is too volatile and so the chloride content diminishes appreciably during pre-treatment. Table 1 shows that by increasing the SO_3 content the energy of activation of the total conversion changes considerably, the energy of activation of the dehydrogenation reaction increases, while that of the dehydration reaction decreases.

BET measurements showed that by the addition of sulphates the surface of zinc oxide is markedly enlarged. The compact catalyst changes into one

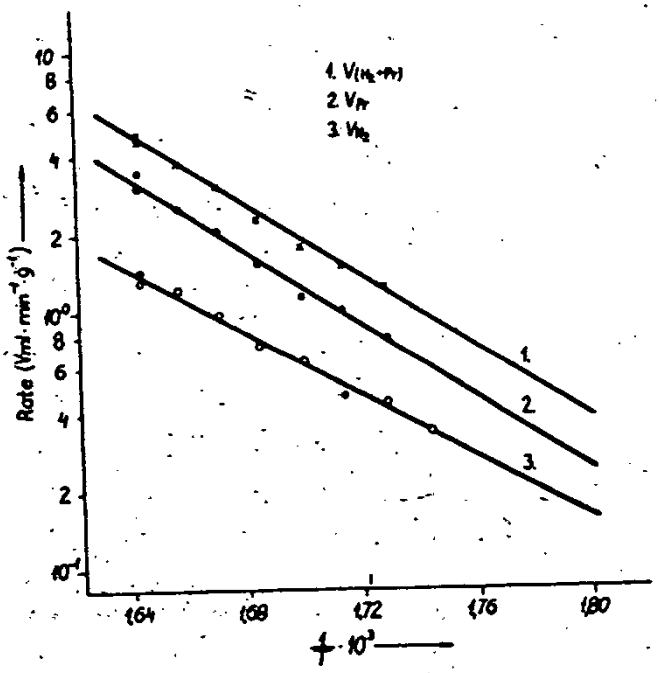

Fig. 1. Arrhenius plot of one exp. of isopropyl alcohol decomposition on ZnO + 2.2 mole % SO_3 catalyst sintered at 500°C for 5 h.

with looser structure. This supports the Schwab-Wheeler theory. But a very important difference must be emphasized here, namely that the marked increase of dehydration, i. e. the decrease of the selectivity factor due to poisoning with SO_3, is not wholly the result of poisoning of dehydrogenating centres. At the same time the dehydration centres remain active since the specific activity of catalysts poisoned with sulphate ions increases for the dehydration reaction in absolute value. Therefore the case is not that the dehydrogenation centres being covered no longer take part in the process and dehydration becomes more apparent.

Variations in the electric conductivity due to poisoning with sulphate ions have also been studied, namely in vacuo, in oxygen and hydrogen atmospheres, and at the same time the energy of activation of conductivity has also been taken in each ambient atmosphere. No very marked differences were found.

This statement is against the effect of the electronic factor, but it is in accordance with Schwab's conception. Anyway, we are of the opinion that the electronic factor cannot be entirely left out of consideration, as it is shown by changes in the selectivity factor of the decomposition of formic acid on a number of other oxides, poisoned with various cations [10]. On *n*-conductor titanic dioxide the selectivity of decomposition of formic acid is shifted towards dehydration when as a result of poisoning the electron concentration decreases. On the contrary, at *p*-conductor chromic oxide with a decrease in the number of electron holes the rate of dehydration reaction also increased. Thus both on *p*- and *n*-conductor oxides, when the

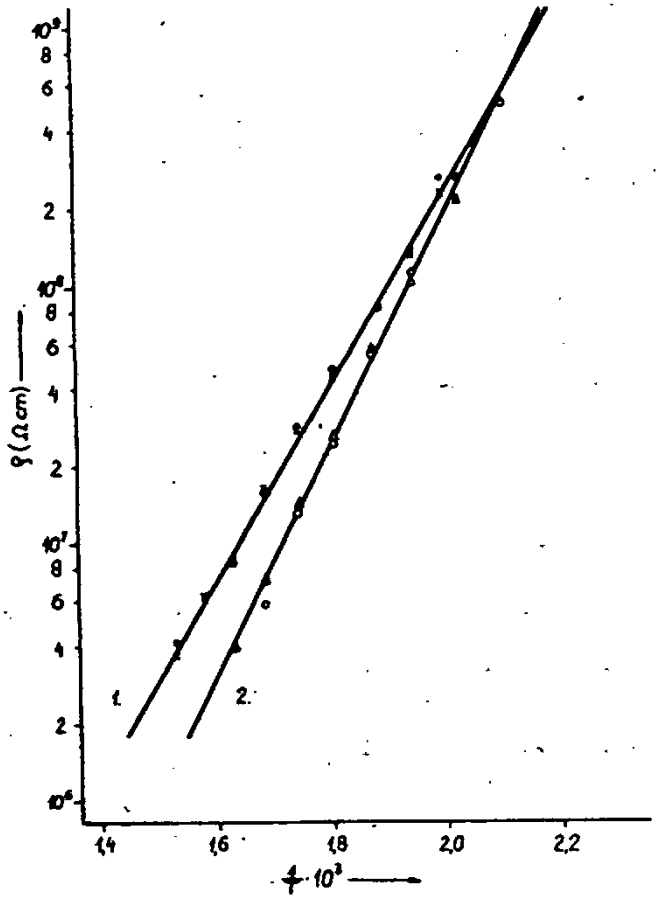

Fig. 2. The dependence of specific resistivity on temperature.
1. ZnO (sintered at 500°C for 5 h)
2. ZnO + 3.8 mole % SO_3 (sintered at 500°C for 5h)
x, Δ upwards in oxygen
•, o downwards in oxygen

conductivity of the catalyst decreases, the dehydrogenation reaction is shifted to the second plane.

The structure of catalysts and the building-in of poisoning ions, respec tively, was controlled by X-ray examinations.

The sulphate ions penetrate the zinc oxide lattice very easily but other poisoning anions do not. This is in accordance with the observation that the latter ions do not affect the selectivity.

4. DISCUSSION

Taking the experimental data above into account we think that it would be erroneous to regard the geometrical factor to be the only significant one in the determination of selectivity. The function suggested by Eucken [1]

$$\frac{(\text{radius of the cation})^3}{(\text{mole} \cdot \text{volume per cation})(\text{charge of cation})}$$

is, perhaps, correct basically, but the deductions made from it are wrong, if the size of the cation, as in Balandin's multiplet theory, is regarded as an independent variable of the catalytic efficiency. The scattered experimental data does not allow that Eucken's function should be regarded valid strictly, with respect to the exponents. However, regarding that the ratio of the valency of a cation and its radius gives the polarizing power, then the changes of selectivity can be related to the character of bonds in the catalyst. Namely, the greater the polarizing power, the more covalent will be the bond formed and the greater the dehydration. In case of low ionic charge and large size the bond between the closely or almost closely packed oxygen ions and the cation is more ionic in character. Oxides of more positive metals are dehydrogenating. Therefore it can generally be said that the more ionic a bond an oxide possesses, the more strongly dehydrogenating it is and the nearer it approaches the covalent bond character, the more dehydrating it is. Knowing this it is obvious that the selectivity factor is not determined by the *n*- or *p*-conducting characteristics of semiconductor oxides, but by the nature of oxygen-cation bonds.

The variation of selectivity due to the basic or acidic character of oxides can also be interpreted so that the strength of the hydrogen coupling to non-deformed (oxides of more positive metals) and to deformed (acidic oxides) oxygen ions is considered. In the first case the hydrogen coupling is strong, i.e., we shall have dehydrogenation and in the second the hydrogen coupling is weak, but a strong hydroxyl coupling becomes possible, consequently dehydration takes place.

Although data on the selectivity factor are rather scattered the following series of oxides can be written:

$$\underset{\text{Dehydrogenation}}{\longleftarrow} \quad \text{CaO} \quad \text{MgO} \quad \text{ZnO} \quad \text{FeO} \cdot \text{Fe}_2\text{O}_3 \quad \text{Cr}_2\text{O}_3 \quad \text{TiO}_2 \quad \text{Al}_2\text{O}_3 \quad \text{SiO}_2 \quad \text{WO}_3 \quad \underset{\text{Dehydration}}{\longrightarrow}$$

This classification, although from a different point of view, to some extent has a similar content to Schwab and his coworkers' statement on the role of Lewis-acids and Broensted-acids [11].

That here the electronic state of the oxygen ions is a controlling factor is proved also by the data obtained on $ZnSO_4$ and Zn_2PO_7. In these salts the oxygens exhibit covalent character and thus the catalytic effect is completely a dehydrating one.

The Authors express their thanks to Mr. K. Jáky and Mrs. E. Takács for their valuable assistance.

REFERENCES

1) A. Eucken, Naturwiss. 36 (1949) 48;
A. Eucken and K. Heuer, Z. physik. Chem. (Leipzig) 196 (1950) 40.
2) E. Wicke, Z. Elektrochem. 53 (1949) 279.
3) H. J. Leugering, Heterogener Wasserstoffisotopen-Austausch an Al_2O_3-Oberflächen mit verschiedener Hydroxylgruppenbelegung. Thesis (Göttingen, 1948).
4) P. Marsh, The Mechanism of Heterogeneous Catalysis, ed. by J. H. de Boer (Elsevier, 1960) p. 50.
5) G. M. Schwab and Elly Schwab-Agallidis, J. Am. Chem. Soc. 71 (1949) 1806.
6) A. Wheeler, Catalysis, ed. by P. H. Emmett, Vol. 2. (New York, 1955) p. 105.
7) K. Hauffe, Angewandte Chemie 67 (1955) 189.
8) Z. G. Szabó and F. Solymosi, Z. Elektrochem. 63 (1959) 1177.
9) G. M. Schwab, XVIIth International Congress of Pure and Applied Chemistry (1959).
10) Z. G. Szabó and F. Solymosi, Acta Chim. Hung. 25 (1960) 145.
11) G. M. Schwab, O. Jenkner and W. Leitenberger, Z. Elektrochem. 63 (1959) 461.

Declassified in Part - Sanitized Copy Approved for Release 2014/03/04 : CIA-RDP80-00247A004200070001-6

SELECTIVE HETEROGENEOUS CATALYTIC OXIDATION OF HYDROCARBONS

I. I. IOFFE
Institute for Organic Semi-Products and Dyes, Moscow

and

L. Ya. MARGOLIS
Institute of Chemical Physics, Academy of Sciences, Moscow, USSR

Abstract: The kinetics of selective heterogeneous catalytic oxidation of hydrocarbons with molecular oxygen is a function of two factors: of the site where a hydrocarbon molecule is attacked with oxygen, which depends on the sum of crystalline, complexing and semiconducting properties of the catalyst, and of the ratio of adsorption to description rates for all intermediate and end-products of the reaction.

Investigations were made on the vapour- and liquid-phase oxidation of olefines and aromatics, on simple and complex oxide systems containing vanadium, molybdenum, tungsten, copper, chromium and bismuth oxides, and also on silver and platinum catalysts. The phase composition of catalysts was studied by X-ray analysis, ESR spectra were interpreted, and the electrophysical properties of catalysts were investigated in vacuum and in the reactant medium.

The oxide catalysts were found to be σ - and π- active. The former are responsible for breaking of CH bonds, and the latter of C=C bonds. The type of activity is a function of electronic structures both of individual cations and of the whole solid crystal.

For all systems studied oxidation proceeded by a parallel-consecutive scheme.

1. INTRODUCTION

Successive development of the catalytic oxidation of hydrocarbons depends on the working out of a proper theory, the determination of the nature, of elementary acts and the relation of these to the catalyst surface properties.

Intermediate steps of heterogeneous reactions proceed on the catalyst surface. The catalytic process of organic oxidation may be conceived as a chain of conversions the route of which is determined by the site of oxygen attack on the molecule. Consequently the problem of selective catalytic oxidation is essentially that of determining the probable site of oxygen inclusion into organic molecules of various solids.

Hydrocarbon oxidation involves the following steps:

1. Transfer of electrons from the hydrocarbon molecule to the catalyst (chemisorption of the hydrocarbon).
2. Transfer of electrons from the catalyst to the oxygen molecule (chemisorption of oxygen).
3. Interaction of the charged particles formed (a radical, an ion-radical or a complex) yielding the oxidation products.

4. Desorption of oxidation products.

The oxidation catalysts should possess two properties: that of forming acceptor-donor bonds with organic compounds and oxygen, and that of transferring electrons from one reacting particle to another. The mechanism of electron transfer may be different for various types of solids.

2. METAL OXIDES

In order to establish the dependence of certain hydrocarbon oxidation rates on the electronic properties of a surface and on metal structures, the authors, together with Lyubarskii, Ezhkova, Krylova, Kazanskii and Isaev, have investigated a number of oxide catalysts in various reactions [1-3].

The characteristic data on catalysts is given in table 1.

Table 1

Characteristic data on oxide catalysts.

Catalyst	Composition atomic percentage	Surface m^2/g
$V_2O_5 + MoO_3$	0 to 25 of Mo	1 to 2.0
	30 to 80 of Mo	1 to 2
$V_2O_5 + Cr_2O_3$	0 to 80 of Cr	1 to 2
$V_2O_5 + Co_2O_3$	0 to 80 of Co	1 to 2
$V_2O_5 + P_2O_5$	0 to 70 of P	1 to 2
$V_2O_5 + Li_2O$	0 to 50 of Li	1 to 2
$MoO_3 + Bi_2O_3$	0 to 80 of Bi	1.4 to 1.5
$WO_3 + Bi_2O_3$	0 to 80 of Bi	7.0 to 8.0
$V_2O_5 + Bi_2O_3$	0 to 43 of Bi	2.6 to 2.8
$V_2O_5 + P_2O_5$	0 to 43 of P	2.6 to 2.8
$MoO_3 + P_2O_5$	0 to 43 of P	1.0 to 1.2
$WO_3 + P_2O_5$	0 to 43 of P	2 to 12

It was shown by X-ray analysis that mixed catalysts (excluding oxides involving pure V_2O_5 and MoO_3 may be divided into two groups: solid solutions and compounds. The results obtained on the phase composition of the metal oxides studied are summarized in table 2. Certain oxide systems were studied earlier by other investigators [4-7], but their results are not always consistent with those obtained by the authors of this paper.

The phase composition of catalysts was determined by X-ray analysis in a PKD chamber, using a chromium anode (k_α-irradiation).

The activity of catalysts was studied from the kinetics of benzene and propene oxidation in flow-circular and flow apparatus [8, 9] with respect to the benzene yield in maleic anhydride, and from the constants of acrolein formation rates with respect to propene. Selectivity was determined from the amount of the main oxygenated product yielded by the hydrocarbon.

The structures were investigated from ESP spectra, using a technique described before [10].

The electronic properties of a surface (the electron work function φ)

were determined from the contact potential difference catalysts and standard electrodes measured by means of the vibrating condensor technique using an apparatus the schematic view of which was given previously [11].

Table 2
Phase composition of mixed oxide catalysts.

Catalyst	Composition atomic percentage	Phase composition
V_2O_5 + MoO_3	0 to 30 of Mo	solid solution
V_2O_5 + MoO_3	30 to 50 of Mo	V MoO_x
V_2O_5 + Cr_2O_3	0 to 50 of Cr	$VCrO_4$
V_2O_5 + Co_2O_3	0 to 30 of Co	V_2O_5 + $Co_2V_2O_7$
V_2O_5 + Co_2O_3	30 to 50 of Co	V_2O_5 + Co_3O_4 + $Co_2V_2O_7$
V_2O_5 + P_2O_5	0 to 3.5 of P	solid solution
V_2O_5 + P_2O_5	3.0 to 50 of P	VPO_x
V_2O_5 + Li_2O	0 to 50 of Li	$LiVO_x$
MoO_3 + Bi_2O_3	0 to 50	Bi_2O_3 MoO_3 Bi_2O_3. $2MoO_3$ Bi_2O_3 $3MoO_3$
WO_3 + Bi_2O_3	0 to 50	Bi_2O_3 WO_3 Bi_2O_3 $3WO_3$

The activity and selectivity of mixed oxide catalysts were correlated with their electrophysical properties and structures. Following were the results obtained.

2.1. *Oxidation of benzene to maleic anhydride*

The maximum activity of a mixed vanadium-molybdenum catalyst corresponds to the solubility limit for molybdenum oxide in vanadium pentoxide. The selectivity, the work function variations and the intensity of ESR signals characteristic of the concentration of V^{4+} ions in the V_2O_5 lattice were observed to change in the same sense (fig. 1).

A small increase in the catalytic activity of V_2O_5 is observed for a vanadium-chromium catalyst in the presence of minor amounts of Cr_2O_3 (about one molecular per cent of Cr_2O_3) the activity and selectivity of the catalyst changing again in the same sense (as in the case of the V_2O_5 + + MoO_3 system).

Addition of more than one percent of Cr_2O_3 will decrease the activity and selectivity of the catalyst (fig. 2).

With mixed vanadium-chromium catalysts two ESR signals are observed simultaneously: a broad signal (δ = 400 gauss) and on the background of it a narrow one (δ = 150 gauss) (fig. 3). The narrow line may be ascribed, by analogy with the V + Mo system, to V^{4+} ions appearing in the solid solution of Cr_2O_3 in V_2O_5. The intensity of this signal is consistent with the catalytic activity and selectivity.

The catalytic activity, selectivity and electron work function of this system change in the same sense as for the V_2O_5 + MoO_3 system. When the

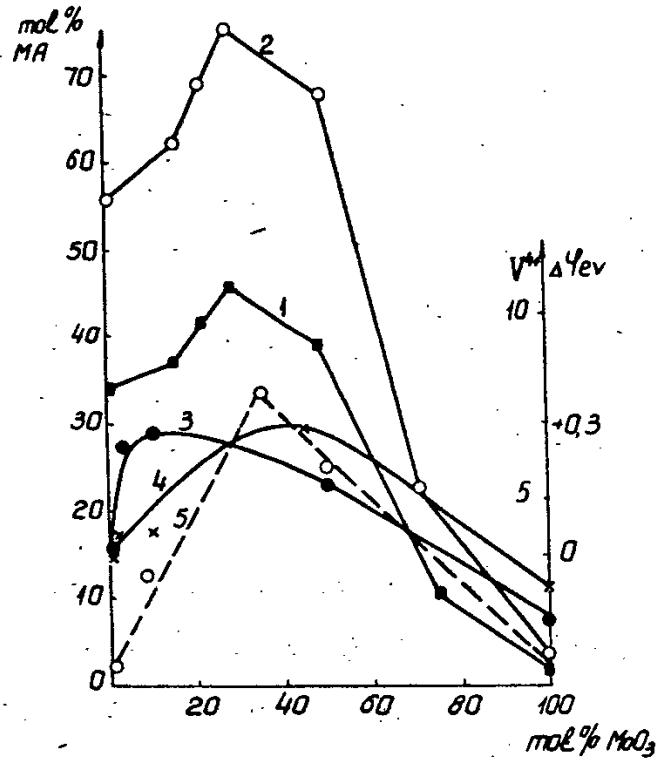

Fig. 1. V_2O_5 + MoO_3 system.
1. Activity. Molar percentage of maleic anhydride with respect to amount of benzene.
2. Selectivity, Percentage with respect to the benzene reacted.
3. $\Delta\varphi$ in vacuum at 20°C (eV).
4. $\Delta\varphi$ after treatment with a benzene-air mixture at 300°C (eV).
5. Content in V^{4+} after contact with the catalyst.

catalyst surface is treated with a benzene-air mixture, the maximum $\Delta\varphi$ value corresponds to the maximum selectivity of the process.

Addition of cobalt oxide to V_2O_5 will decrease the activity and selectivity of the catalyst; the work function value will also drop, though a small increase in $\Delta\varphi$ would be observed with addition of 1% of Co_2O_3, the reaction selectivity remaining unaffected (fig. 4). The V_2O_5 + Co_2O_3 system shows no ESR signals.

Investigations on the activity of vanadium-phosphorus catalysts in the oxidation of benzene to maleic anhydride have shown that the influence of P_2O_5 is negative. With an increasing content of P_2O_5 in V_2O_5 the activity and selectivity of a sample show a monotonic decrease.

ESR signals from vanadium-phosphorus catalysts involving more than 5% of P_2O_5 represent a single line of about 200 gauss. With increase in P_2O_5 the intensity of ESR signals becomes higher. A correlation with X-ray data shows that the signal is due to formation of a chemical V_2O_5 + P_2O_5 compound.

The addition of P_2O_5 also decreases the electron work function, as well as the activity and selectivity of the catalyst. Only at phosphorus concentrations up to 5%, when a solid solution is possible, the $\Delta\varphi$ value will increase

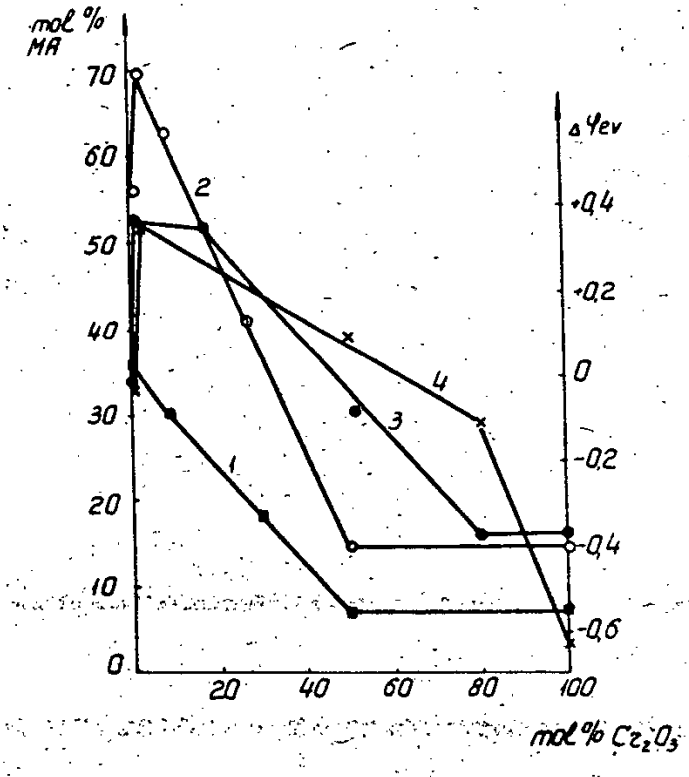

Fig. 2. V_2O_5 + Cr_2O_3 system.
1. Activity. Percentage of maleic anhydride with respect to the amount of benzene.
2. Selectivity. Percentage with respect to the benzene reacted.
3. $\Delta\varphi$ in vacuum at 20°C (eV).
4. $\Delta\varphi$ after treatment with a benzene-air mixture at 300°C.

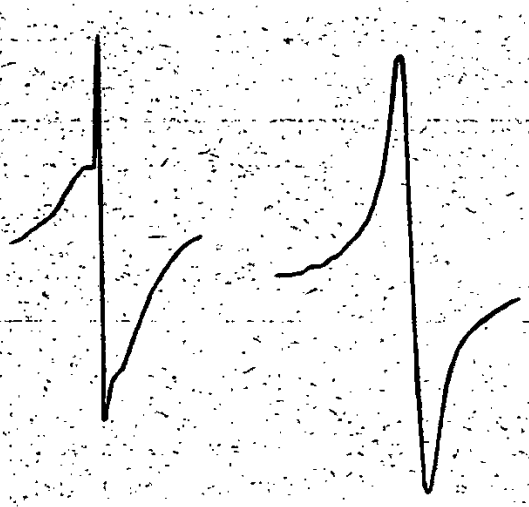

Fig. 3. ESR spectra of vanadium-chromium catalysts.
a) Composition: 5 mol% of Cr_2O_3 + 95 mol% of V_2O_3.
b) Composition: 50 mol% of Cr_2O_3 + 50 mol% of V_2O_3.

by 0.1 eV without changing the characteristics of the catalytic process.

A change in the catalytic activity of V_2O_5 with addition of Li_2O in benzene oxidation to maleic anhydride resulted in a monotonic decrease in activity and

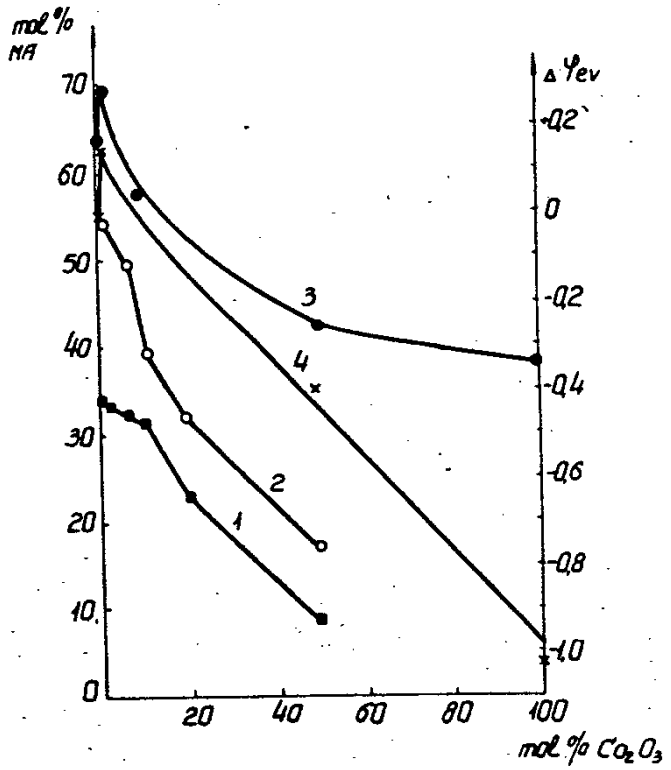

Fig. 4. V_2O_5 + Co_2O_3 system.
1. Activity. Percentage of maleic anhydride with respect to the amount of benzene.
2. Selectivity. Percentage of maleic anhydride with respect to the benzene reacted.
3. Δφ in vacuum at 20°C (eV).
4. Δφ after treatment with a benzene-air mixture at 300°C (eV).

selectivity. ESR signals increasing in intensity with a greater amount of the substance added are observed for the V_2O_5 + Li_2O system. These are due to V^{4+} ions in the chemical compounds formed by interaction between V_2O_5 and oxides of alkali metals.

A monotonic decrease in the work function with increasing amount of Li_2O is observed for the V_2O_5 + Li_2O system, and, consequently, the activity and work function will change in the same sense.

2.2. *Oxidation of propene to acrolein*

The oxidation of propene to acrolein [12] over vanadium and molybdenum oxides was investigated earlier and the rate of acrolein fromation was shown to decrease continuously with increasing concentration of MoO_3 in V_2O_5.

Variations in the selectivity of propene oxidation and in the electron work function depending upon the composition of mixed catalysts, MoO_3 + Bi_2O_3 and WO_3 + Bi_2O_3, are shown in fig. 5. The maximum selectivity corresponds to maximum increase in the work function. The electronconductivity builds up in a way similar to that observed for the work function. It was shown by X-ray analysis of these systems [6,7] that $Bi_2O_3 MoO_3$, $Bi_2O_3 2MoO_3$ and and $Bi_2O_3 \cdot 3MoO_3$ compounds were formed within the range of 0 to 40 % of

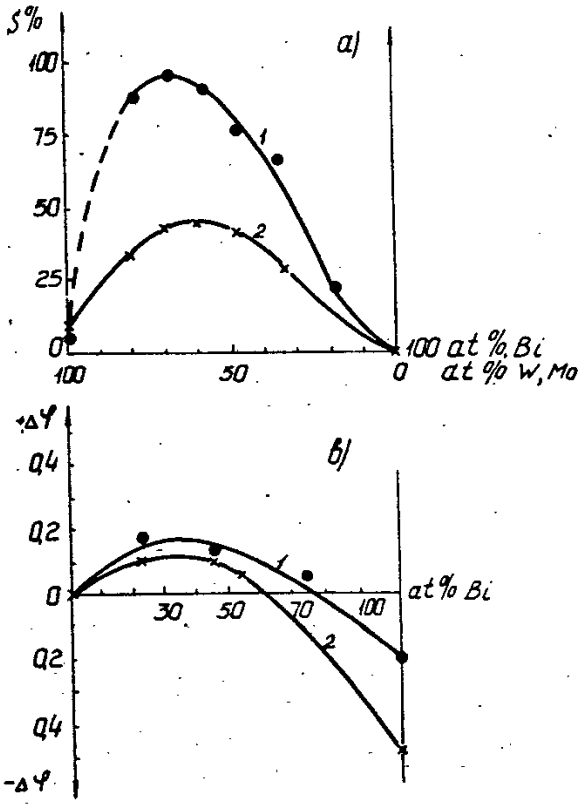

Fig. 5. Variations in the electron work function ($\Delta\varphi$, eV) and selectivity percentage (S) as a function of the composition of bismuth molybdenum and tungsten catalysts
a) S1 – Bi + Mo 2 – Bi + W
$\Delta\varphi$1 – Bi + Mo 2 – Bi + W.

the Bi_2O_3 concentration in MoO_3. Propene oxidation over V_2O_5 yields acrolein, saturated aldehydes and acids, Co_2, and H_2O. The addition of bismuth oxide results in a lower catalytic activity, but the relation between the rates of formation of acrolein and saturated aldehydes from propene remains almost unchanged. With a bismuth-vanadium catalyst the rate of formation of acids is lower (43% at Bi in V_2O_5). Vanadates of various structure were found to form in the presence of Bi_2O_3.

The formation of new compounds was established by X-ray analysis of V_2O_5, MoO_3, and WO_3 systems in the presence of P_2O_5. The selectivity of propene oxidation over vanadium, molybdenum, and tungsten phosphates increased with decreasing specific catalytic activity. The activation energies for CO_2 formation were by 8 to 10 kcal/mole lower than for pure oxides. An interesting feature of the $V_2O_3 + P_2O_5$ system is a change of the oxidation route, due to suppression of reactions induced by breaking of the double bond in a propene molecule. Similar observations were made by Kernos and Moldavskii [13] for the oxidation of butenes to maleic anhydride over phosphorus-vanadium catalysts.

The addition of various compounds to oxide catalysts is known to change the selectivity of oxidation of unsaturated hydrocarbons. Modifying additions increasing the work function and displaying a highed electronegativity than that of Cu_2O will increase the selectivity of propene oxidation, while an oppo-

site effect would be observed with additions decreasing the work function. Catalysts with a higher φ value will show greater coverage with positively charged propene, as compared with Cu_2O, while increased coverage with negatively charged oxygen will be characteristic of catalysts with a lower φ value.

3. METALS

Platinum, palladium, copper and silver are the most widespread metal catalysts for oxidation. Complete destruction of the hydrocarbon molecule skeleton to CO_2 and H_2O will be observed in the gas-phase oxidation of hydrocarbons over these catalysts. Silver is the only active catalyst inducing incomplete oxidation of ethylene to ethylene oxide. Investigation of oxygen adsorption and of oxygen isotope exchange [2] over these metals has shown that chemisorption of oxygen yielded molecular and atomic oxygen ions, the ratio of which is a function of temperature and the surface condition. Vol and Shishakov [14] have shown by electron diffraction that the interaction between silver and oxygen at 100 to 200° yields silver peroxide which is decomposed by ethylene. With platinum and palladium catalysts the mobility of oxygen at these temperatures will be considerably lower. The interaction between saturated hydrocarbons and an oxygen-covered platinum surface results in the formation of an intermediate complex readily decomposed by oxygen of the gas phase, the reaction continuing in the gas phase at 50 to 70°. The oxidation of unsaturated hydrocarbons on silver was not found to continue in the gas phase.

Variations in the electron work function, in the electroconductivity of the compounds added, and the selectivity of ethylene oxidation to ethylene oxide on modified silver are shown in fig. 6.

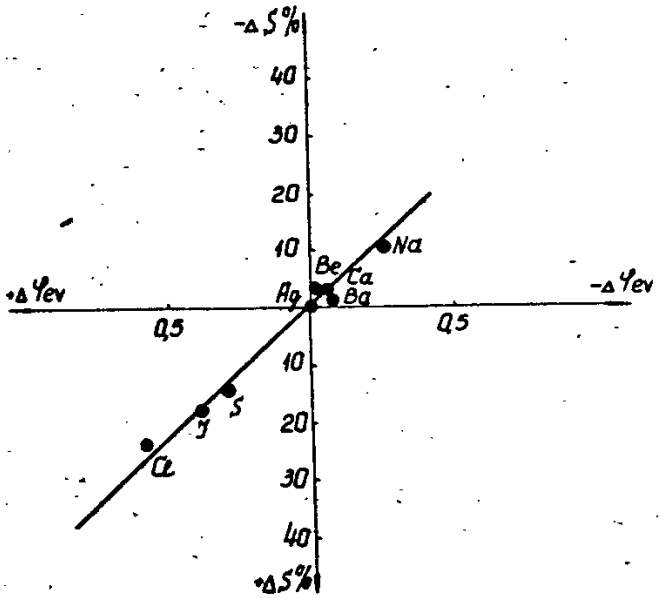

Fig. 6. Variations in the selectivity (Δ S, %) of ethylene oxidation to ethylene oxide over silver as a function of variations in the electron work function (Δφ, eV).

Additions involving alkali and earth-alkali metals will decrease, while metalloids will increase the electron work function. Elements displaying a lower electroconductivity than that of silver will decrease φ and the selectivity, while higher electronegativity results in increased and selectivity of ethylene oxidation.

Variations in φ in the adsorption of various atoms on metals are considered as due to the formation of a dipole layer on the surface. Dipoles are formed also by chemisorption of oxygen and hydrocarbons, and the interaction between these dipoles and those formed by additives seems to induce changes in the surface coverage with oxygen and ethylene.

4. LIQUID-PHASE OXIDATION OF HYDROCARBONS

The liquid-phase oxidation of hydrocarbons has been investigated less extensively than that in the gas phase. It was shown by experiment that transient metal oxides and certain metals may be used as catalysts for liquid-phase oxidation. Oxidation of toluene by air over a mixed vanadium-tungsten catalyst at 200° and a pressure of 80 atm yields 71 mol % of benzoic acid and about 10 mol % of benzoic aldehyde. With the same catalyst and under similar conditions toluene will yield 7.2 mol % of acid and 1.5 mol % of aldehyde. In a number of cases, depending on the hydrocarbon structure and oxidation conditions, the part played by oxide and metal catalysts comes to initiation of a homogeneous chain reaction [16, 17]. The products yielded by catalytic reactions are similar in composition with those formed in liquid-phase reactions involving homogeneous initiators. In other cases reactions on solid catalysts proceed in a more specific way [15]. The main products of *n*-heptane oxidation on vanadium and tungsten oxides are butyric and valeric acids, while mainly acetic and propionic acids are formed with soluble catalysts. In the presence of heterogeneous catalysts the yield in carbonyl compounds is several times higher. In this case liquid-phase oxidation will proceed mainly on the surface, and not in the gas phase.

5. DISCUSSION OF THE RESULTS OBTAINED

It was shown by analysis of the results obtained that the mixed and modified catalysts studied may be divided into two groups: solid inclusion and substitution solutions, and chemical compounds (vanadates, molybdates, etc).

The introduction of minor amounts of molybdenum and chromium oxides to vanadium pentoxide results in the formation of solid solutions containing V^{4+} ions.

The addition of minor amounts of molybdenum and chromium oxide to solid vanadium pentoxide results in the formation of solid solutions containing V^{4+} ions. These catalysts display increased activity and selectivity with respect to benzene oxidation. This is not so for butene oxidation to maleic anhydride [13] or of propene to acrolein [2]; the addition of MoO_3 to V_2O_5 will decrease the activity and selectivity. A relation was found to exist between the electron work function and the selectivity of both reactions.

The formation of chemical compounds from vanadium pentoxide and from

chromium, molybdenum, and cobalt oxides resulsts in decreased activity and selectivity of benzene oxidation, while molybdenum and bismuth tungstate increase the selectivity of propene oxidation to acrolein. Vanadium phosphates accelerate butene oxidation to maleic anhydride and slow down its formation from benzene. A relation between the electronic properties of the catalyst and the selectivity is observed for chemical compounds, same as with solid solutions.

All systems of the oxidation catalysts studied contain transient metals, and surface formation of various complexes with the lattice cations seems to be possible in the adsorption of hydrocarbons. Hydrocarbon molecules involving a double bond with the transient metal atoms may form π-complexes [15]. The π-complexing capacity is a function of the electronic structures of cations and of organic molecules. Possible is also σ-complexing involving the breaking of C-H bonds in the hydrocarbon.

At the catalyst surface the complexes seem to convert into ion radicals forming peroxide ion radicals by reaction with oxygen [2].

The first group of catalysts may be called π-active, and the second σ-active.

Similarly to homogeneous catalysts, reduction of transient metal ions may occur in the solid lattice, following the scheme

$$RCH + Me^{n(+)} \rightarrow RCH^{(+)} + Me^{(n-1)(+)} .$$

The superposition of d-orbitals with the formation of a generalized electron conduction band is not observed for metal oxides with open d-shells [16], and displacement of current carriers proceeds by charge exchange between ions, as suggested by Verwey [17]. The redox potential value characteristic of the electron or hole transfer from one ion to another is a measure for determining the redox capacity of ions in solutions. When electronic levels form no band, as is the case for the systems studied, the redox potentials will be a function of the activity and selectivity of catalysts in hydrocarbon oxidation. For these catalysts the work function (φ) will be related to the distribution of electronic levels in the lattice of the solid. The acceptor capacity of the surface, thus the coverage with electron donors, that is with hydrocarbons, will increase with increasing φ. Additions to metals and to oxide catalysts result in the formation of solid solutions of heterogeneous systems. With metals (in contrast to oxides) the main part will be played by oxygen activation at the surface resulting in charged molecular (oxide) and atomic forms.

The reaction selectivity is a function not only of the chemical composition and electronic properties of the catalyst, but also of the ratios of rates for individual steps. Selectivity is a function either of the relation between formation rates for various products, or of the destruction rate of the final product. This question was widely discussed and it was shown that oxidation of hydrocarbons proceeds by a parallel-consecutive mechanism. When the time of a reaction product desorption is comparable with that of its formation a subsequent surface conversion of this product becomes possible. Interesting results were obtained for the liquid-phase oxidation of o-xylene on a vanadium catalyst. Instead of the expected phtaleic anhydride, o-toluene acid was formed.

The reason for it probably is the shortage of time the products remain on the surface, and desorption of these into the gas phase. A similar effect is observed for gas-phase oxidation in the presence of water vapour. An example of it would be the increase in selectivity in propene oxidation to acrolein [22], or in that of furfurole to maleic anhydride [23].

REFERENCES

1) I.I.Ioffe, Z.I.Ezhkova and A.G.Lyubarskii, Kinetika i Kataliz 2 (1962) 194.
2) L.Ya.Margolis, Geterogennoye Katalyticheskoye Okislenyi Uglevodorodov (Gostoptekhizdat, 1962).
3) Z.I.Ezhkova, I.I.Ioffe, V.B.Kazanskii, A.V.Krylova, A.G.Lyubarskii and L.Ya.Margolis, Kinetika i Kataliz 4 (1963) 187.
4) A.Magnalli and B.M.Oughton, Acta Chem. Scandinavica 5 (1951) 581.
5) R.Tarama, Sh.Teranishi and T.Jasui, J. Chem. Soc. Japan, Industr. Chem. 60 (1957) 1222.
6) I.N.Belyaev and N.P.Smolyaninov, Zhurn. Neorgan. Khimii 7 (1962) 1126, 2521.
7) G.Gattow, Z. anorgan. Chem. 298 (1959) 64.
8) I.I.Ioffe and A.G.Lyubarskii, Kinetika i Kataliz 2 (1962) 261.
9) O.V.Isaev and L.Ya.Margolis, Kinetika i Kataliz 1 (1960) 237.
10) V.B.Kazanskii, Z.I.Ezhkova, A.G.Lyubarskii, V.V.Voevodskii and I.I.Ioffe, Kinetika i Kataliz 2 (1961) 862.
11) E.Kh.Enikeev, L.Ya.Margolis and S.Z.Roginskii, Dokl. Akad. Nauk SSSR 130 (1960) 807.
12) L.N.Kutzeva and L.Ya.Margolis, Zhur. Obshch.Khim. 32 (1962) 102.
13) Yu.D.Kernos and B.L.Moldavskii, Kinetika i Kataliz 2 (1962) 271.
14) Yu.U.Vol and N.A.Shishakov, Izv. Akad. Nauk SSSR,Otdel. Khim. Nauk, No. 4 (1962) 586.
15) I.I.Ioffe and N.V.Klimova, Kinetika i Kataliz, 4 (1963) No. 5.
16) J.Burger, C.Meyer, G.Clement and J.C.Balaceanu, Compt. Rend. 252 (1961) 2235.
17) E.A.Blumberg, M.G.Bulygin, L.Ya.Margolis and N.N.Emanuel, Dokl. Akad. Nauk SSSR 150 (1963) 1066.
18) Ya.K.Syrkin, Zhur. Strukt. Khim. 1 (1960) 189.
19) I.I.Ioffe, Kinetika i Kataliz 2 (1962) 175.
20) F.Y.Morin. Semiconductors (ed. by M.B.Hanney, N.Y., 1961).
21) E.Y.W.Verwey, Semiconducting Material (1951) p. 151.
22) A.G.Polkovnikova, A.N.Shatalova and L.L.Tzeitina, Neftekhimya 3 (1963) 246.
23) V.A.Slavinskaya, M.A.Shimanskaya, C.A.Giller and I.I.Ioffe, Kinetika i Kataliz 2 (1961) 252.

THE INFLUENCE OF SELECTIVE PROPERTIES OF MOLECULAR SIEVES ON CATALYTIC DEHYDRATION OF ETHANOL

Miloš RÁLEK and Oto GRUBNER

Institute of Physical Chemistry, Czechoslovak Academy of Sciences, Prague

Abstract: The catalytic dehydration of ethanol and diethylether has been studied. Model catalysts used were molecular sieves. It has been found, that the rate of transport of reaction components in the microporous structure of molecular sieves substantially influences the selectivity of the reaction. Results obtained confirm the simultaneous mechanism of the reaction.

1. INTRODUCTION

The catalytic dehydration of ethanol and diethylether, taking place on alumina and aluminosilicate catalysts, is a complex reaction which includes equilibria and chemical reactions between the individual components (ethanol, diethylether, water, ethylene) [1].

The conversion of ethanol to diethylether, in dependance on time of contact, runs through a maximum. Conversion to ethylene increases with increasing time of contact. Conversion of diethylether to ethanol shows a similar maximum.

The conversion curves have been described by Brey and Krieger [2]. These authors have studied the dehydration of ethanol on aluminas, treated in different ways, using kinetic equations derived under the assumption that water and ethanol are sorbed strongly on the catalysts and that the rate of reaction is determined by the rate of the chemical conversion of the adsorbed intermediary complex to ethylene. They have made use of Whitmore's conception [3] assuming that the intermediary complex, forming on the catalyst surface, is a carbonium ion. The carbonium ion concentration is proportional to the surface concentration of ethanol and its formation is conditioned by interactions of active centers of the catalyst, where non-saturated valence forces exist, with molecules of the substrate. The reaction takes place simultaneously according to the scheme:

$$C_2H_5OH \overset{-OH^-}{\rightleftharpoons} C_2H_5^+ \overset{-H^+}{\longrightarrow} C_2H_4$$
$$\Big\Downarrow +C_2H_5O^-$$
$$(C_2H_5)_2O$$

Balaceanu and Jungers [4] have studied the dehydration of ethanol and ether at low temperatures on alumina. In agreement with opinions expressed

earlier in the literature [5], they have come to the conclusion, that this is a consecutive reaction and they have proposed the following scheme:

$$2\ C_2H_5OH \longrightarrow (C_2H_5)_2O + H_2O \longrightarrow C_2H_4 + C_2H_5OH + H_2O$$

Topshievā and Yun-Pin [6] have derived kinetic equations for the dehydration of ethanol and diethylether on alumina and aluminosilicate catalysts of various composition. The equations apply to the consecutive scheme of the reaction under the condition that sorption of water on the catalyst prevails appreciably over the sorption of the other components. The rate constants in the temperature range of 375 to 450°C are comparable and directly proportional to the Al_2O_3 content of the catalysts. The activation energy for the dehydration of ethanol and ether to ethylene is the same for all the catalysts (14.5 kcal/mole). At a reaction temperature of 250°C the main product of ethanol dehydration is diethylether. Ethylene is formed in slight amounts (2%).

When later analysing the results, the authors have come to the conclusion that the reaction proceeds by a simultaneous mechanism, through a surface compound of the type of aluminium alcoholate, which is formed on the catalyst surface according to the scheme

$$C_2H_5OH + HO\text{-}Al \overset{I}{\rightleftharpoons} C_2H_5\text{-}O\text{-}Al \overset{II}{\rightleftharpoons} \tfrac{1}{2}(C_2H_5)_2O + HO\text{-}Al$$

$$\Big\downarrow III$$

$$C_2H_4 + OH\text{-}Al$$

Reactions I and II are reversible, the decomposition of the intermediary complex (III) is non-reversible. During a short contact time, equilibrium between the reactions I and II is not obtained on the catalyst surface. In ethanol dehydration a reaction is preferred in this case, which supports the establishment of equilibrium, i.e., ether formation, ether passing by desorption into a gaseous phase. When the time of contact is increased, decomposition of the intermediary complex to ethylene takes place in a greater measure. The equilibrium concentration of ethylene is renewed by the reaction of ether from the gaseous phase, resulting in decreased ether production. A similar process takes place in the case of diethylether dehydration, the dependance of ethanol production on the time of contact passing through a maximum.

The kinetic relations and assumptions of the reaction mechanism derived from these are based on measurements of catalytic activity in the kinetic region, where conversions measured are independent of the particle size of the catalysts.

Boreskov [7] has found, that at particle size of the alumina of 3 mm, inner diffusion becomes important and the relatic amounts of products change. Reactions in the region of inner diffusion take place at a lower rate. With the same amount of reacting alcohol, ether production is roughly half of that, which is produced when the reaction takes place in the kinetic region. Qualitatively the results agree with theoretical conclusions on the influence of inner diffusion on catalyst selectivity.

The aim of this work was the application of the shape selectivity of

molecular sieves to the confirmation of the proposed mechanism, and an elucidation of the influence of pore size on catalytic selectivity.

The molecular sieves are crystalline aluminosilicates with defined pore size, comparable with the size of the molecules of some of the reacting substances. They are therefore suitable for use as model catalysts.

2. EXPERIMENTAL PART

The molecular sieves have been synthesised in the sodium form [8,9] and their purity was checked by means of X-ray methods [10,11]. The calcium and potassium forms were prepared from the sodium form by means of ion exchange. In the dehydrated state, the molar composition of the catalysts was:

molecular sieve 3A	0.81 K_2O . 0.18 Na_2O . Al_2O_3 . 1.98 SiO_2
molecular sieve 4A	0.98 Na_2O . Al_2O_3 . 1.98 SiO_2
molecular sieve 5A	0.72 CaO . 0.26 Na_2O . Al_2O_3 . 1.98 SiO_2
molecular sieve 10X	0.87 CaO . 0.12 Na_2O . Al_2O_3 . 2.6 SiO_2
molecular sieve 13X	1.0 Na_2O . Al_2O_3 . 2.6 SiO_2

Alumina, prepared by the hydrolysis of aluminium alcoholate, was used as comparison catalyst. Its specific surface was 200 m^2/g, the diameter of the most frequent pores was 40 Å (sample B I, having the properties described in ref. 12).

Microcrystalline catalyst samples were pelletised by pressure and grains of 0.2 to 0.4 mm size were used for the experiments.

A registering microbalance was used to measure the rate of ethanol and ether sorption on molecular sieves 5A and 10X at temperatures at which no reaction occurs yet. Values of the apparent diffusion energy E_a for ethanol and ether into these catalysts were calculated from these measurements. The calculations were performed by means of the relation [13]

$$R \frac{\partial}{\partial(1/T)} \ln \frac{d(Q_t/Q_\infty)}{d\sqrt{t}} = -\tfrac{1}{2} E_a$$

(Q_t is the amount sorbed in the time t at the temperature T°K, Q_∞ corresponds to the equilibrial sorption value at the same temperature). The dependance of Q_t on $\sqrt{t}$ was linear up to $Q_t = 0.6\ Q_\infty$. It has been found, that the apparent activation energy of ethanol diffusion in molecular sieves 5A and 10X is the same and is equal to 1.4 kcal/mol. The apparent activation energy of ether diffusion in molecular sieve 10X is equal to 2.1 kcal/mol. The apparent activation energy of ether diffusion in molecular sieve 5A was substantially higher (6.4 kcal/mol).

The catalytic dehydration of ethanol has been studied in a circulating flow apparatus with differential reactor [14]. Pure nitrogen was used as carrier gas. Ethanol feed was controlled by the saturator temperature. Reaction components have been analysed by means of gas chromatography.

Overall catalytic activity values, expressed as fraction of reacted alcohol amounts, in dependance on the reciprocal value of the feed, are shown

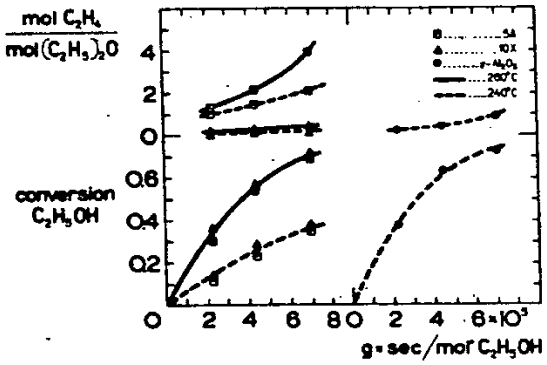

Fig. 1. Overall catalytic activity of molecular sieves 5A, 10X and γ-alumina, and the value of the molar ratio of ethylene-diethylether, in dependance on the reciprocal value of the feed.

in the lower part of fig. 1. Values of the molar ratio of ethylene and diethylether, formed by the reaction, are shown in the upper part of fig. 1. The overall activity of both types of molecular sieves is practically identical in the temperature range of 240 to 260°C. On the small-pore molecular sieve 5A, ethylene is mainly formed, whereas ether is the main product obtained on the molecular sieve 10X, which has wider pores. With decreasing feed total ethanol conversion increases. The value of the molar ratio ethylene/ether increases much more rapidly in the case of molecular sieve 5A than in the case of molecular sieve 10X.

Alumina is a more active catalyst than both types of molecular sieves described. Its activity at 240°C corresponds roughly to the activity of molecular sieves at 260°C. Alumina produces mainly ether, similarly as sieve 10X.

Molecular sieve 13X has, in the temperature range studied, approximately 40% of the activity of molecular sieve 10X, and forms mainly ether.

Molecular sieves 3A and 4A are non-active in the temperature range studied. A measurable catalytic reaction takes place only at higher temperatures (~300°C).

The dehydration of ethanol and diethylether on sieves 5A and 10X and alumina has been studied furthermore by means of the microcatalytic pulse technique [15]. In the dehydration of ethanol molecular sieve 5A formed mainly ethylene. Under comparable conditions, molecular sieve 10X and alumina formed mainly ether.

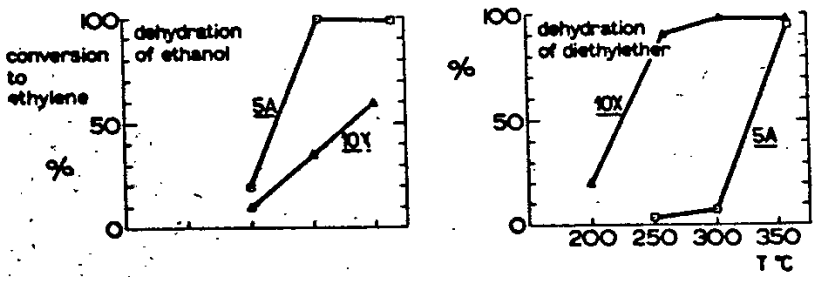

Fig. 2. Dehydration of ethanol and diethylether on molecular sieves 5A and 10X using the pulse microcatalytic technique, in dependance on temperature.

The dehydration of ether took place easier on molecular sieve 10X and on alumina than on molecular sieve 5A. Comparing the behaviour of both types of molecular sieves on the basis of the amount of ethylene formed by catalytic reaction, we obtain the dependance shown in fig. 2. The figure shows, that molecular sieve 5A dehydrates diethylether relatively with great difficulty.

3. DISCUSSION

From the results of this work follows:

The activity of the model catalysts, used for the dehydration of ethanol, decreased in the series: alumina, molecular sieves 5A and 10X, molecular sieve 13X. Molecular sieves 3A and 4A were non-active, due to the small dimensions of their pores, which made it impossible to utilise the inner pore surfaces.

On molecular sieve 5A, ethanol dehydration proceeded selectively to ethylene in a temperature range, where alumina and molecular sieve 10X gave mainly ether.

Diethylether has been dehydrated easily by alumina and by molecular sieve 10X, with difficulty by molecular sieve 5A.

In catalytic action, alumina and molecular sieve 10X are more similar to each other, although these two substances are chemically and crystallographically different, than both molecular sieves, which have similar chemical compositions and character of the arrangement of the inner surface.

The cause for this difference in behaviour must be searched for in the differing pore size, which influences the rate of mass transport into the catalysts. This effect is most distinct in the case of ether diffusion into molecular sieve 5A, whose activation energy is substantially higher than for the other components, corresponding roughly to one half the value of activation energy of the dehydration of ether to ethylene. The high activation energy of the diffusion of ether into molecular sieve 5A is the direct cause of the fact, that the dehydration of ether in the pulse microcatalytic arrangement takes place more slowly than the dehydration of ethanol, because the relative frequency of ether molecules which have access to the inner catalytic surface, is decreased. In the case of catalysts with wider pores, the reaction is not slowed down by transport effects, and dehydration of ether is easy. Steric effects, influencing ether transport, may explain the increased selectivity of molecular sieve 5A in the dehydration of ethanol to ethylene. Schemes of the simultaneous mechanisms of dehydration reactions are based on the establishment of equilibria between the intermediary surface complex and ethanol or ether. In the case of the narrow-pore sieve 5A, transport of ether formed by ethanol, from catalyst cavities into the gaseous phase is retarded by slow diffusion. The equilibrium concentration of the ether-complex is therefore established easily. The intermediary complex decomposes to ethylene, and its equilibrium concentration is constantly amplified by ethanol, coming from the gaseous phase. Due to these processes the catalytic reactions produce mainly ethylene.

Among the two dehydration mechanisms proposed, the carbonium mechanism seems to be less probable, because no parallel has been found between the acidity of catalysts - which increases in the series 5A, 10X, 13X [16] - and their catalytic activity. Our results show, that there exists a relation between the content of Al_2O_3 and the overall catalytic activity, which has been found in the work of Topshieva and Boreskov.

The explanation of the observed catalytic effects also agrees with the work of Brey and Krieger, from which follows that aluminas, structurally modified by the influence of steam at elevated temperatures (leading to decrease of the specific surface values and thus also to the loss of the very small pores), have produced under otherwise equal conditions a larger amount of ether than the initial catalysts.

It has been observed in the present work, that on the molecular sieves appreciable ether sorption takes place even at temperatures close to the reaction temperatures. A similar observation has also been made by Balaceanu and Jungers in the course of determining the adsorption coefficients of ethanol, ether and water on alumina. Kinetic equations given in the literature do not respect sufficiently this fact, and therefore it cannot be assumed that they describe the kinetics of these dehydration reactions fully.

It seems probable, that selective catalytic effects of molecular sieves, caused by transport phenomena, will be observed in a number of other reactions also.

REFERENCES

1) M.E.Winfield, in: Catalysis (Reinhold, New York, 1960) Vol. 7, p. 93.
2) W.S.Brey and K.A.Krieger, J. Am. Chem. Soc. 71 (1949) 3657.
3) F.C.Whitmore, J. Am. Chem. Soc. 54 (1932) 3274.
4) J.C.Balaceanu and J.C.Jungers, Bull. Soc. Chim. Belg. 60 (1951) 476.
5) Alvarado, J. Am. Chem. Soc. 50 (1928) 790.
6) K.V.Topshieva and K.Yun-Pin, Zhur. Fiz. Khim. 29 (1955) 1678, 1854, 2976.
7) G.K.Boreskov, V.A.Dzisko and M.C.Borisova, Zhur. Fiz. Khim. 28 (1954) 1055.
8) O.Grubner, M.Rálek and P.Jiru, Chem. prům. 11 (1961) 521.
9) P.Jiru, O.Grubner and M.Rálek, Chem. prům. 11 (1961) 20.
10) R.M.Barrer, J.W.Baynham, F.W.Bultitude and W.M.Meier, J. Chem. Soc. (1959) 195.
11) T.B.Reed and D.W.Breck, J. Am. Chem. Soc. 78 (1956) 5972.
12) V.Bosáček, R.Polák, E.Kučera and V.Daneš, Coll. Czech. Chem. Commun. 27 (1962) 2575.
13) R.M.Barrer, Trans. Faraday Soc. 45 (1949) 358.
14) M.I.Temkin, C.L.Kiperman and L.I.Lukjanova, Doklady Akad. Nauk SSSR 74 (1950) 763.
15) R.C.Stein, J.J.Feeman, G.P.Thomson, J.F.Shultz, L.J.E.Hofer and R.B. Anderson, Ind. Eng. Chem. 52 (1960) 671.
16) C.J.Norton, Chem. Ind. (1962) 258.